DEVELOPING AN ADENO-ASSOCIATED VIRAL VECTOR (AAV) TOOLBOX FOR CNS GENE THERAPY

A Dissertation Presented
By

SOURAV ROY CHOUDHURY

Submitted to the Faculty of the

University of Massachusetts Graduate School of Biomedical Sciences, Worcester

in partial fulfillment of the requirements for the degree of

DOCTOR OF PHILOSOPHY

JANUARY 7, 2016

INTERDISCIPLINARY GRADUATE PROGRAM

DEVELOPING AN ADENO-ASSOCIATED VIRAL VECTOR (AAV) TOOLBOX

FOR CNS GENE THERAPY

A Dissertation Presented
By

SOURAV ROY CHOUDHURY

The signatures of the Dissertation Defense Committee signify completion and approval as to style and content of the Dissertation

_____
Miguel Sena-Esteves, Ph.D., Thesis Advisor

_____
Guangping Gao, Ph.D., Member of Committee

_____
Sean P. Ryder, Ph.D., Member of Committee

_____
Claudio Punzo, Ph.D., Member of Committee

_____
Luk H. Vandenberghe, Ph.D., Member of Committee

The signature of the Chair of the Committee signifies that the written dissertation meets the requirements of the Dissertation Committee

_____
Jeffrey A. Bailey, M.D., Ph.D., Chair of Committee

The signature of the Dean of the Graduate School of Biomedical Sciences signifies that the student has met all graduation requirements of the school.

_____
Anthony Carruthers, Ph.D.,
Dean of the Graduate School of Biomedical Sciences

INTERDISCIPLINARY GRADUATE PROGRAM

January 7, 2016

To my parents.

Acknowledgements

This body of work would not have been possible without the contributions of several people.

I owe *everything* to **my parents**. They have sacrificed so much selflessly, wordlessly for me. They have been my first mentors, guiding lights, moral compasses and *heroes*. It breaks my heart to know that they are thousands of miles away from me now, at a point of time in their lives when they most need me to be around. This thesis is more theirs than mine.

I met **Ribhu Nayar** during a very low point in my life. She rescued me, stubbornly refused to give up on me, moved across half the world with me, and last year (against all better judgment) decided to marry me. She *even* taught me core course, that superwoman. I shudder at the thought of going through graduate school without her.

I had burned through five laboratory rotations, and was a literal week away from having to leave this country, when I showed up at **Miguel Sena-Esteves**' office. I am very grateful for the (life-changing) opportunity he gave me. Some of my favorite memories of graduate school involve talking shop with him. His edits to my first drafts have basically taught me how to write.

A recommendation from **Guangping Gao** got (a paper-less and unemployable) me a postdoctoral position in my dream lab, and for this I will always be indebted. He has been a solicitous TRAC Chair for me in every way possible.

Special thanks to my TRAC members **Jeffrey Bailey**, **Sean Ryder** and **Daryl Bosco** for their time, suggestions and telling me when it was time to wrap up. I am sad that Daryl could not be on my DEC, and thankful to have **Claudio Punzo** step in to fill that gap. I am also thankful to **Luk Vandenberghe** for agreeing to be my DEC external – there is no more appropriate person for this thesis.

I would like to thank all the collaborators I have had the good fortune to work with during graduate school - **Anne Harris**, **Damien Cabral**, **Allison Keeler**, **Ellen Sapp**, **Jennifer Ferreira**, **Heather Gray-Edwards**, **Jacob Johnson**, **Aime Johnson**, **Qin Su**, **Lorelei Stoica**, **Zachary Fitzpatrick**, **Stacy Maitland**, **Yuanfan Zhang**, **Shan Ma**, **Rohit Sharma**– and the PIs - **Marian DiFiglia**, **Neil Aronin**, **Laura Alonso**, **Claudio Punzo**, **Kathryn Wagner**, **Casey Maguire**, **Robert Kotin**, **Douglas Martin**, and **Guangping Gao**. I am grateful to **Xandra Breakefield** for giving me the opportunity to co-write a review with her. I apologize that this reads like a mere roll call of names – I truly value the contribution of each and every member of this group.

A sizable number of the above names are from the **Sena-Esteves laboratory**, which illustrates the level of help I have received from all present and past members. I thank them all for putting up with my idiosyncrasies. Conversations with **Christian Mueller** have shaped my thinking about gene therapy. The **office staff** has been an immense help all through the seven years at UMass.

Finally, a big chunk of the credit for my continued sanity through graduate school must go to my good friends – **Sophia Todeasa, Florie Borel, Dwijit**

Guhasarkar, Leticia Fridman, Lorelei Stoica, Gabriela Toro and many others

– for an ear or a shoulder at an appropriate time.

Abstract

Neurological disorders – disorders of the brain, spine and associated nerves – are a leading contributor to global disease burden with a sizable economic cost. Adeno-associated viral (AAV) vectors have emerged as an effective platform for CNS gene therapy and have shown early promise in clinical trials. These trials involve direct infusion into brain parenchyma, an approach that may be sub-optimal for treatment of neurodegenerative disorders, which often involve more than a single structure in the CNS. However, overall neuronal transduction efficiency of vectors derived from naturally occurring AAV capsids after systemic administration is relatively low. We have developed novel capsids AAV-AS and AAV-B1 that lead to widespread gene delivery throughout the brain and spinal cord, particularly to neuronal populations. Both transduce the adult mouse brain >10-fold more efficiently than the clinical gold standard AAV9 upon intravascular infusion, with gene transfer to multiple neuronal sub-populations. These vectors are also capable of neuronal transduction in a normal cat. We have demonstrated the efficacy of AAV-AS in the context of Huntington's disease by knocking down huntingtin mRNA 33-50% after a single intravenous injection, which is better than what can be achieved by AAV9 at the particular dose. AAV-B1 additionally transduces muscle, beta cells, pulmonary alveoli and retinal vasculature at high efficiency, and has reduced sensitivity to neutralizing antibodies in human sera. Generation of this vector toolbox represents a major step towards gaining genetic access to the entire CNS, and provides a platform to develop new gene therapies for neurodegenerative disorders.

Table of Contents

List of tables

List of figures

Preface

Part of Chapter I is in submission as a first-author review at *Neuropharmacology*. Xandra O. Breakefield contributed content, and is the corresponding author. Eloise Hudry, Casey A. Maguire, Miguel Sena-Esteves and Paola Grandi are co-authors. Emily Mills illustrated **Figure 1.2**.

Chapters II, III and IV are sections of first-author manuscripts currently under review. Figures were renumbered to include supplementary figures.

For Chapter III, Anne F. Harris, Damien J. Cabral, Allison M. Keeler, Ellen Sapp, Jennifer S. Ferreira, Heather L. Gray-Edwards, Jacob A. Johnson, Aime K. Johnson, Qin Su, Lorelei Stoica, Marian DiFiglia, Neil Aronin, Douglas R. Martin and Guangping Gao were involved in generating experimental data, and are co-authors on the corresponding manuscript.

For Chapter IV, Zachary Fitzpatrick, Anne F. Harris, Stacy A. Maitland, Jennifer S. Ferreira, Yuanfan Zhang, Shan Ma, Rohit B. Sharma, Heather L. Gray-Edwards, Jacob A. Johnson, Aime K. Johnson, Laura C. Alonso, Claudio Punzo, Kathryn R. Wagner, Casey A. Maguire, Robert M. Kotin and Douglas R. Martin were involved in generating experimental data, and are co-authors on the corresponding manuscript.

Miguel Sena-Esteves supervised all research, and is the corresponding author on manuscripts derived from Chapters II, III and IV.

CHAPTER I

Introduction

Viral vectors for gene therapy of neurological disorders

In recent years, gene therapy using viral vectors – encoding a therapeutic gene or inhibitory RNA into a "gutted" viral capsid and supplying it to the nervous system - has emerged as a clinically viable option for therapy of brain disorders largely due to the success and safety of the current generation of virus-based vectors[1]. In general viral vectors have proven more efficient at gene delivery *in vivo* than synthetic nanoparticle and liposome vectors, and in most diseases the goal is to transduce as many affected cells as possible. Within the nervous system, phase 1/2 clinical trials have shown benefit for several neurologic diseases involving replacement of defective genes. This includes: restoration of vision, at least for an extended period, in Leber's congenital amaurosis (LCA) using adeno-associated virus (AAV) vectors[2]; curtailment of further brain neurodegeneration in the brain in metachromatic leukodystrophy (MLD)[3] and adrenoleukodystrophy (ALD)[4] using *ex vivo* genetic modification of hematopoietic stem cells with lentivirus vectors; and safety for oncolytic vectors in clinical trials[5]. Success has also been reported in blocking human immunodeficiency virus (HIV) infection in a single individual using *ex vivo* gene editing of autologous CD4 T cells to disrupt the viral receptor gene *CCR5*[6].

It is hardly surprising that viruses have led the field in gene therapy, as they have evolved to deliver their genes efficiently in the form of RNA or DNA into mammalian cells. In many cases their aim is to replicate in and kill the host cell in the process, as in the case of adenovirus and herpes simplex virus (HSV). In other cases they may be non-pathogenic such as AAV, or may either become latent in the host cell for long periods (e.g. HSV in trigeminal neurons) or

integrate into the host cell genome at different sites as with retrovirus and lentivirus. Viruses have evolved very efficient mechanisms to deliver their genome into cells. In the case of HSV and retrovirus/lentivirus their genome is carried within a proteinaceous capsid surrounded by a lipid membrane envelope. This envelope can efficiently fuse with the plasma membrane of the cell delivering its contents directly into the cytoplasm with subsequent release of nucleic acids from the capsid, and either conversion to DNA (in the case of retro/lentivirus vectors) or delivery of DNA (in the case of HSV) into the cell nucleus. Other viruses, such as AAV and adenovirus, have a proteinaceous capsid that is taken up by endocytosis and have evolved ingenious means to escape the endosome/lysosome compartment to deliver the viral DNA to the nucleus. By “gutting” the virus of its own genes and just retaining the packaging signals, one can package viral vectors in culture using viral genes in *trans* for replication and virus structure and generate an efficient delivery vehicle for the transgene of interest with no viral genes.

As in pharmacology, it is a therapeutic advantage if the cause of the disease (target) is known, as in monogenic hereditary diseases. For these diseases, gene therapy strategies using virus vectors include gene replacement by bringing in a normal copy of a defective gene using AAV vectors that establish themselves as stable “episomes” in the cell nucleus, and lentivirus vectors that integrate transgenes into the genome. Both AAV and lentivirus vectors are capable of infecting dividing and non-dividing cells, but the latter are a better choice for permanent modification of dividing cell populations as genomic integration ensures the progeny generated from the primary target cell is also genetically modified. These same vectors can be used to deliver siRNAs (shRNAs)/miRNAs

that can downregulate a dominant-negative mutant mRNA/protein, sometimes also decreasing copies of the normal mRNA. In the future with CRISPR or other gene editing technology combined with virus vectors, it should be possible to correct gene defects in recessively inherited diseases and to eliminate mutant genes in dominantly inherited diseases in mammalian brain[7]. For diseases of unknown etiology, strategies have evolved to deliver neurotrophic factors, neurotransmitters, compensatory proteins, and selectively toxic proteins into the brain.

Some general principles of intervention are becoming clear. 1) *Treat early.* Excluding prenatal gene therapy, which is not considered ethical at this stage, and given that most neurologic diseases have progressive sequelae, it is best to begin treatment as early as possible. For example, for spinal muscular atrophy (SMA) in which motor neurons are lost leading to death within months for some babies, AAV gene replacement is being tested in babies 2-9 months of age (NCT02122952). In MLD and ALD where gene therapy can arrest neurodegeneration, it is important to treat before extensive damage to the brain has already occurred[3, 4]. 2) *Too much has to be okay*. With the current generation of promoters, the levels of transgene expression cannot be regulated. You have the choice of using strong or weak, constitutive or cell specific promoters, but not of adjusting levels of expression or turning off expression after delivery. 3) *Transgene size is limited*. The two vectors for which we have the most clinical experience, AAV and lentivirus, have a limited transgene cassette capacity (includes regulatory sequences, promoter, cDNA, and polyA sequence, etc.), with a maximum size of about 4-5 kb for AAV and about 8.5 kb for lentivirus. For some hereditary diseases, such as ataxia telangiectasia or neurofibromatosis

type 1 (NF1) with cDNAs of 9.6 kb and 8.4 kb respectively, this presents a difficult hurdle. In the case of dystrophin (11 kb), mutated in Duchenne's muscular dystrophy, a condensed version of the gene (minigene) has been developed which lacks repeat sequences and fits into an AAV[8]. 4) *Pick realistic outcome measures*. It is difficult to monitor benefit if the natural history of the disease is variable and the phenotypic traits are not quantitative and are protracted over time. For example, neurotrophic therapy in Parkinson's disease (PD) may work, but the outcome measures are subjective and the time to measureable clinical improvement may be unrealistically long[9]. Realistic outcome measures include, for example, metabolite levels, lesion size using a variety of imaging methods, and nerve conduction velocity, with improvements occurring in the scale of months. 5) *You only get one shot*. For now, given the immunogenicity of viral vectors, efficient delivery will only occur on the first exposure to the vector. Thus, it is a disservice to the patients to try non-therapeutic doses that may exclude the patient from future doses deemed therapeutic. This is a difficult problem as the increasing dose regime is an inherent part of the evaluation of toxicity in a phase 1 trial.

Which vector – why and when?

A number of different viruses have been explored for gene delivery or cancer oncolytic therapy. The viruses most commonly used in clinical trials include retrovirus vectors, lentivirus vectors, adenovirus vectors, herpes simplex virus type 1 (HSV-1) and AAV vectors.

Retroviral vectors derived from Moloney murine leukemia virus (MoMLV) were the first vectors to be used for FDA-approved clinical trials. While direct *in vivo* administration does not result in a therapeutic outcome[10], pseudotyped retroviral vectors has been used clinically for *ex vivo* correction in human progenitor cells, followed by autologous transplantation[11]. Retrovirus vectors are generally not useful for neurological applications, as they cannot be used for gene transfer to non-dividing cells, such as neurons, although they can be used for lineage determination in embryos[12, 13]. While retroviral vectors have a modestly large packaging capacity (7-9 kb), they are produced at relatively poor titers and require proviral integration into the host genome for expression. The latter aspect is particularly concerning, as a trial for retroviral-mediated *ex vivo* gene therapy in children with X-linked severe combined immune deficiency (SCID) resulted in some patients developing leukemia as a result of activation of the LMO2 proto-oncogene due to proviral integration[14]. However, SCID was cured by the treatment in all cases, and the few patients who developed leukemia were treated and survived[15]. Several features of retrovirus integration, including tendency to integrate into promoter regions of genes combined with intact (long terminal repeat) LTR elements with enhancer activity in these early vectors has led to improvements in vector design[1].

Lentiviral vectors derived from HIV-1 can mediate gene transfer to both dividing and non-dividing cells. Importantly, lentiviral vectors integrate preferentially in introns of transcriptionally active genes, and the use of self-inactivating designs that eliminate the promoter elements from LTRs in the provirus have reduced dramatically the oncogenic potential[16, 17]. Further, they can be pseudotyped with VSV-G (vesicular stomatitis virus G envelope protein) to allow purification to titers higher than MoMLV vectors, and have a similar transgene capacity as retroviral vectors. While lentiviral vectors can mediate long-term expression (years) in the non-human primate brain[18, 19], their infection efficiency after direct injection is low. They have mainly been used for *ex vivo* gene therapy applications. A particularly successful example has been the halt of neurodegeneration in infants and children afflicted with X-linked ALD (X-ALD) and MLD in clinical trials involving transplantation of lentivirally-corrected autologous CD34+ hematopoietic cells[3, 4].

Adenoviral (Ad) vectors have some potential advantages over the abovementioned vectors: first, transgene packaging capacity can be up to 36 kb in high-capacity Ad vectors devoid of viral genes, albeit these “gutless” vectors are difficult to generate at high titers; second, the standard Ad vectors can be manufactured at titers up to 1,000-fold higher than retro- and lentiviral vectors; and third, the transgene does not integrate into the host genome and instead remains episomal, leading to stable and sustained expression in brain for at least up to a year[20]. Direct infusion into brain parenchyma results in gene transfer to a broad range of cell populations, including neurons, astrocytes, microglia, oligodendrocytes and ependymal cells[21, 22]. A major limitation, however, is the strong innate immune response to the Ad capsid itself, as well as continuing low

level expression of viral genes in the standard vectors producing a secondary transgene/viral gene-dependent immune response, even after direct intraparenchymal infusion into the brain[23]. While this antigenicity facilitates their use as an immunogenic adjuvant, *in vivo* delivery at high doses can result in severe inflammation and cytotoxicity, which resulted in the death of a patient in an ornithine transcarbamylase (OTC) deficiency clinical trial[24]. Nevertheless, this continues to be a very popular vector, especially for clinical trials in cancer[25].

Herpes simplex viral (HSV) vectors can efficiently infect neurons and other cell types *in vivo*, and are capable of both anterograde and retrograde transport within neurons[26, 27]. This makes them attractive candidates for neurological gene therapy. HSV vectors can broadly be classified into two main categories: recombinant vectors, which have a packaging capacity of 50 kb, can be purified to high titers (up to 10^{11} particles per mL) and can persist as episomes post-infection; and plasmid-based HSV amplicons, which have a capacity of up to 150 kb, but are difficult to generate and can only be purified at 10^{8} particles per mL[28, 29]. Recombinant HSV vectors, in turn, can be sub-divided into replication-competent and replication-defective vectors depending on whether they can undergo a lytic cycle, and both have found therapeutic use in a broad range of neurological disorders[30].

Adeno-associated virus (AAV) vectors are a relatively recent addition to this list of viral vectors, but have emerged as one of the most important ones for therapy of neurological disorders. It is currently the most frequently used viral vector for central nervous system (CNS) clinical trials (**Table 1.1**). AAV vectors are close to the ideal CNS gene therapy vector as they: a) can mediate gene

Disease	Vector	Transgene	Phase	Trial code
AADC deficiency	AAV	AADC	I, II	NCT01395641
Alzheimer's disease	AAV	NGF	I, II	NCT00087789, NCT00876863
Batten disease	AAV	CLN2	I	NCT00151216
Batten disease	AAV	CLN2	I, II	NCT01414985
Canavan disease	AAV	ASPA	I	Leone et.al., 2012
Giant axonal neuropathy	AAV	GAN	I	NCT02362438
Leber's hereditary optic neuropathy	AAV	MT-ND4	I	NCT02161380
Metachromatic leukodystrophy	AAV	ARSA	I, II	NCT01801709
MPS IIIA (Sanfilippo Disease Type A)	AAV	SGSH, SUMF1	I, II	NCT01474343, NCT02053064
Parkinson's disease	AAV	GAD	I, II	NCT00195143, NCT00643890
Parkinson's disease	AAV	NTRN	I, II	NCT00252850, NCT00400634
Parkinson's disease	AAV	GDNF	I	NCT01621581
Parkinson's disease	AAV	AADC	I, II	NCT02418598
Parkinson's disease	AAV	AADC	I	NCT00229736
Pompe disease	AAV	GAA	I, II	NCT00976352
Pompe disease	AAV	GAA	I	NCT02240407
Spinal muscular atrophy type 1	AAV	SMN	I	NCT02122952

Table 1.1: AAV-mediated clinical trials for neurological disorders. Data obtained from *clinicaltrials.gov*.

transfer to both mitotic and post-mitotic cells, albeit the transgene is lost over time in dividing cells; b) are neurotropic after direct infusion into brain parenchyma[31]; c) can exist stably in an episomal state with a low rate of genomic integration[32]; d) exhibit no pathogenicity or cytotoxicity; e) have very mild immunogenicity, mostly humoral[33]; and f) can be manufactured at high titers (10^{13}-10^{14} particles per mL, depending on the production method) and at high purity[34, 35]. AAV vectors have been shown to mediate stable transgene expression in the human brain for >10 years[36]. However, a significant limitation of AAV vectors is their small packaging capacity (4.5 kb for single stranded vectors, 2.4 kb for self-complementary vectors), which places severe limitations on the therapeutic cargo size. Recently, vexosomes, which are hybrid viral vectors comprising AAV associated with extracellular vesicles, have been shown to enhance considerably the gene transfer properties of AAV[37, 38].

Other viral vectors that infect neurons and thus can potentially be used for CNS gene therapy applications include RNA viruses, such as poliovirus replicon vector[39, 40], Semliki Forest virus (SFV)[41, 42] and Sindbis virus vectors[43], as well as DNA viruses, such as SV40[44, 45].

Modes and sites of delivery

Within the context of delivery to the brain, virus vectors can be injected directly into regions of pathology using strategies that either limit or extend the range of transduction, or through intrathecal (IT), intraventricular, or intravascular routes. Of these, the intravascular route has historically been restrictive due to the blood-brain-barrier (BBB), but new serotypes of AAV, modifications of AAV and hematopoietic stem cell-derived vehicles have now breached this barrier.

Direct injection into brain parenchyma. Most clinical trials to date have investigated the therapeutic efficacy of direct neurosurgical infusion of virus vectors into the brain parenchyma. This approach bypasses the need to cross the BBB and works for well for AAV vectors. Among AAV serotypes, AAV2, the first discovered serotype, was used in all first generation clinical trials as it is highly neurotropic, but its distribution out from the injection site is relatively poor. Newer serotypes of AAV capsids discovered in the intervening years have dramatically improved transduction efficiency and volumetric spread. Different AAV serotypes have different preferential patterns of cell transduction. For example, while AAV1, AAV8 and AAV9 and AAVrh10 are primarily neurotropic[46], AAV4 preferentially infects astrocytes and ependymal cells[47], and AAV5 transduces both astrocytes and neurons[31]. Part of this cell preference is probably due to differential binding of AAV serotypes to cell-surface receptors prior to internalization[48-50]. AAV9 and AAVrh10 are the leading candidates for intraparenchymal infusion, not only because of their vector spread but also because it can be transported along axons at high efficiency[51, 52]. Neurodegenerative disorders are often multifocal, affecting more than a single

structure in the CNS[53]. Therefore, global distribution of viral vectors, which is not limited to the site of injection, is desirable. Intracranial infusion of AAV vectors into axonally connected structures of the brain, such as the ventral tegmental area (VTA) or thalamus allows for widespread distribution of either AAV or encoded gene products that spread to distal projection sites by axonal transport[51, 54, 55]. Use of pressurized convection-enhanced delivery (CED) and magnetic resonance imaging (MRI)-guided infusion can lead to significantly better distribution compared to single injections of smaller volumes[56]. Facilitated access across the BBB with AAV has also been achieved using focused ultrasound and microbubbles[57].

Infusion into cerebrospinal fluid (CSF). In addition to being spatially restricted[58], intraparenchymal infusion is invasive and carries risk of surgery-related side effects. To avoid these complications, an alternate less invasive route is administration into the CSF, where the viral vector can cross directly into the brain. This can be achieved by intracerebroventricular (ICV) or intrathecal (IT) injection of AAV vectors. Infusion into the lateral ventricles (ICV) in adult mice primarily results in transduction of the surrounding ependymal cell layer[31], which can be extended to the brain parenchyma by intravenous co-administration of mannitol to raise osmolarity and thereby open up junctions between ependymal cells. ICV injection of AAV into neonatal mice provides a means of widespread gene delivery of many cell types throughout the brain and spinal cord[59, 60]. On the other hand, IT injection into the CSF, either at the subarachnoid space in the cisterna magna or into the intervertebral cistern in the lumbar spinal cord, is less invasive than ICV delivery and results in robust and widespread transduction of spinal cord motor neurons, as well as dorsal root ganglia (DRG) in mice[61]. In

higher species such as pigs and non-human primates, the spread of gene transfer after IT injection is much wider, with multiple cell populations (including neurons) in the brain and brainstem being transduced at high efficiency[62-64]. However, this route has some limitations. There are contradictory reports as to whether AAV administration via intra-CSF route shields against anti-AAV neutralizing antibodies[64, 65]. There is also some concern that the distribution results arise partly from AAV vector leaking from the subarachnoid CSF space into systemic circulation[66].

Delivery via the vasculature. Systemic administration has the potential to mediate gene transfer to the entire CNS ubiquitously and non-invasively with every cell in the brain being a maximum of 40 microns from endothelial cells[67]. AAV9 was the first AAV serotype to be shown to cross the BBB without pharmacological intervention[68], and remains the gold standard for CNS therapy by intravenous delivery. Other serotypes, such as AAVrh8 and AAVrh10, were subsequently demonstrated to lead to robust and sustained CNS transduction following intravascular administration, transducing both neuronal and non-neuronal cell populations[69, 70]. The mechanism of this BBB circumvention is not yet known. It is possible that such a mechanism might be serotype-specific, as exemplified by the observation that while transient opening of BBB tight junctions by mannitol leads to increased AAV2 CNS gene transfer[71, 72], it does not enhance transport of AAV9 into the brain[73]. There are conflicting reports on the extent of neuronal transduction upon systemic administration in adults, possibly due to variations in dosage and promoter usage[68, 74]. Several concerns for clinical development exist. The first is significant vector loss and concerns of toxicity[75] due to high off target peripheral biodistribution, especially to the liver, which can

be somewhat reduced by restricting blood flow by occlusion[76] or by choosing to express a therapeutic gene under a neuronal promoter. The other major concern is that the presence of neutralizing antibodies to AAV in monkeys and humans can severely limit the extent of gene transfer by systemic infusion[65, 73].

Age at time of infusion. The timing of AAV administration is one of the key factors that determine the extent of CNS transduction and the relative transduction of cell populations in the CNS. In general, transport across the BBB is higher in younger individuals[77]. Irrespective of the injection route, there are multiple reports suggesting that injection of AAV9 at P0 (post-natal day 0) in mice results in widespread neuronal transduction, while administration at older ages results primarily in glial and endothelial cell transduction, both with IV[65, 68, 76] and ICV[78] infusion. The switch away from neuronal transduction at older ages results in loss of therapeutic efficacy of AAV9-based approaches for some neurodegenerative diseases such as SMA where therapy is highly dependent on motor neuron transduction[79].

Therapeutic modalities for neurological diseases

a. Gene replacement or inhibition

Canavan disease (CD) is a pediatric leukodystrophy, characterized by accumulation of N-acetyl aspartate (NAA) in the brain due to mutations in the aspartoacylase (ASPA) gene[80]. CD gene therapy has historical significance, as the disorder represents both the first clinical trials for a neurodegenerative disorder (ICV administration of lipid-encapsulated plasmid DNA (LPD) containing hASPA cDNA[81], and the first AAV-based FDA-approved clinical trial for a brain disorder[82]. This later Phase I/II clinical trial involved intraparenchymal infusion of AAV2-hASPA vector into the brain, and was based on pre-clinical proof-of-principle studies on a transgenic rat model of CD[83]. No toxicity or long-term adverse effects were evident. Importantly, a significant decline in the elevated NAA levels was observed in the brains of all treated patients, albeit only modest neurological improvement was reported[36]. Although anti-capsid neutralizing antibodies could be detected, no correlation to clinical outcome was found. A recent preclinical study with intravenous delivery of AAV9 has shown seemingly complete phenotypic rescue of disease in a CD genetic mouse model[84].

Lysosomal storage disorders (LSDs) include over 50 rare individual genetic disorders resulting in defective metabolism and lysosomal accumulation, which collectively have a frequency of one per 7000-8000 live births[85]. Enzyme replacement therapy is the most common clinical treatment for this group of disorders, but is less effective for the neurological symptoms due to the inability of the enzymes to cross the BBB. LSDs are a good target for gene replacement therapy, as correction of even 5-10% of normal enzyme levels is enough to stop

disease progression, and genetically modified cells can cross-correct neighboring cells through enzyme secretion and uptake by the mannose-6-phosphate receptor pathway[86]. A Phase I/II clinical trial for MLD involving transplantation of autologous hematopoietic stem cells corrected *ex vivo* with a lentiviral vector expressing functional arylsulfatase A (ARSA) enzyme, reported stable ARSA gene replacement, no aberrant clonal cell expansion and no manifestation of disease 7-21 months after the predicted disease onset[3]. Gene therapy for LSDs involving *in vivo* AAV gene replacement have been successful in preclinical models, but less so in clinical trials. Numerous pre-clinical studies with gene replacement by *in vivo* intracranial AAV administration have shown partial to complete phenotypic correction in animal models of several LSDs. These include MPS I[87], MPS IIIA[88], MPS IIIB[89, 90], MPS VII[51], MLD[91, 92], multiple sulfatase deficiency (MSD)[93], Niemann-Pick A disease[94], Pompe disease[95], GM1-gangliosidosis[96], Tay Sachs disease[97] and Sandhoff disease[98].

On the other hand, clinical trials have proved less effective. While intracranial administration of an AAV2-CLN2 vector in late-infantile Batten disease (late-infantile neuronal ceroid lipofuscinosis, LINCL) patients in a Phase I/II clinical trial was found to be safe, there was no significant clinical improvement[99]. Similar results were found in a Phase I/II trial for Sanfilippo syndrome type A (mucopolysaccharidosis IIIA, MPS IIIA), where intracranial administration of AAVrh10-SGSH-SUMF1 vector was well tolerated in the patients, but resulted in only minor improvement in clinical outcomes[100]. Other clinical trials for LINCL (NCT01414985) and MPS IIIA (NCT02053064) based on the above two studies have been initiated. Clinical trials for Pompe disease (NCT02240407, NCT00976352), MLD (NCT01801709), giant axonal neuropathy (GAN)

(NCT02362438) and a proposed trial for MPS IIIB, all based on gene replacement *in vivo* by AAV vectors, are currently being initiated. The modest outcomes in human trials may be related to the doses that have been tested which have yet to reach doses successfully tested in animal models. In addition the choice of delivery routes and target sites/structures which are effective to treat a small mouse brain may not be adequate to achieve widespread distribution of functional enzyme in the ~2,000-fold larger human brain.

X-linked adrenoleukodystrophy (X-ALD) is caused by mutations in the ABCD1 gene, which results in the accumulation of very long-chain fatty acids (VLCFA) in the body. The cerebral form of the disease is fatal. Hematopoietic stem cell transplantation of CD34+ cells corrected *ex vivo* by a lentiviral vector encoding ABCD1 gene into two X-ALD patients with cerebral demyelination resulted in reversal of demyelination and alleviation of associated neurological symptoms in both patients[4]. Further, no clonal cell expansion or preference for oncogenic site of genome integration could be detected, highlighting the safety profile of such a therapy. A recent preclinical study in *Abcd1* knock-out mice showed that *in vivo* delivery of AAV9-ABCD1 could reduce VLCFA levels in the CNS[101].

Spinal muscular atrophy (SMA) is a fatal infantile motor neuron disorder, resulting from loss of the *SMN1* gene. Gene replacement by intravascular AAV9 administration has proved effective in preclinical studies in both mice and non-human primates[79, 102-105]. Based on these studies, a Phase I clinical trial (NCT02122952) with intravenous administration of AAV9-SMN1 has been initiated in babies 2-9 months of age.

Other disorders. Pre-clinical *in vivo AAV* gene therapy studies have been carried out for several other disorders involving both gene replacement in recessive disorders or inactivation of mutant genes in dominant disorders. These include Rett syndrome (delivery of MeCP2[106]), amyotrophic lateral sclerosis (ALS) (shRNA targeting SOD1[107]; delivery of ADAR2[108]; delivery of single chain antibody targeting misfolded SOD1[109]), Huntington's disease (shRNA targeting HTT[110]; artificial miRNA targeting HTT[111, 112]) and Machado-Joseph disease (artificial miRNA targeting ATXN3[113]).

b. Trophic factor support and neurotransmitter modulation

Parkinson's disease and AADC deficiency. Parkinson's disease (PD) is an age-related neurodegenerative disorder that affects about one in every 100 people older than 60 years of age worldwide, and as many as one million people in the United States alone. PD is characterized by the loss of dopaminergic neurons in the substantia nigra with resulting loss of dopamine in the putamen[114]. The current standard of care involves dopamine replacement by administration of levodopa and deep brain stimulation; however, levodopa becomes ineffective in advanced stages of the disease, probably because of the continuing loss of dopaminergic neurons.

Clinical intervention for PD by intraparenchymal delivery of viral vectors can broadly be divided into two strategies: overexpression of enzymes involved in neurotransmitter synthesis; and overexpression of neurotrophic factors that can promote neuron survival. One clinical trial was based on the first approach, where AAV2 encoding glutamic acid decarboxylase (GAD) was injected into the subthalamic nucleus of PD patients to generate the inhibitory transmitter gamma

amino-butyric acid (GABA[115]), which satisfied the Phase I safety criteria. However, a Phase II clinical trial, resulting from the findings of this study, showed only modest efficacy[116]. Infusion of AAV encoding aromatic L-amino acid decarboxylase (AADC), which converts L-dopa to dopamine, into the putamen was also shown to be safely tolerated in two Phase I clinical trials[117, 118]. While long-term stable AADC expression could be detected by PET scanning, the initial clinical improvement deteriorated over 4 years even with continued administration of L-dopa[119]. A new Phase I trial based on combined pressurized CED and MRI-guided infusion into the putamen is currently recruiting participants. A Phase I/II dose escalation study involving infusion of ProSavin, a tricistronic self-inactivating lentiviral vector encoding tyrosine hydroxylase (TH; the first and rate limiting enzyme in dopamine synthesis), AADC and GTP cyclohydrolase I (GCH1; which generates the biopterin cofactor for TH) was found to be well tolerated with no toxicity, and even showed improvement in motor function in combination with L-dopa administration in patients injected at the higher dose[120]. These interventions to alter firing patterns or increase dopamine levels in the brain have to be seen in the context of degeneration of dopaminergic neurons, which continues unabated.

The second approach is based on the expression of neurotrophic growth factors. The prime example is neurturin (NRTN), a natural analog of glia-derived neurotropic factor (GDNF), which has been shown to protect dopaminergic neurons in pre-clinical studies[121-123]. Again, while Phase I clinical trials with CERE-120 AAV2-NRTN vectors showed no adverse effects[124], Phase II efficacy results were modest with no significant improvement in primary outcome measure at 1 year, albeit with some improvement at a later time[125]. Injection into

both putamen and substantia nigra in a Phase IIb clinical trial did not improve this disappointing clinical outcome[126]. A third emerging approach is to decrease levels of alpha-synuclein expression, which accumulates in the brains of PD patients, using an AAV vector encoding a short hairpin (sh) RNA targeting the mRNA for this protein[127], which has yet to be tested in patients.

While AAV2-AADC delivery to the putamen resulted in modest clinical outcomes in PD patients, a similar strategy used in a Phase I study to treat AADC deficiency (a fatal loss-of-function disorder with a high prevalence in Taiwan) showed highly promising results[128]. Treated children that are otherwise unable to move showed improved motor function and increased dopamine in the CSF, with no AAV-associated toxicity. This may have implications for PD therapy, as it could indicate that clinical intervention may become less effective at a later age.

c. Compensatory proteins

Alzheimer's disease (AD) is one of the main causes of dementia in the elderly, affecting 6% of individuals 65 years and older[129]. The vast majority of patients suffer from the sporadic form of the disease, but numerous predisposing genes[130], as well as environmental risk factors, such as traumatic brain injury[131], diabetes[132], stroke and hypertension[133] have been identified over the years. The defining neuropathologic characteristics are accumulation of Aβ peptide, a cleaved product of amyloid precursor protein (APP), in toxic amyloid fibrils forming extracellular plaques, in association with abnormally hyperphosphorylated tau filaments composing intraneuronal neurofibrillary tangles. These hallmarks are associated with elevated levels of inflammatory cytokines, including interleukin1β and TNFα, disregulated calcium homeostasis,

synapse collapse, neuronal dysfunction and death (especially of cholinergic neurons[134]. The multiple etiologies of this disease make it hard to identify a therapeutic target, although the consensus seems to be that decreasing levels of Aβ peptides and/or preventing abnormal tau phosphorylation and aggregation is an important goal.

The devastating consequences of this disease have elicited a broad range of gene therapy strategies[135] with only a recent subset listed below. The most straightforward strategies have aimed at directly inhibiting the production of neurotoxic species of amyloid, either via viral vector expression of Aβ degrading enzymes, such as Neprilysin[136, 137], or anti-Aβ single-chain antibodies to achieve passive immunization[138]. Alternatively, targeting the cleavage of APP has been attempted, with genetic transfer of siRNA specific for β-secretase[139] or shRNA to knock-down the orphan G protein-coupled receptor that regulates activity of γ-secretase[140], the first and second enzymes, respectively, controlling the proteolysis of APP to produce the neurotoxic amyloid peptides, respectively. Additionally, AAV-mediated expression of CD74, a chaperone that directly binds to the APP, also prevents the accumulation of Aβ in the hippocampus and improves cognitive deficits of AD mice[141].

Because of the complexity of the molecular mechanisms underlying AD neuropathological changes and the relatively low success of therapeutic strategies directly based on the “amyloid hypothesis” in clinical trials, other alternative approaches have emerged. Based on genetic risk studies, it was found that individuals who inherit the rare apolipoprotein E (APOE) ε2 allele have a markedly reduced risk of developing AD by about 50%. Expressing this specific

isoform of APOE in the brains of a mouse model of AD after ICV infusion of an AAV4 vector reduced amyloid plaque formation and associated synapse loss[142]. Potentially, viral vectors could also be used to express anti-ApoE antibodies, an alternative immunotherapy approach that has proven effective in AD mouse models[143]. Recently, silencing expression of acylCoA-cholesterol acyltransferase, an important enzyme regulating lipid metabolism, as well as APP processing, using a vector encoding an artificial miRNA was shown to alleviate both amyloid and tau pathology in a transgenic AD mouse model[144]. Finally, hippocampal delivery of an AAV vector encoding cholesterol-24S-hydroxylase, an enzyme that regulates neuronal cholesterol efflux, ameliorated cognitive deficits and spine defects associated with a murine model of tauopathy without impacting Tau hyperphosphorylation[145]. This approach was also shown to reduce dramatically the Aβ burden and neuropathology in the brain of APP23 mice[146].

Other therapeutic approaches to AD gene therapy are more tangential, including AAV delivery of a FK506-binding protein (FKBP1b) that stabilizes Ca++ release from the endoplasmic reticulum in neurons[147] or delivery of growth factors that help neurons survive toxic injury, including delivery of cerebral dopamine neurotrophic factor (CDNF)[148], insulin growth factor[149], brain-derived neurotrophic factor (BDNF)[150] and nerve growth factor (NGF)[151] to the brain using different virus vectors. The latter has proceeded to promising clinical trials.

d. Potential for genome engineering *in vivo*

While lentiviral vectors have been used as the vector of choice for *ex vivo* gene transfer[4], AAV vectors are emerging as the leading delivery vehicle for *in vivo* gene transfer, including for genetic engineering. This is largely due to high

efficiency gene delivery to a large number of tissues including brain, excellent long-term safety profile in clinical trials[152, 153], and low rates (~0.1%) of random chromosomal integration[32]. This last point may be somewhat controversial, as there may be some concerns of integration 'hotspots', particularly in unstable[154, 155] and transcriptionally active regions of the genome[156]. Most studies on AAV mediated genome editing have been based on homologous recombination (HR) between AAV-encoded transgenes and a specific chromosomal locus[157]. The transgene typically contains genomic sequences flanking the locus, allowing site-specific insertion via the canonical HR pathway. While the majority of the work using this method has been done *in vitro* to create modified cell lines[158, 159], there have been several *in vivo* studies. These include correction of β glucuronidase for mucopolysaccharidosis VII[160], fumarylacetoacetate hydrolase (Fah) for hereditary tyrosinemia[161], and factor IX (FIX) for hemophilia B[162]. The FIX study used a promoter-less editing strategy, relying on insertion of the transgene into the transcriptional unit of the albumin locus, which increases the safety of this approach[162]. However, the frequency of gene correction observed in these studies was extremely low (fraction of corrected cells ranging from 10^{-4} to 10^{-2}). This frequency may be too low for clinical applications outside the liver, particularly in the CNS.

The field of genome engineering has been revolutionized by the discovery of targeted nucleases. These include zinc-finger nucleases (ZFNs), TALENS, and most recently CRISPR-Cas9[163]. These methods allow creation of site-specific double strand breaks in the genome, allowing for either disruption of gene function, or gene correction by homology repair at those sites using a normal oligonucleotide spanning the mutation. Therapeutic benefit from AAV-mediated *in*

vivo genome editing has been demonstrated in both neonatal[164] and adult[165] mouse models of hemophilia B, as well as in a mouse model of Huntington's disease[166]. Genome editing by CRISPR-Cas9 represents the most recent advance in this field, and this technology has found use in many fields including generation of mouse models of human disease, cancer biology, drug development, *etc*[167]. AAV-mediated genome editing using CRISPR-Cas9 has been shown to be effective in liver[168] and more crucially in the context of neurological disorders, in brain[7]. Co-injection of two AAV vectors encoding SpCas9 and sgRNAs targeting the *Mecp2* gene (mutated in Rett syndrome) into the visual cortex of mice resulted in effective gene editing at this locus and a resulting electrophysiological response[7]. Limitations of such therapy include the relatively large size of SpCas9 relative to the transgene capacity of AAV (hence the need for two vectors), the potential antigenic nature of this bacterial protein, and off-target effects in the genome that might accumulate with long-term expression of these transgenes. The first can be resolved by using shorter Cas9 from other bacterial species[168]. Non-Cas9 CRISPR effectors are also being developed[169]. Overall, this is a very promising field that is likely to foster the next generation of CNS gene therapy.

The AAV capsid

AAV is a parvovirus of the genus *Dependovirus*, classified thus because AAV depends on co-infection of an unrelated helper virus (adenovirus or herpesvirus) for productive infection. The AAV virion consists of a non-enveloped icosahedral capsid and an encapsidated 4.7-kilobase (kB) single-stranded DNA viral genome[170]. For wild-type AAV (wtAAV), this genome comprises of two open reading frames (ORFs), *rep* and *cap*, flanked by two inverted terminal repeats (ITRs)[171] (**Figure 1.1**). The *rep* ORF encodes four overlapping proteins: Rep78, Rep68, Rep52 and Rep40, which play crucial roles in AAV replication and packaging. DNA replication depends on the two larger proteins (Rep78 and Rep68), which have single-strand endonuclease, DNA helicase and ATPase activity, while the two smaller proteins (Rep52 and Rep40) are required for AAV packaging and only have helicase activity. Expression of these four proteins is initiated from the p5 and p19 promoters. The p40 promoter, present on the *rep* ORF, initiates transcription of two alternatively spliced mRNAs from the *cap* ORF that encode three capsid viral proteins (VPs): VP1, VP2 and VP3, and an assembly activating protein (AAP). The larger of these mRNAs encodes for VP1 and comprises the entire *cap* ORF, while the other mRNA is smaller and encodes for VP2 and AAP from weak non-canonical start codons (ACG and CTG, respectively), and VP3 from a conventional downstream ATG start codon. The capsid proteins VP1 (87 kDa), VP2 (73 kDa) and VP3 (61 kDa) assemble in a ratio of ~1:1:10 to yield the AAV capsid with a diameter of ~20 nm. The 145-bp ITRs form stable T-shaped hairpin structures at either end of the genome and function as start sites of DNA replication and play a key role in viral genome integration.

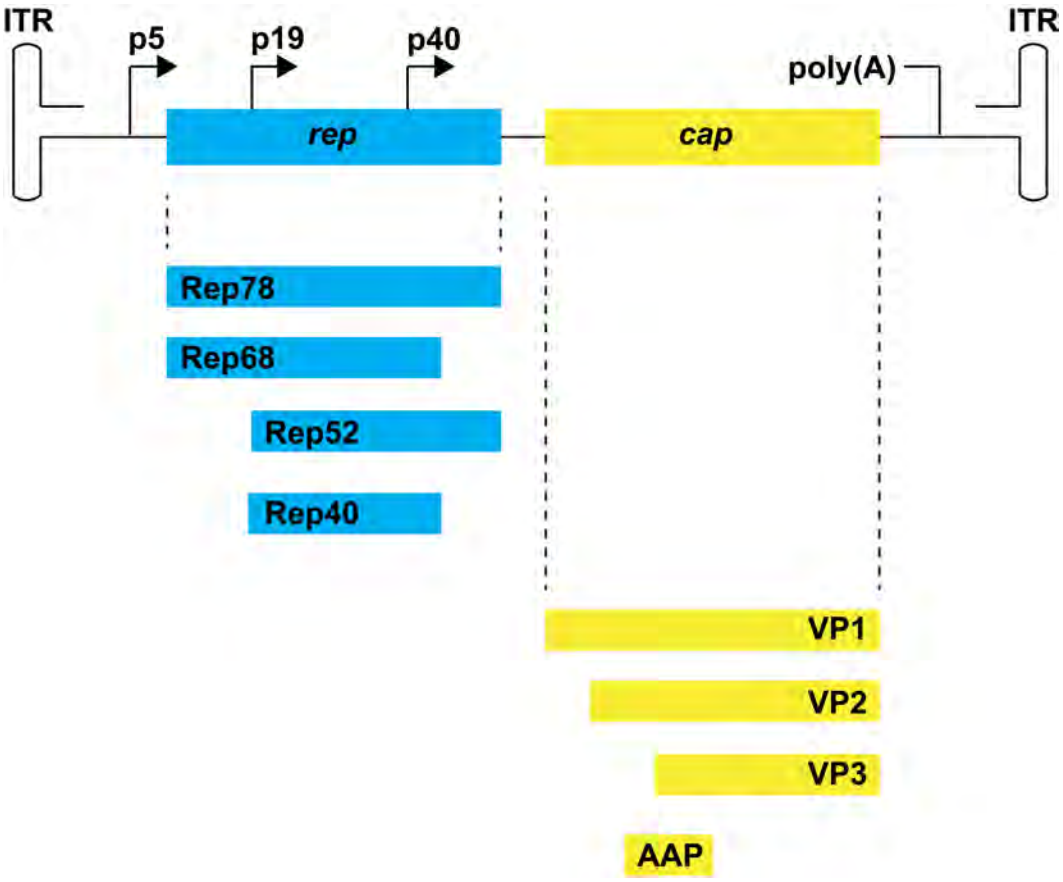

Figure 1.1: Map of wild type AAV genome. The ~4.7 kB genome contains two ORFs, *rep* and *cap*. The *rep* ORF (blue) codes for four Rep proteins: Rep78, Rep68, Rep52 and Rep40. These play crucial roles in AAV DNA replication and packaging. The *cap* ORF (yellow) codes for three capsid proteins: VP1, VP2 and VP3. These assemble in ~1:1:10 ratio to form the AAV capsid. The VP3 protein forms the capsid shell, while VP1 and VP2 are thought to be in the interior of the capsid. In addition, the *cap* ORF also codes for assembly activating protein (AAP) that promotes assembly and maturation of the capsid, but is not present in the capsid. The *rep* and *cap* ORFs are flanked by inverted terminal repeats (ITRs) that are start sites of replication and also play a role in integration into host genome.

The ITRs are the only necessary *cis* elements in the viral genome. Recombinant AAVs (also commonly known as AAV vectors or rAAV) used for gene delivery approaches are generated by replacing the viral genes with a transgene cassette while retaining the ITRs *in cis*. *Rep* and *cap* genes are supplied *in trans* during vector production, along with adenoviral helper genes. Properties of such resulting vectors have been listed in previous sections.

AAV capsid structure

Discovered 50 years ago as a contaminant in adenoviral stocks[172, 173], 12 distinct AAV serotypes (AAV1 – 12) have been identified from human and non-human primate (NHP) to date[174-178]. Based on serologic cross-reactivity and amino acid sequence, these can be broadly divided into 8 clades[174]: A-F and isolates AAV4 and AAV5 (on account of the divergence of these two serotypes from the others), with the clades sharing varying levels of sequence homology (60-99%) with each other. Numerous variants within each clade have been isolated. Elucidation of crystal structures of representative members of all the antigenic clades (AAV1[179], AAV2[180], AAV3B[181], AAV4[182], AAV5[183], AAV6[184], AAV7[185], AAV8[186], AAV9[187]) as well as of AAVrh8[188] (not part of the major clades) and the modified capsids AAVrh32.33[189] and AAV-DJ[190], has helped correlate some of the structural elements with associated capsid functions.

The VP monomers assemble in the host nucleus to form the T=1 icosahedral capsid with two-, three- and five-fold axes of symmetry[191]. These symmetry interactions create characteristic topological features on the assembled AAV capsid: depressions at the two-fold axes, protrusions and depressions at the three-fold axes, and channels at the five-fold axes. The AAV capsid is comprised

of 8 highly conserved β-sheets (βB-βI), arranged as a "jelly-roll" β-barrel and form the contiguous shell of the capsid, and a highly conserved α-helix (αA). Conversely, surface exposed loops (located between the β-strands) differ in their amino acid composition across serotypes. These loops form most of the outer surface of the capsid, and play critical roles in transduction, receptor binding and antigenic response. Nine such clustered loops (VR-I to –IX; variable region) exist, and most serotypes differ in one or more of these loops. However, it is difficult to predict the properties of any particular serotype by the surface topology alone.

The published structures, for AAV or any parvovirus, are determined only for the overlapping C-terminus sequence, *i.e.* VP3. The N-terminal sequences (unique VP1 N-terminus, *i.e.* VP1u, and VP2 N-terminus) are thought to be "disordered"[180] and experimental evidence suggests they are located in the interior of the capsid (according to cryo-EM studies of empty capsids)[192]. The cause of this "disorder" is not clear so far. The requirement of VP1 and VP2 for capsid formation is controversial, with conflicting reports on whether VP3 alone is sufficient for capsid assembly[193-197]. It is generally agreed that the nuclear localization signal[195] and AAP[198], both located upstream of VP3 ORF, are required along with VP3 for successful formation of virus-like particles (VLPs).

Role of capsid in AAV life cycle

The role of the capsid is not only limited to protecting the encapsidated genome/transgene, but includes mediating such essential functions as host cell recognition and receptor binding, endosomal entry and trafficking, and nuclear entry (**Figure 1.2**). Information for receptor recognition is available for several

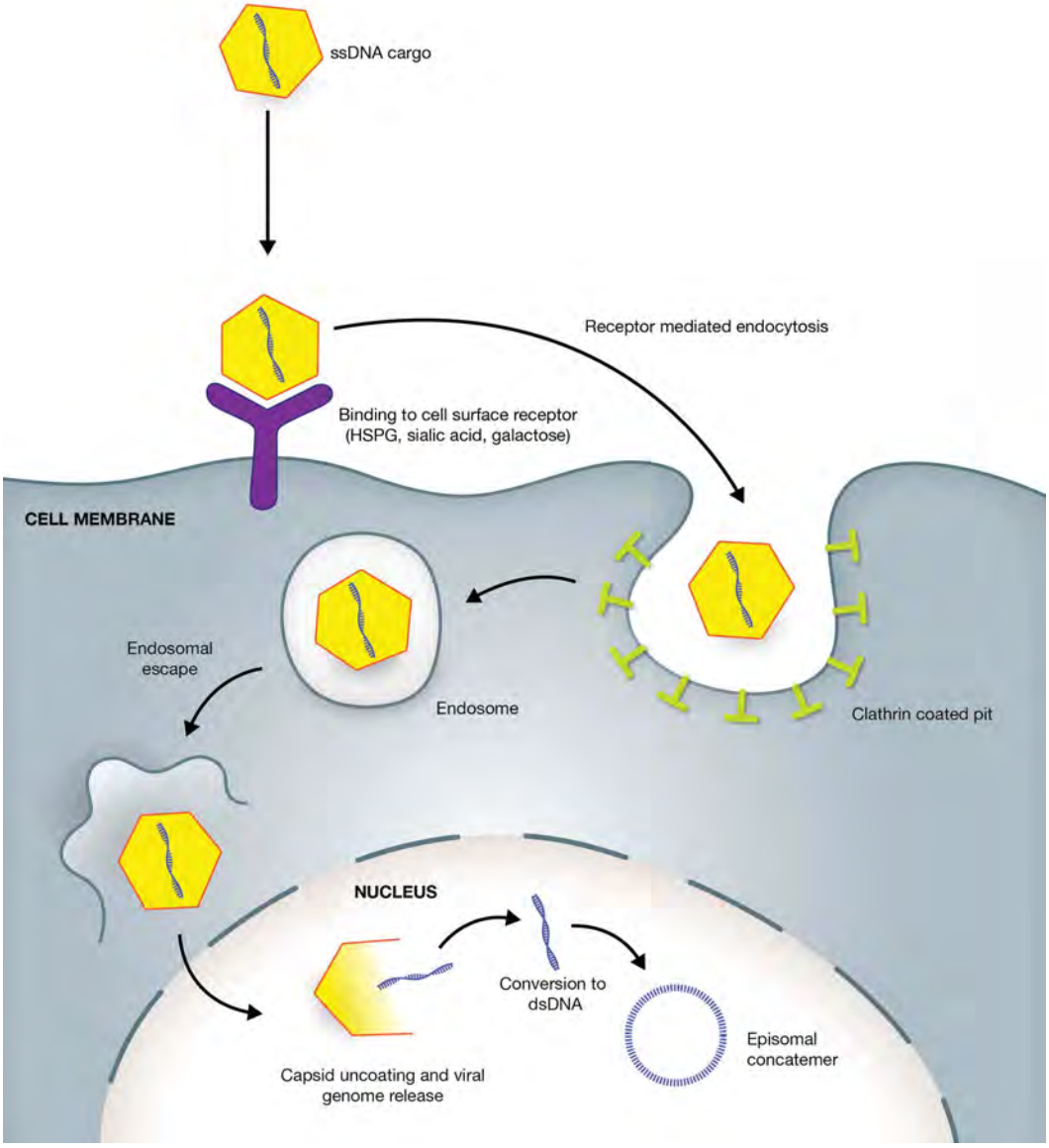

Figure 1.2: AAV vector entry into cells. Receptor footprints on the surface of AAV capsids vary with serotype, which allows them to bind to a variety of glycan receptors on the host cell surface (HSPG, N- and O-linked sialic acids, galactose). Once bound, the virion gets internalized via clathrin-coated vesicles and trafficked to the nuclear area while encapsulated in an endosome. Endosomal acidification leads to release of the virion, which is transported into the nucleus. Capsid uncoating in the nucleus is followed by conversion of the single-stranded vector genome to double-stranded DNA. In case of AAV vectors, the double-stranded vector genome persists as stable circular and concatemeric extrachromosomal episomes.

serotypes; however, much of the data on subsequent steps has only been elucidated for AAV2, the most studied AAV serotype.

Binding to cell surface receptors: After multiple cell surface contact events[199], the essential first step of the AAV infection cycle is attachment to a host cell surface receptor. These glycan receptors vary with serotype[48, 200-205], and choice of receptor is the primary determinant of cell transduction properties for a particular serotype. Subsequent interaction of the AAV capsid with co-receptors stabilizes the low-affinity binding to the primary receptor. AAV clades can be re-organized into 3 major groups, according to their primary receptor preference: those binding to (a) heparan sulfate proteoglycan (HSPG): AAV2[201], AAV3[202] and AAV6[206]; (b) sialic acid: AAV1[200], AAV4[48], AAV5[48, 203] and AAV6[200]; and (the most recently discovered) (c) galactose: AAV9[50, 205]. Primary glycan receptors for AAV7 and AAV8 are not yet known. While most clades show a clear preference for one or the other of these 3 receptors, AAV6 can bind to either HSPG or N-linked sialic acid. A list of primary receptors and co-receptors for each serotype is provided in **Table 1.2**. It is important to note that irrespective of serotype, receptor-binding sites map near the protrusions surrounding the icosahedral three-fold axes of symmetry[48, 180, 204, 207]. This region of the capsid is therefore the primary structural determinant of receptor recognition, possibly providing the first indication of how AAV structure has evolved to generate phenotypic variability across clades.

Internalization: Binding to the primary receptor induces a structural rearrangement of the capsid, required for subsequent internalization[208]. The process of internalization is dependent on the co-receptors. Growth factor

Serotype	Clade	Origin	Primary glycan receptor	Co-receptors	PDB ID of crystal structure
AAV1	A	NHP	α2-3/α2-6 N linked SA		3NG9
AAV2	B	Human	HSPG	hFGFR1, hHGFR, α5β1- and αVβ5-integrins, 37/67 kDa LamR	ILP3
AAV3	C	NHP	HSPG	hFGFR, hHGFR, 37/67 kDa LamR	3KIC (AAV3B)
AAV4	AAV4 clonal isolate	NHP	α2-3 O linked SA		2G8G
AAV5	AAV5 clonal isolate	Human	α2-3 N linked SA	PDGFR	3NTT
AAV6	A	Human	HSPG, α2-3/α2-6 N linked SA	EGFR	3OAH
AAV7	D	NHP			
AAV8	E	NHP		37/67 kDa LamR	2QA0
AAV9	F	Human	Galactose	37/67 kDa LamR, αV-integrins	3UX1
AAV10	E	NHP			
AAV11	AAV4 clonal isolate	NHP			
AAV12	AAV4 clonal isolate?	NHP			

Table 1.2: AAV serotypes and their receptors/co-receptors. Data on Protein Data Bank (PDB) IDs obtained from *rcsb.org*. Abbreviations: EGFR, epidermal growth factor receptor; hFGFR, human fibroblast growth factor receptor; hHGFR, human hepatocyte growth factor receptor; HSPG; heparan sulfate proteoglycan; LamR, laminin receptor; NHP, non-human primate; PDGFR, platelet-derived growth factor receptor; SA, sialic acid.

receptors[209-211] and laminin receptor[212] are thought to facilitate capsid structural rearrangement and increase the affinity of the capsid to the host cell. Integrins[208, 213, 214] likely induce cytoskeletal rearrangements in the host cell and thus play a role in endocytosis of the virion. AAV2 is internalized by either dynamin-dependent clathrin-coated pit pathway[215, 216], and/or by a recently elucidated clathrin- and dynamin-independent CLIC/GEEC pathway[217]. Other AAVs may use different internalization pathways[218]. Motifs on the AAV2 capsid surface that interact with the co-receptors have been identified[208, 213], and are again localized near the base of the three-fold protrusions, but are only partially surface-exposed.

Endosomal trafficking and release: AAV2 appears to localize in both late (Rab7) and recycling (Rab11) endosomes, although trafficking via the Rab11 pathway leads to higher AAV transduction[219]. Endosomal acidification triggers conformational changes in the viral capsid (possibly by selective cleavage of capsid proteins by acid-dependent endosomal proteases)[216]. This causes the phospholipase A2 (PLA2) domain located in VP1u to become surface-exposed[192], likely through the five-fold channel, which leads to escape of the virion from the endosomal compartment through an unknown mechanism.

Cytoplasmic processing: After the virion is released from the endosomal compartment, further processing in the cytoplasm occurs prior to nuclear entry. This includes the capsid being phosphorylated and then ubiquitinated, tagging the capsid for proteasomal degradation[220-222]. Mutation of capsid surface tyrosines, thought to be sites of phosphorylation, decreases proteasomal degradation and in turn, enhances transduction[220, 221].

Movement through cytoplasm and across nuclear membrane: The AAV virion moves through the cytoplasm to the perinuclear region along a microtubule network[223, 224], although this may not be the only mechanism of motility as free diffusion in the cytoplasm has also been reported[199]. The mechanism of transport across the nuclear membrane is even less understood, although putative nuclear localization signals in the VP1/VP2 N-termini are accessible on the capsid surface at this stage and are thought to play a role in nuclear transport activity[216, 225]. Whether the transport occurs through the nuclear pore complex, or through an unidentified pathway involving perforation of the nuclear membrane is unclear[226-228].

Capsid uncoating and genome release: It is generally agreed that capsid uncoating occurs in the nucleus[214, 216, 226, 229] allowing for release of the ssDNA viral genome, although some contradictory evidence suggests that it could occur in the perinuclear region prior to nuclear entry[215]. While the mechanism of this uncoating process is unknown, a putative CDK2/cyclin A kinase binding motif in the VP1/VP2 N-termini has been implicated[230].

Subsequent steps: Once released, the ssDNA viral genome converts to the double stranded (ds) form. In the absence of helper virus, *rep*-containing wild type AAV enters a latent cycle by integrating into the host genome preferentially at the AAVS1 locus on chromosome 19 in human[231, 232]. This process involves the Rep proteins binding both the viral genome at the ITRs and a homologous sequence at the AAVS1 locus[233-235]. Infection by helper virus can “rescue” this integrated genome to package progeny AAV particles, by inducing replication and gene expression of the viral proteins. The AAV capsid is not known to play a

role in the steps post genome release and prior to capsid assembly and genome encapsidation.

Re-engineering the AAV capsid

AAV is close to the ideal gene therapy vector, due to their ability to mediate long-term gene expression *in vivo*, and their excellent safety profile in several clinical trials[152, 153, 236]. However, specific applications require improved versions of the AAV capsids isolated from human and NHP samples. Properties of capsids derived from natural AAV isolates have been altered to improve their biological properties, such as tropism and transduction efficiency, to re-direct to non-natural receptors, or to shield from host immune responses. Re-engineering of the discrete surface-exposed variable loops (and other regions, in some cases) has been achieved by several techniques to yield novel AAV capsids. These techniques can be broadly divided into 5 major classes: 1) ***genetic grafting of peptides*** onto the capsid surface to re-direct tropism, 2) generating ***hybrid or chimeric capsids*** derived from *cap* genes of two serotypes, in order to combine properties of both into a single vector, 3) ***rational mutagenesis*** of a natural AAV isolate, based on structural information of the capsid, 4) ***chemical or non-genetic conjugation*** of receptor-binding or masking moieties directly onto the surface of a fully assembled virion, and 5) ***biopanning*** from a library of chimeric AAV capsids to isolate a unique variant with a desired phenotype. Some select re-engineered capsids and their properties have been tabulated in **Table 1.3**.

Genetic grafting of peptides

A natural AAV capsid can be re-targeted by (ideally) eliminating the interaction with its native receptor and grafting a peptide onto the capsid surface that can re-direct the capsid to bind to an alternate receptor. The earliest approaches tried to identify suitable sites on the AAV capsid for peptide insertion. Sites were chosen

Modified capsid	Method of modification	Target
AAV-PFG[237]	Peptide insertion	Disease-altered brain vascular endothelium
DARPin-inserted AAV2s[238, 239]	Peptide insertion	Target based on receptor (tumor cells, lymphocytes)
AAVrh32.33[240]	Rational hybrid	Lower seroprevalence in human population[241, 242]
AAV2i8[243]	Rational hybrid	Muscle, detargeted from liver
AAV2.5[244]	Rational hybrid	Muscle, used in Phase I clinical trial
AAV Y/F and T/V mutants[221]	Rational mutagenesis	Ubiquitous, enhanced transduction
AAV9.45, AAV9.61[245]	Rational mutagenesis	Detargeted from liver
AAV-DJ[246]	*In vitro* biopanning	Liver, resistant to Nabs
AAV-M41[247]	*In vivo* biopanning	Cardiac muscle
AAV-7m8[248]	*In vivo* biopanning	Photoreceptors (from the vitreous)
AAV-LK03[249]	*In vivo* biopanning	Human hepatocytes
Anc80[250]	*In silico* reconstruction	Broad (muscle, liver, retina)

Table 1.3: Select re-engineered capsids.

where insertion does not drastically decrease capsid assembly and vector packaging yield, while ensuring that the inserted peptide be presented on the surface of the capsid to be able to demonstrate biological activity. Scanning mutagenesis across the AAV2 *cap* gene has yielded several such promising sites[197, 225]. Two positions that have been primarily used are 1) at amino acid positions 138 and 139 (in the VP1/VP2 N-terminus)[196, 225, 238, 239, 251, 252], and 2) at positions 587 and 588 (in the common VP3 C-terminus)[237, 253-263]. Insertions at the first locus are expressed fused only to the VP1 and VP2 capsid proteins[196], and thus have a low copy number in the virion, compared to insertions at the latter locus, which is expressed in every monomer. While the VP1/VP2 N-terminus is conventionally thought to be expressed in the interior of the capsid[192] and thus is not surface-exposed, there is evidence that genetic insertion at that locus allows for exposure of the exogenous peptide on the capsid surface[196, 238, 239], perhaps mimicking the escape of VP1/VP2 N-terminus and exposure of PLA2 domain during endosomal escape. However, depending on the peptide size, insertions at this location marginally[251] or drastically[196] reduces VP3 expression. While providing VP3 *in trans* restores capsid assembly, vector yields and infectivity can remain lower than the unmodified capsid[196]. In addition, the modified capsid still retains its natural tropism, which can lead to significant off-targeting *in vivo*. This appears to be (at least) in part due to the presence of capsids containing only VP1 and VP3, and thus on-target specificity can be improved by selecting capsids that incorporate VP2[239]. Insertion at the 587/588 site, on the other hand, can directly interfere with AAV2 binding to HSPG[264], thus ablating natural tropism in some insertion vectors[253, 255-257] and increasing likelihood of being re-directed to the desired non-HSPG receptor. The peptides screened thus far primarily at these two loci have not only been those with known

receptor binding properties, but also those identified through biopanning of peptide libraries and thus with unknown host receptors[237, 263]. Peptides are not required to be short, and can be as large as full-length proteins[196, 265], depending on the site of insertion. Several re-targeted novel capsids have been generated by this technique, including those with increased *in vivo* gene transfer to vascular tissue[260, 262], disease-altered brain vascular endothelia[237], lung[266, 267], skeletal[268, 269] and cardiac[270] muscle, lymphocytes[239], retina (by intravitreal injection)[248] and several types of implanted tumor cells[238, 239, 254, 267].

Hybrid/chimeric capsids

Initial efforts were directed at producing mosaic capsids, which could (in theory) combine the phenotypic properties of different serotypes. Mosaic capsids containing VP monomers from two or more different serotypes in a single virion are generated by co-transfecting *cap* genes of the serotypes during viral production. Examples of successful mosaic capsids include an AAV1/2 hybrid that combined the HSPG mediated gene transfer to liver of AAV2 with the muscle tropism of AAV1[271], and an AAV3/5 hybrid that can bind both HSPG (like AAV3) and mucin (like AAV5)[272]. Deeper understanding of capsid structure-function relationship and in particular, knowledge of receptor “footprints” of particular serotypes has allowed for more precise attempts at producing hybrid capsids. Prominent examples are AAV2i8[243], an AAV2/8 hybrid created by replacing six amino acids on AAV2 capsid responsible for HSPG binding with corresponding AAV8 residues; and AAV2.5[244], an AAV2/1 hybrid created by replacing five amino acids on AAV2 capsid with corresponding AAV1 amino acid residues responsible for skeletal muscle tropism. The former displayed improved muscle tropism combined with reduced hepatic tropism, while the latter demonstrated

enhanced muscle transduction while preserving HSPG binding, and was used in a Phase I clinical trial for Duchenne muscular dystrophy. Rational grafting of galactose-binding footprint of AAV9 generated AAV2G9, an AAV2/9 hybrid with dual binding capacity to galactose and heparin receptors, and AAV2i8G9, an AAV2i8/9 hybrid with muscle gene transfer efficiency comparable to AAV9 while retaining the reduced liver tropism of AAV2i8[273]. Other examples include AAV2/1 hybrid with reduced sensitivity to AAV2-specific neutralization[274], AAV1/6 hybrids[206] and even an AAV2/canine parvovirus hybrid[275].

Rational (structure-guided) mutagenesis

Improved understanding of AAV structure has allowed for not only precise hybrid capsid engineering, but also mutation or substitutions of specific amino acids responsible for a certain vector function. Several liver de-targeted (such as AAV9.45) and liver- and muscle-detargeted mutants (such as AAV9.47) have been generated by mutagenesis of AAV9 along the surface-exposed three-fold axes[245]. AAV6.2, a single amino acid mutant of AAV6, displayed superior gene transfer to airway epithelium[240, 276]. Identification of antibody recognition motifs on the capsid surface has led to development of AAV2 mutants with a reduced neutralization profile while retaining other properties[277, 278]. A prime example of structure-guided mutagenesis is the generation of AAV2-based capsids where surface-exposed tyrosines, serines and threonines are mutated[221]. As mentioned in an earlier section, these residues on the capsid surface are thought to act as sites of phosphorylation during cytoplasmic processing following cell entry, leading to ubiquitination and subsequent proteosomal degradation of capsid[220-222]. Tyrosine, serine or threonine mutants display enhanced transduction efficiency of

various cell populations *in vivo* in mice[221, 279-283] and dogs[284, 285], although whether this effect extends to other serotypes such as AAV8 and AAV9 is controversial[286].

Chemical conjugation

Coating the AAV capsid surface can physically prevent the virion from interacting with its native receptors and can also shield it from neutralizing antibodies. This can be achieved by chemical conjugation of the capsid to various polymers such as polyethylene glycol (PEG)[287] and poly-[N-(2-hydroxypropyl) methacrylamide] (HPMA)[288], and selective masking of surface-exposed arginine residues by glycation using α-carbonyl compounds[289]. Conjugation of bioactive molecules such as antibodies specific to $\alpha_{IIb}\beta_3$ integrin[290], or EGF[291] can further enhance transduction to target cells overexpressing the respective receptors. However, this approach to capsid engineering has had scant success *in vivo*.

Library biopanning

While most of the above approaches demand at least partial understanding of the transduction process, biopanning does not require any such prior mechanistic insight. This high throughput approach instead applies a screening process to enrich for capsids with a particular biological property from an initial pool. This process therefore, imitates natural evolution with the exception that all genomic variants are present simultaneously in the starting pool, which allows for scanning through a large pool of capsid variants in one (library selection) or a few (directed evolution) cycles, rather than the geologic timescales of natural evolution. For directed evolution, after each cycle, the selected variants are rescued (either by helper virus infection or PCR amplification), diversified further

by additional mutagenesis, and used as the starting material for the next cycle of selection. Starting libraries can be created by subjecting natural AAV isolates to one of two processes: 1) error-prone PCR[292, 293] which introduces nucleotide substitutions across the *cap* of a particular serotype, or 2) DNA shuffling[246, 294, 295], where *cap* genes of several serotypes are fragmented by nuclease digestion and randomly re-assembled by PCR to produce chimeric genomes. Care must be taken to ensure capsid-genome correlation during encapsidation of the chimeric genomes, although a recent study has suggested that production of the virus-like AAV libraries naturally result in very low cross-packaging[296]. Directed evolution has been particularly successful *in vitro*, yielding capsid variants capable of selective and enhanced transduction of a variety of cell types[297-300], with the particular examples of adult and pluripotent stem cells[301-303] which are typically refractory to AAV transduction. Several variants capable of evading neutralizing antibodies present in the human sera have also been isolated by this technique[246, 292-295, 304]. This is particularly relevant in the clinical setting where a majority of the human population has a high prevalence of neutralizing antibodies to natural AAV isolates[242, 305], thus posing a critical challenge for intrahepatic and intravenous AAV administration[306, 307]. Success *in vivo* has been comparatively limited, with only a few studies succeeding in selecting novel capsid variants capable of targeting cardiomyocytes[247], transducing Müller cells in the retina through intravitreal injection[308], crossing the seizure-compromised blood-brain barrier[309], transducing photoreceptors from the vitreous humor[248], or targeting xenotransplanted human hepatocytes[249]. Next generation sequencing has allowed the simultaneous characterization of hundreds of capsids variants, providing insight into several capsid functions[310, 311].

In addition to the above techniques, a novel approach to identify putative ancestral AAVs by *in silico* reconstruction has yielded vectors with broad *in vivo* gene transfer properties[250, 312].

Concluding remarks

The first generation of AAV gene therapy for neurological diseases is based on intracranial injections into target structures and has proven effective in numerous mouse and large animal models of neurodegenerative diseases[313, 314]. The efficacy of intraparenchymal infusion of AAV vectors for CNS gene therapy has improved through the identification of new AAV capsids with better transduction and distribution properties[315-317], as well as the use of convection-enhanced delivery techniques[56] and magnetic resonance imaging (MRI)-guided infusion[318]. Several clinical trials have been conducted or are currently underway to test intracranial injection of AAV vectors for different neurodegenerative diseases[36, 99, 100, 118, 128, 319].

There is an increasing recognition that many neurodegenerative diseases affect more than a single structure in the CNS and dominant phenotypic manifestations driven by a particular structure may be a reflection of different kinetics of disease progression across neuronal populations. Therapeutic efficacy in these disorders will therefore depend heavily on efficiently targeting all structures involved in disease pathophysiology. Huntington's disease (HD) is an example of an evolving perspective on target structures for therapeutic intervention. A recent study using transgenic HD mice showed that combined deletion of mutant huntingtin (Htt) in cortical and striatal neurons is necessary to ameliorate all behavioral deficits and neurodegeneration, while deletion in each population individually resulted only in partial effects[53]. The implication is that transformative clinical outcomes in a disease like HD may only be achieved when therapeutic interventions are effective across multiple brain structures. The same case could

be made for numerous other neurodegenerative diseases with diverse neuropathological features. Achieving global gene transfer to the CNS using intraparenchymal injections is a daunting, perhaps impossible task, especially considering the complex geometry and volume of the cortices. Transport of AAV vectors from the injection site to axonally connected structures can expand the therapeutic reach of local interventions[51, 320-322], but massive doses may be needed to achieve significant transduction and coverage in distal structures.

The discovery that AAV9 can cross the blood-brain barrier (BBB) after intravascular delivery in neonatal and adult animals was a critical step for AAV-based CNS gene therapy[68]. Other AAV capsids such as AAVrh8 and AAVrh10 were subsequently shown to share this property[69, 323]. Several studies have demonstrated the therapeutic efficacy of intravenously delivered AAV9 vectors in animal models of spinal cord motor neuron degeneration[79, 107] and neurometabolic disorders[84, 88, 90]. However, while intravascular infusion of AAV9 is efficient for gene delivery to spinal cord motor neurons[68, 69], dorsal root ganglia[324] and enteric nervous system neurons[325, 326], the vast majority of transduced cells in the brain are either glia or endothelial cells with sparse neuronal transduction[68, 70]. The tropism of AAV9 to spinal cord motor neurons, which is consistent across species[68, 76, 324], contributed to the phenotypic rescue of spinal muscular atrophy mice treated at post-natal day 2 (PND2) by systemic infusion of an AAV9 vector encoding survival motor neuron (SMN) protein[79]. However the effectiveness of AAV9-SMN treatment declined rapidly with age and infusion at PND5 showed only a modest survival benefit and no effect by PND10[79]. The reduced therapeutic benefit with age correlated with declining transduction of spinal cord motor neurons at older ages when most transduced

cells were glia[79]. While systemic delivery of AAV9 vectors has proven exceptionally efficient in mouse models of Canavan disease treated as late as PND20[84] and in adult models of lysosomal storage diseases[88, 90], therapeutic efficacy in these diseases is likely less dependent on neuronal transduction. In Canavan disease, it is possible that any transduced cell overexpressing aspartoacylase may function as a metabolic sink for NAA[84]. In lysosomal storage disorders, there is a cross correction mechanism in which AAV transduced cells secrete large quantities of functional enzyme that is taken up and correctly targeted to the lysosomes of enzyme deficient cells. Therefore, disperse NAA metabolic sinks or sources of functional lysosomal enzymes throughout the CNS, regardless of phenotype, are likely to exert a powerful therapeutic effect. Most neurological diseases however are unlikely to benefit from such mechanisms and will require efficient neuronal gene transfer to change the course of disease progression. There is therefore a clear need for AAV capsids with improved neuronal transduction properties to develop the next generation of gene therapies for multi-focal neurodegenerative diseases. Here we have developed a toolbox of AAV capsids with novel or enhanced properties through peptide display on capsids of natural and re-engineered AAV isolates (**Chapter 3**) and biopanning of shuffled AAV capsid library (**Chapter 4**).

CHAPTER II

Materials and Methods

Generation of packaging constructs

AAV9.47 *trans* packaging plasmid was generated by replacing a portion of the AAV9 cap sequence in packaging plasmid pAR-9 with a *de*-novo synthesized fragment carrying the following mutations S414N, G453D, K557E and T582I described in the original work[245] (GenScript USA Inc., Piscataway, NJ) (amino acid numbering beginning at VP1) using In-Fusion cloning kit (Clontech Laboratories Inc., Mountain View, CA). Packaging plasmid necessary to express either only VP1 and VP3 capsid proteins, or VP2 protein fused to peptide were generated by introducing point mutations (T138A substitution to generate VP1,3 plasmids; M1L for VP2 plasmids) as described for AAV2[196]. Peptide and linker (G_4S) coding sequences were cloned at the N-terminus of VP2 using In-Fusion cloning kit to generate peptide-VP2 expression plasmids.

Library construction

PCR-based DNA shuffling was performed similar to a previously described protocol[295]. Capsid ORFs from AAV1, 2, 4, 5, 6, 8, 9, rh8, rh10, rh39 and AAVrh43 were PCR amplified with primers designed to insert unique *Hind*III and *Xba*I sites at the 5' and 3' end of *cap* gene, respectively, cloned into an universal vector (Zero Blunt TOPO, Life Technologies, Grand Island, NY) and digested with *Hind*III and *Xba*I. Equimolar amounts of the resulting digested *cap* fragments were mixed together and fragmented with DNase I (Roche Diagnostics, Mannheim, Germany). Fragments less than 500 bp in length were gel purified and assembled by cycling 250 ng of purified DNA using *Taq* polymerase (Platinum *Taq* DNA Polymerase High Fidelity, Thermo Scientific, Rockford, IL).

Cycling conditions were as follows: 94°C, 5 mins; 35 cycles of (94°C, 30 secs; slow ramping from 65°C to 41°C over 10 mins; 72°C, 4 mins); 72°C, 7 mins. Chimeric cap genes were amplified from assembled DNA (Extensor Long Range PCR Enzyme, Thermo Scientific), digested with *Hind*III and *Xba*I and subcloned into pSub201 packaging plasmid digested with the same restriction enzymes. Shuffled plasmid library was generated by transformation of the subcloned library into high efficiency bacterial cells (MegaX DH10B T1 electrocompetent cells, Thermo Scientific), followed by isolation of plasmid DNA. Maximum theoretical diversity of plasmid library was calculated based on colony counts obtained from representative aliquot of bacteria transformed with plasmid library.

Packaging of the viral library was done as previously described[293]. Briefly, HEK293T cells grown in 150 mm dishes were transfected with 4 ng shuffled plasmid library and 25 µg each of pBluescript and pFΔ6 adenoviral helper plasmid using HEPES-buffered saline (HeBS) / calcium chloride co-transfection method. 72 h after transfection, cells were harvested and viral library was purified by iodixanol gradient ultracentrifugation[327], 100 kilodalton molecular weight cutoff (MWCO) concentration and dialysis in 1X PBS. DNase resistant vector genome titer was determined by quantitative PCR (qPCR). Details of virus purification and titration are provided in a subsequent section.

In vivo library selection

$1x10^{11}$ or $5x10^{11}$ vector genomes of viral library were infused into adult 6-8 week old male C57BL/6J mice through intravenous route (tail vein) (N=1). 3 d after infusion, mice were euthanized, and brain and liver harvested. Total DNA were

isolated using DNeasy Blood and Tissue kit (Qiagen, Hilden, Germany) and tissue-resident capsid genes were amplified by nested PCR using primers designed to bind to 5' and 3' ends of *cap* region. Nucleotide and amino acid alignment and homology quantification were performed using Geneious (Biomatters, Auckland, New Zealand).

Vector particle production, titer quantification and quality analysis

The self-complementary AAV-CBA-GFP vector used in these studies carries an expression cassette comprised of the CBA promoter without an intron to drive expression of GFP and a rabbit β-globin poly-adenylation signal[69].

Sequences targeting mouse *Htt* mRNA were embedded into the artificial miR-155 scaffold to generate the following cassette: 5'-ctggaggcttgctgaaggctgtatgctg**TTTAGACTTGTGTCCTTGACCT**gttttggccactgactg acTGGCAAAGCACAAGTCTAAAcaggacacaaggcctgttactagcactcacatggaacaaatg gcc-3' (targeting sequence in bold uppercase). This artificial miRNA targets position 1090 in exon 8 of mouse huntingtin gene. eGFP and artificial miRNA cassette were expressed under the control of the cytomegalovirus enhancer/chicken β-actin promoter (CBA) containing the β-actin exon and chimeric intron.

To generate AAV vectors, HEK293T cells were co-transfected with the following mix of plasmids using the calcium phosphate precipitation method: 7.96 μg transgene plasmid, 25.6 μg adenoviral helper plasmid pFΔ6, 12.2 μg AAV-B1 or AAV9 *rep-cap* packaging plasmid, per 2.1 x 10^7 cells plated. To generate peptide-grafted AAV vectors, the single *rep-cap* packaging plasmid was

substituted by a 5:1 ratio of VP1,3 packaging plasmid and peptide-VP2 packaging fused expression plasmid in *trans,* for a total amount of 12.2 µg, per 2.1 x 10^7 cells plated. 72 hours post transfection, cells were harvested and cell lysates prepared by 3 cycles of freeze-thaw and treated with Benzonase (Sigma-Aldrich, St. Louis, MO) (50 U/mL cell lysate, 37°C, 30 min). AAV was purified from cell lysates by iodixanol density gradient ultracentrifugation[327] (Optiprep density gradient medium, Axis-Shield, Oslo, Norway). Residual iodixanol was removed by replacing with Buffer B (20 mM TRIS, 0.5 M NaCl, pH 8.5) using a 100 kilodalton (kDa) cutoff centrifugation device (Amicon Ultra-15, Merck Millipore Ltd., Cork, Ireland) by three rounds of centrifugation at 1500x g and dialyzed twice using a 10,000 molecular weight cutoff (MWCO) dialysis cassette (Slide-A-Lyzer, Thermo Scientific, Rockford, IL) against a 1,000-fold volume of PBS for >2h and once overnight at 4°C. After treatment of stocks with DNase I (Roche Diagnostics GmbH, Mannheim, Germany, 2 U/µL vector, 37°C, 30 min), the titer of AAV vectors was determined by real-time quantitative PCR (qPCR) using probe and primers specific for the rabbit β-globin polyA sequence (Integrated DNA Technologies, Coralville, IA). For stoichiometric analysis of capsid proteins, 1 x 10^{10} vector particles of purified vector were subjected to Western blotting by standard SDS-PAGE technique. AAV capsid proteins were detected using mouse monoclonal anti-AAV capsid protein antibody clone B1 (1:500, American Research Products, Inc., Waltham, MA, 03-65158), peroxidase linked anti-mouse secondary antibody (1:2000, GE Healthcare UK Ltd., Buckinghamshire, UK, 380199) and ECL Western Blotting Substrate (Pierce Protein Research Products, Rockford, IL).

Vector administration and tissue processing

The Institutional Animal Care and Use Committees at the University of Massachusetts Medical School and Auburn University reviewed and approved all experiments in mice and cats, respectively, in compliance with guidelines from the National Institutes of Health.

For studies with AAV-AS vector, AAV vectors were administered via the tail vein in a volume of 200 µL into 6-8 week-old male C57BL/6J mice (Jackson Laboratory, Bar Harbor, ME). A dose of 5×10^{11} vg/mouse was administered for immunochemical studies and biodistribution analysis.

For immunochemical and GFP fluorescence studies, mice were trans-cardially perfused at 4 weeks post-injection first with ice cold 1x phosphate buffer saline (PBS), followed by 4% paraformaldehyde solution (Fisher Scientific, Fair Lawn, NJ). Tissues were harvested and post-fixed in 4% paraformaldehyde solution at 4°C for an additional 24 h. Post-fixed tissues were transferred to 30% sucrose in 1x PBS for cryoprotection. Tissues were embedded in Tissue-Tek O.C.T. compound (Sakura Finetek, Torrance, CA) and frozen in a dry-ice-isopentane bath and stored at -80°C.

For studies with AAV-B1 vector, AAV vectors were administered via the tail vein in a volume of 200 µL into 6-8 week-old male C57BL/6J mice (Jackson Laboratory, Bar Harbor, ME). A dose of either 5×10^{11} or 2×10^{12} vector genomes (vg)/mouse was administered for immunochemical studies, while a dose of 5×10^{11} vg/mouse was administered for biodistribution analysis.

For immunochemical studies of CNS and GFP fluorescence studies of liver, mice injected at a dose of 2 x 10^{12} vg/mouse were trans-cardially perfused at 4 weeks post-injection first with ice cold 1x phosphate buffer saline (PBS), followed by 4% paraformaldehyde solution (Fisher Scientific, Fair Lawn, NJ). Tissues were harvested and post-fixed in 4% paraformaldehyde solution at 4°C for an additional 24 h. Post-fixed tissues were transferred to 30% sucrose in 1x PBS for cryoprotection. Tissues were embedded in Tissue-Tek O.C.T. compound (Sakura Finetek, Torrance, CA) and frozen in a dry-ice-isopentane bath and stored at -80°C. For all other immunochemical and GFP fluorescence analysis, mice injected at a dose of 5 x 10^{11} vg/mouse were trans-cardially perfused at 4 weeks post-infusion with ice-cold 1x PBS. Retinas were removed prior to perfusion. Lungs were inflated in 0.5% low melting point agarose in 10% formalin-PBS solution post perfusion.

For biodistribution analysis with either vector, mice were trans-cardially perfused at 4 weeks post-infusion with ice-cold 1x PBS. Tissues were harvested immediately, frozen on dry ice and stored at -80°C.

Cat studies

AAV-AS vector was packaged by University of Massachusetts Medical School Viral Vector Core by transient transfection followed by purification by cesium chloride sedimentation[175, 328], and administered through the carotid artery into a 2 month old normal domestic short haired cat at a dose of 1.29x10^{13} vg. The cat was not screened for pre-existing anti-capsid neutralizing antibodies. AAV-B1 vector was packaged and purified by iodixanol gradient purification as described

in an earlier section, and administered through the carotid artery into a 2 month old normal domestic short haired cat at a dose of $3.4x10^{12}$ vg.

At 4 weeks post infusion, the injected cats was trans-cardially perfused with cold 1x PBS. Various tissues were harvested and fixed in 4% paraformaldehyde in PBS at 4°C. The brain was cut into 0.6 cm coronal blocks prior to immersion in fixative. Processing of post-fixed brains and spinal cords for immunohistochemical (IHC) and immunofluorescence studies was identical to that for mouse studies.

Immunohistochemical detection of GFP expression

For chromogenic IHC, 40 µm serial sections of brains and 30 µm serial sections of spinal cord were incubated for 96 h in anti-GFP primary antibody (ABfinity rabbit monoclonal anti-GFP 1:1000, G10362, Life Technologies, Grand Island, NY), or overnight in anti-GFAP (rabbit polyclonal anti-GFAP 1:500, Z0334, Dako, Glostrup, Denmark) or anti-Iba1 (rabbit polyclonal anti-Iba1 1:1000, 019-19741, Wako, Osaka, Japan) at 4°C. After washing with 1x PBS, sections were incubated in appropriate biotinylated secondary antibody (biotinylated anti-rabbit antibody, Vector Laboratories Inc., Burlingame, CA), followed by incubation in ABC reagent (PK-6100, Vector Laboratories Inc.). Sections were developed with 3,3′-diaminobenzidine reagent (DAB) according to the manufacturer's instructions (SK-4100, Vector Laboratories Inc.), dehydrated with increasing concentrations of ethanol, cleared with xylene and mounted using Permount mounting medium (Fisher Scientific).

For immunofluorescence studies, 40 µm sections of brains and 30 µm sections of spinal cord were incubated for 24 h in a cocktail of appropriate primary antibodies at 4°C. The primary antibodies used were: rabbit polyclonal anti-GFP (1:1000, Life Technologies, A11122), chicken polyclonal anti-GFP (1:2000, Abcam, ab13970), mouse monoclonal anti-NeuN (1:500, EMD Millipore, MAB377), mouse monoclonal anti-DARPP32 (1:250, BD Biosciences, 611520), mouse monoclonal anti-tyrosine hydroxylase (1:100, EMD Millipore, MAB318), mouse monoclonal anti-calbindin-D-28K (1:500, Sigma, C9848), mouse monoclonal anti-APC (1:1000, EMD Millipore, OP80), rabbit polyclonal anti-CD31 (1:50, Abcam, ab28364) and mouse monoclonal anti-GFAP (1:500, Abcam, ab4648). After washing in 1x PBS, sections were incubated for 1 h at room temperature in appropriate secondary antibodies, washed in 1x PBS and mounted using Permafluor mounting media (Thermo Scientific). Native GFP fluorescence in liver and skeletal muscle (quadriceps) was analyzed in 30 µm sections mounted using Permafluor mounting media. Native GFP fluorescence in liver and muscle groups was analyzed in 30 µm formalin fixed sections, and 10 µm frozen sections, respectively. 7 µm formalin fixed pancreatic sections were analyzed with the following primary antibodies: rabbit polyclonal anti-GFP (1:1000, Life Technologies, A11122), and guinea pig polyclonal anti-insulin (1:200, Abcam, ab7842). GFP expression in 10 µm formalin fixed lung sections was detected by chromogenic IHC after 24 h incubation with rabbit polyclonal anti-GFP antibody (1:1000, Life Technologies, A11122). Retinas were immunochemically processed as previously described (Punzo 2009), using rabbit polyclonal anti-GFP (1:1000, Life Technologies, A11122). All images were captured on a Leica DM5500 B microscope (Leica Microsystems Inc., Buffalo Grove, IL), except the muscle groups, which were imaged on a Zeiss microscope with Axiocam system. Post-

processing of images was performed using Adobe Photoshop CS6 (Adobe Systems, San Jose, CA).

Quantification of GFP-positive neurons in striatum and thalamus

Chromogenic IHC staining of 40 µm mouse brain sections was performed as described in an earlier section. Five 663.28 µm x 497.40 µm regions were randomly chosen from the striatum or thalamus (n=4 biological replicates per vector) of the stained sections. Neurons were identified by their morphology and counted by individuals blinded to the study design. All statistical analyses were performed using GraphPad Prism (GraphPad Software, Inc., La Jolla, CA). Total neurons in the 663.28 µm x 497.40 µm fields were counted in Nissl (cresyl violet acetate) stained brain sections using ImageJ software. Significance was determined by Student's unpaired two-tailed T-test. A $p<0.05$ was considered to be significant.

Biodistribution analysis

Vector genome copy numbers from various mouse tissues were determined by qPCR after extraction of total DNA using DNeasy Blood and Tissue kit (Qiagen). Tissues were mechanically lysed using TissueLyzer II (Qiagen GmbH, Hilden, Germany). Vector genome content in each tissue was determined using 100 ng total DNA using the same qPCR method described above for AAV vector titration using a plasmid-based standard curve, and a viral vector internal control for quality assurance. All statistical analyses were performed using GraphPad Prism.

Significance was determined by Student's unpaired two-tailed T-test. A $p<0.05$ was considered to be significant.

Western blotting to detect GFP protein levels in various tissue types was performed using primary antibodies detecting GFP (chicken polyclonal anti-GFP, 1:2000, Aves Labs Inc., Tigard, OR, GFP-1010) and mouse β-actin (mouse monoclonal anti-β-actin, 1:1000, Sigma-Aldrich, St. Louis, MO, A5441), followed by appropriate IRDye secondary antibodies (LI-COR Inc., Lincoln, NE). Total protein was isolated from harvested tissues by bead lysis in T-PER tissue extraction reagent (Life Technologies) and quantified by Bradford assay. 20 µg of total protein was loaded onto each well of 4-20% Mini-PROTEAN TGX gels (Bio-Rad Laboratories Inc., Hercules, CA). Tissues from two representative mice per group were used for analysis. Detection and quantification were done with Odyssey infrared imaging system (LI-COR Inc.).

In vitro binding assay

Pro5 and Lec2 CHO cell lines were gifts from Dr. Aravind Asokan (University of North Carolina, Chapel Hill, NC) and binding assay was performed as previously described[205]. Briefly, cells were pre-chilled for 30 min at 4°C in serum-free DMEM (Life Technologies), followed by incubation with AAV vectors at $4x10^4$ vg/cell in cold serum-free media DMEM at 4°C. 90 min later, cells were washed thrice with cold serum-free DMEM to remove loosely bound vector particles. Cells were harvested and total DNA was extracted using DNeasy Blood and Tissue kit (Qiagen). Vector genome copy numbers of cell surface bound virions was quantified by qPCR as described earlier.

In vitro knockdown assay

A 159 bp sequence containing the *Htt* mRNA target sequence was cloned into pSiCHECK-2 vector (Promega Corporation, Madison, WI) between the XhoI and NotI restriction sites in the 3' UTR of the *Renilla* luciferase gene. Luciferase assays were performed by co-transfection in 24 well plates with 0.025 µg/well of the Htt target- containing pSiCHECK-2 reporter and 0.6 µg/well of GIPZ or AAV transgene plasmid containing either *Htt* targeting- artificial miRNA sequence (miR^{Htt}) or scrambled miRNA sequence. Transfections were performed using Lipofectamine 2000 (Invitrogen Corporation, Carlsbad, CA), according to the manufacturer's protocol. 48 hours after transfection the cells were lysed for 20 min in 1x passive lysis buffer (Promega). Luciferase activity was read in 96-well plates with the Dual-luciferase assay kit (Promega) using the GloMax multi-detection system (Promega). *Renilla* luciferase values were normalized for intraplasmid transfection efficacy to firefly luciferase signal. All statistical analyses were performed using GraphPad Prism. Significance was determined by Student's unpaired two-tailed T-test. A $p<0.05$ was considered to be significant.

Analysis of *in vivo Htt* knockdown

AAV vectors were administered intravascularly via the tail vein into 6-8 week-old male C57BL/6J mice (Jackson Laboratory, Bar Harbor, ME) at a dose of $9.4x10^{11}$ vg/mouse. Mice were euthanized at 4 weeks post-injection and the brain sectioned in 2 mm coronal blocks using a brain matrix. Biopsy punches of

different diameters (2 or 3 mm) were used to sample motor cortex (2 mm), striatum (3 mm) and thalamus (3 mm). Cervical spinal cord and liver were also included in the analysis. Tissue samples were mechanically homogenized using a TissueLyzer II and 5 mm stainless steel beads (Qiagen) in Trizol (Life Technologies). Total RNA was isolated using Direct-zol RNA MiniPrep kit (Zymo Research Corporation, Irvine, CA) according to manufacturer's protocol. Total RNA (400-1000 ng) was reverse transcribed using High Capacity RNA to cDNA kit (Applied Biosystems, Foster City, CA). Relative mouse *Htt* mRNA expression was assessed by qPCR using TaqMan gene expression assays for mouse *Htt* (Mm01213820_m1, Applied Biosystems) and hypoxanthine phosphoribosyltransferase 1 (Hprt1; mm00446968_m1, Applied Biosystems). Changes in Htt mRNA for groups injected with AAV9 or AAV-AS vectors were calculated relative to PBS-injected mice using the $2^{-\Delta\Delta CT}$ method[329]**.** Significance was determined by Student's unpaired two-tailed T-test. A $p<0.05$ was considered to be significant.

For protein analysis, a frozen punch from each region (motor cortex, striatum, thalamus, cervical spinal cord, and liver) was homogenized in 75-300 µl 10mM HEPES pH7.4, 250mM sucrose, 1mM EDTA + protease inhibitor tablet (cOmplete mini, EDTA-free, Roche), 1mM NaF and 1mM Na_3VO_4 on ice for 30 strokes. Protein concentration was determined by Bradford method (BioRad) and 10µg motor cortex, striatum, and thalamus or 20µg cervical spinal cord and liver were loaded onto 3-8% Tris-Acetate gels (Life Technologies) and separated by SDS-PAGE. Proteins were transferred to nitrocellulose using a TransBlot Turbo apparatus (BioRad) then blots were cut horizontally at 72kD. Blots were washed in TRIS-buffered saline + 0.1% Tween 20 (TBST) and blocked in 5%

milk/TBST. The top half of the blot was incubated in anti-Htt antibody Ab1[330] (1:2000) and the bottom half in anti-tubulin antibody (1:4000, Sigma) or anti-GAPDH antibody (1:6000, Millipore) diluted in 5% milk/TBST overnight at 4°C. Blots were washed in TBST then incubated in peroxidase conjugated secondary antibodies diluted in 5% milk/TBST for 1 hour at room temperature, washed, and proteins were detected using SuperSignal West Pico Chemiluminescent Substrate (Thermo Scientific) and FluoroChem SP (Alpha Innotech) and Hyperfilm ECL. The bottom blots were reprobed with anti-GFP antibody (1:3000, Cell Signaling). Densitometry was performed using ImageJ software.

Structural analysis

Alignment of AAV-B1 capsid protein sequence with parental serotypes was carried out using Cobalt Constraint-based Multiple Protein Alignment Tool. The capsid sequence ordering was arranged using Chimera (http://www.cgl.ucsf.edu/chimera) in descending percent identities referenced to AAV8. The 3D model of AAV-B1 was generated using SWISS MODEL subroutine[331] based on coordinates from the AAV8 crystal structure[186] (PDB accession no. 2QA0) as a template. Surface mapping was performed using Pymol (http://www.pymol.org).

Antibody neutralization assay

Anti-AAV neutralization assay was performed as previously described[332]. Briefly, AAV vectors were mixed with varying concentrations of Gammagard S/D purified

intravenous immunoglobulin (IVIg), (Baxter, Deerfield, IL, gift from Dr. Luk H. Vandenberghe, Harvard Medical School, MA) in serum-free media, incubated for 1 h at 37°C and then added to HeLa cells at $3.5x10^4$ v.g./cell at 37°C. AAV incubated with PBS (no IVIg) served as control. 90 min later, cells were washed thrice with cold serum-free media and replacing with complete media, cells were incubated for 48 h prior to trypsinization and preparation for flow cytometry. Cell samples were analyzed for GFP expression using the blue laser of a BD LSR Fortessa™ flow cytometer (San Jose, CA) running BD FACSDiva™ software (v6.1.3). Flow data was analyzed using FLOWJo software (FLOWJo, LLC, Ashland, OR). To calculate % transduction of control for the samples mixed with IVIg, % GFP positive cell values for each sample were plotted as a percentage of the AAV transduction sample without IVIg, which was set to 100%.

CHAPTER III

Widespread CNS gene transfer and silencing after systemic delivery of novel AAV-AS vector

Abstract

Effective gene delivery to the central nervous system (CNS) is vital for development of novel gene therapies for neurological diseases. Adeno-associated virus (AAV) vectors have emerged as an effective platform for *in vivo* gene transfer, but overall neuronal transduction efficiency of vectors derived from naturally occurring AAV capsids after systemic administration is relatively low. Here we investigated the possibility of improving CNS transduction of existing AAV capsids by genetically fusing peptides to the N-terminus of VP2 capsid protein. A novel vector AAV-AS, generated by the insertion of a poly-alanine peptide, is capable of extensive gene transfer throughout the CNS after systemic administration in adult mice. AAV-AS is 6- and15-fold more efficient than AAV9 in spinal cord and cerebrum, respectively. The neuronal transduction profile varies across brain regions but is particularly high in the striatum where AAV-AS transduces 36% of striatal neurons. Widespread neuronal gene transfer was also documented in cat brain and spinal cord. A single intravenous injection of an AAV-AS vector encoding an artificial microRNA targeting huntingtin (Htt) resulted in 33-50% knockdown of Htt across multiple CNS structures in adult mice. This novel AAV-AS vector is a promising platform to develop new gene therapies for neurodegenerative disorders.

Results

Insertion of poly-alanine peptide in AAV9.47 capsid enhances neuronal gene transfer in adult mice

We chose AAV9.47 as the capsid in which to test our peptide grafting approach as this quadruple mutant of AAV9 (S414N, G453D, K557E, T582I) has comparable CNS gene transfer properties to AAV9 but decreased tropism to liver[245] (**Figure 3.1**). Peptides were grafted on the AAV9.47 capsid surface via genetic fusion to the N-terminus of VP2 using a previously described approach[196] (**Figure 3.2a**). Unexpectedly, one of the control vectors used for this screen, a peptide-modified AAV9.47 vector carrying a string of 19 alanines in the VP2 capsid protein, designated as AAV-AS (**Figure 3.2b**), showed a remarkable increase in CNS transduction efficiency compared to AAV9 after systemic delivery in 6-8 week old C57BL/6 mice (**Figure 3.3a**). AAV-AS vector transduced diverse neuronal populations, glia and endothelia throughout the brain and spinal cord, including extensive transduction of neurons in motor cortex and striatum (**Figure 3.3b**). We also observed efficient transduction of granule cells in the dentate gyrus as well as motor neurons and interneurons in the spinal cord (**Figure 3.3b**). The identity of GFP-positive cells with neuronal morphology in cortex, striatum and spinal cord was confirmed by co-localization of GFP and NeuN (**Figure 3.3c**). GFP-positive neurons in the striatum were shown to be DARPP32-positive medium spiny neurons (**Figure 3.3c**). Neuronal transduction was apparent in many brain regions of AAV-AS injected mice with the exception of thalamus and hypothalamus where only sparse transduction was observed (**Figure 3.4**). AAV-AS also transduced GFAP-positive astrocytes (**Figure 3.3c**),

oligodendrocytes in the corpus callosum and Bergmann glia in the cerebellum (**Figure 3.4**). The transduction profile of AAV9 was limited to glial cells and endothelia in most CNS regions analyzed (**Figure 3.3b** and **Figure 3.4**).

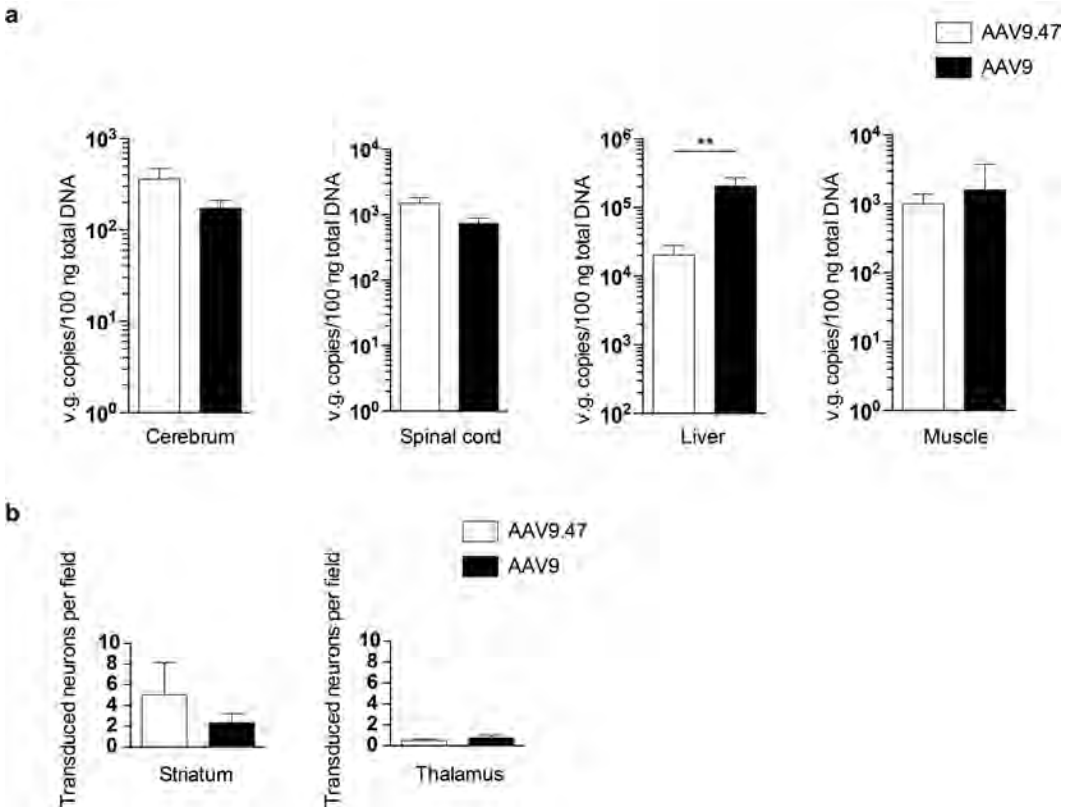

Figure 3.1: Biodistribution profile of AAV9.47. (**a**) AAV vector genome content in cerebrum, spinal cord, liver and muscle of mice injected intravenously with AAV9.47-GFP or AAV9-GFP vectors ($5x10^{11}$ vg/mouse) (n=4 animals per group). (**b**) Quantification of GFP-positive neurons per high power field in striatum and thalamus of injected mice (n=4 biological replicates per group). Data shown as mean ± SD. **p < 0.01 by Student's unpaired two-tailed t-test.

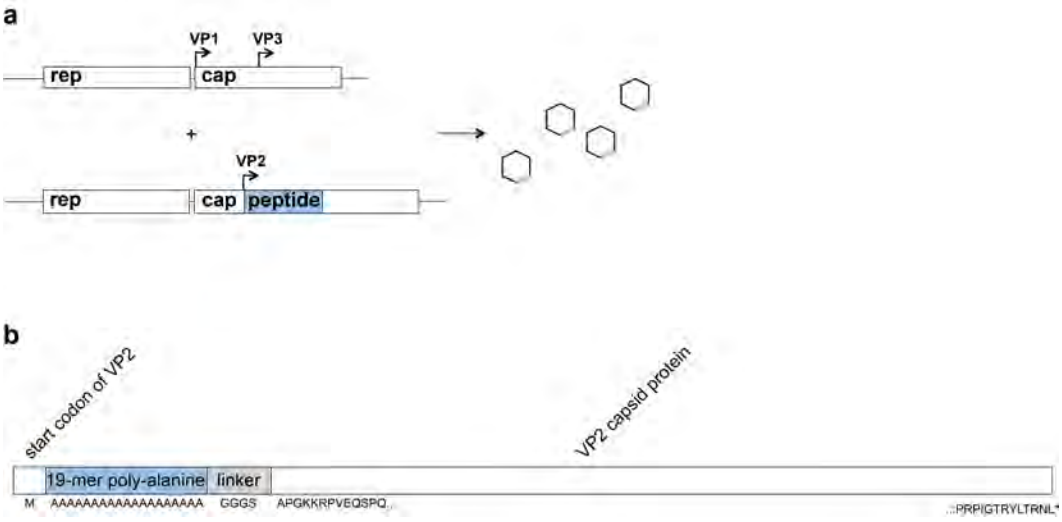

Figure 3.2: Construction of AAV-AS vector. (**a**) Illustration of packaging strategy. VP1 and VP3 are expressed separately (top) from VP2 fused with peptide (below). (**b**) Schematic diagram of VP2 capsid protein showing insertion site of AS peptide and G_4S linker.

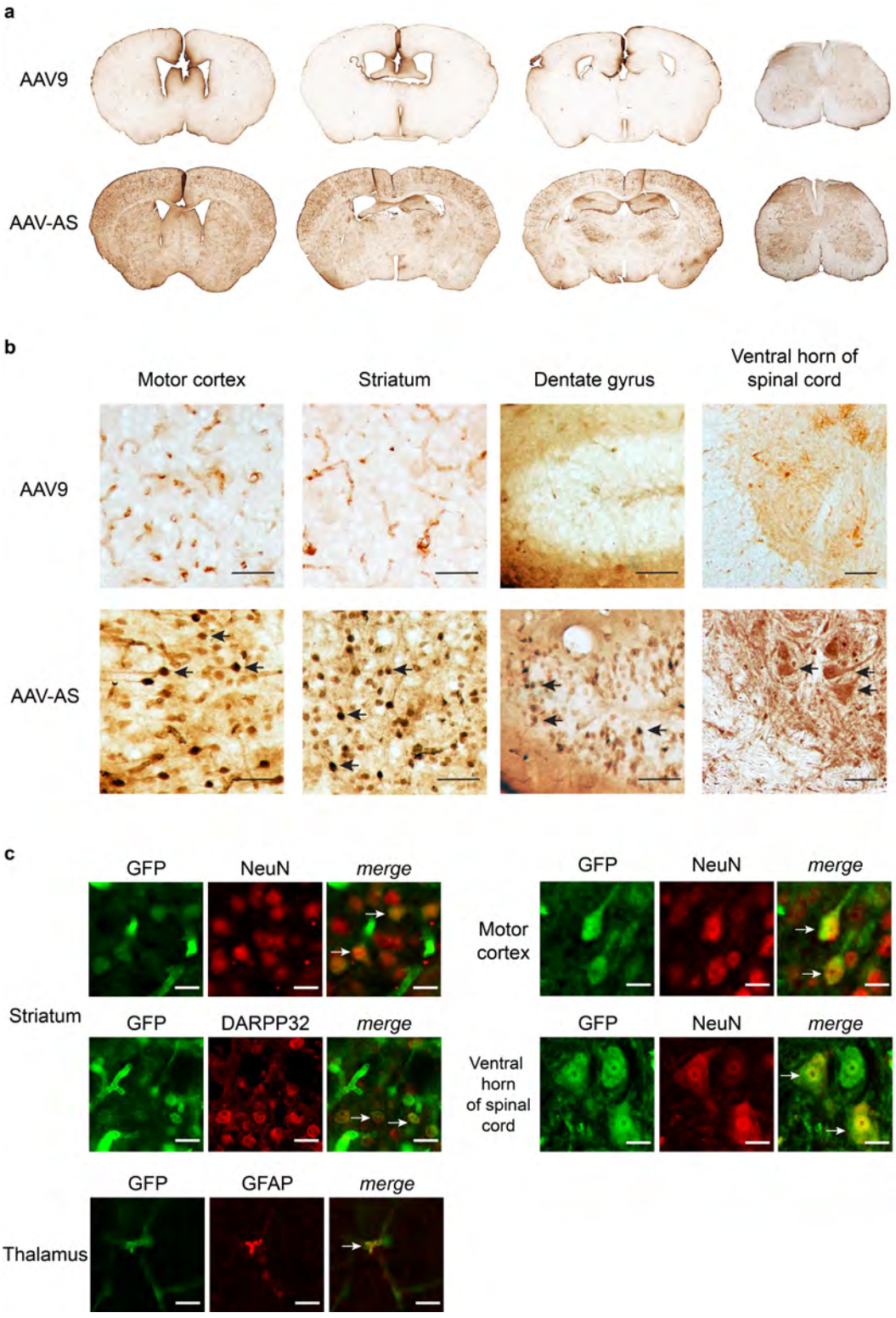

Figure 3.3: CNS transduction profile of AAV-AS vector after vascular infusion in adult mice.

Figure 3.3: CNS transduction profile of AAV-AS vector after vascular infusion in adult mice. a. Overview of GFP distribution in brain and spinal cord in AAV-AS and AAV9 injected mice ($5x10^{11}$ vg/mouse)**.** Representative images of coronal brain sections located in relation to bregma at +0.5mm, -0.5mm and -1.80mm, and cervical spinal cord (left to right) are shown. **b.** Transduction of neuronal populations in different brain regions. Black arrows indicate examples of GFP-positive neurons identified by morphology. Bar = 50 µm. **c.** Phenotype of transduced cells was identified by double immunofluorescence staining with antibodies to GFP, pan-neuronal marker NeuN, striatal medium spiny neuron marker DARPP32 or astrocyte marker GFAP. Neuronal transduction in spinal cord was examined in sections stained for GFP and NeuN. The large size and morphology of GFP-positive neurons in the ventral spinal cord suggest a motor neuron identity. White arrows indicate examples of GFP-positive neurons. Bar = 10 µm.

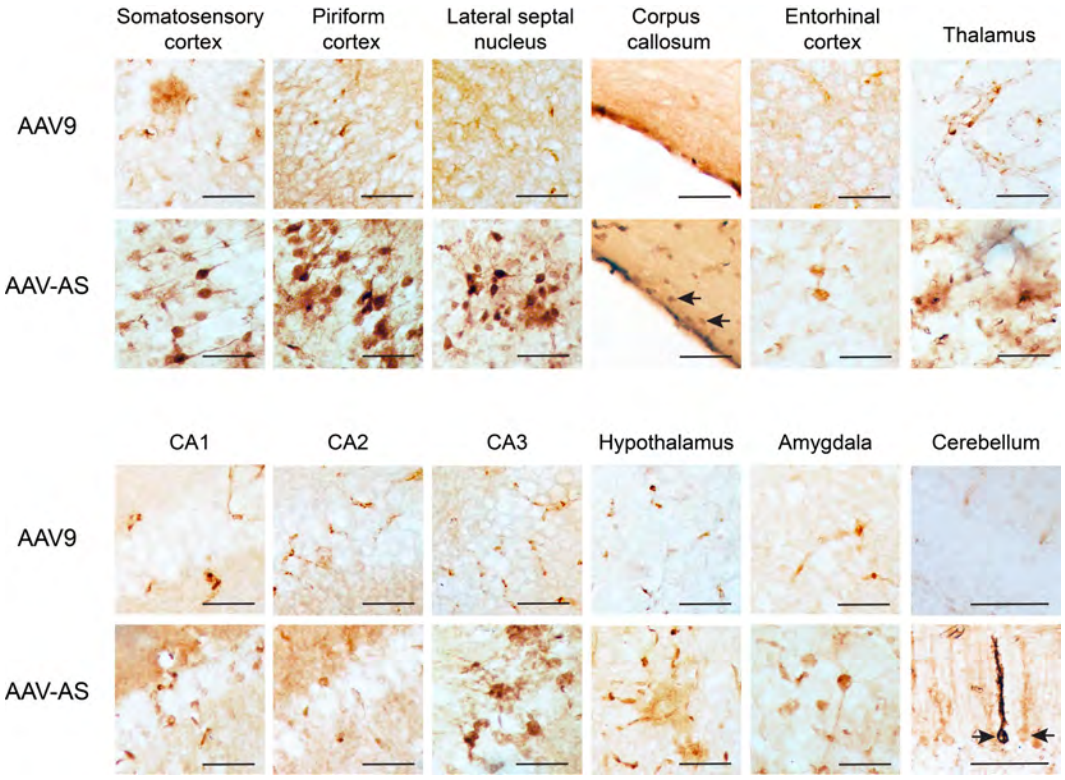

Figure 3.4: Transduction profile of AAV-AS and AAV9 vectors across multiple CNS regions after systemic delivery. Bar = 50 μm. Black arrows in corpus callosum indicate GFP-positive oligodendrocytes, and in the cerebellum indicate Bergmann glia.

Western blot analysis of AAV preparations confirmed incorporation of the chimeric poly-alanine VP2 protein in the AAV-AS capsid (**Figure 3.5a**). Quantification of GFP-positive neurons revealed AAV-AS transduced as many as 36% of striatal neurons compared to only 0.45% by AAV9 (**Figure 3.5b**). In contrast, the increase in transduced thalamic neurons was more modest (**Figure 3.5b**). The CNS transduction efficiency of AAV-AS vector was also reflected in its biodistribution profile. More vector genomes were found in the cerebrum and spinal cord of AAV-AS injected animals compared to AAV9 (15-fold and 6-fold, respectively) (**Figure 3.5c**). These findings were corroborated by comparable increase in GFP protein in cerebrum and spinal cord (**Figure 3.5d**). The increased gene transfer efficiency for AAV-AS vector compared to AAV9 appears to be restricted to CNS, as transduction of liver, muscle, lung, pancreas and kidney was identical for both AAV vectors based on analysis of vector genome content (**Figure 3.5e and Figure 3.6**) and GFP protein levels (**Figure 3.5f**). No inflammatory response characterized by reactive astrogliosis or microgliosis was observed due to AAV-AS infusion (**Figure 3.7**).

As a first step to understand how the poly-alanine peptide enhances CNS transduction of AAV9.47, we carried out a cell culture study to determine whether it changes the capsid interaction with exposed galactose residues on cell surface glycans. Terminal N-linked galactose is the primary cell surface receptor for AAV9[50, 205]. Binding studies in parental (Pro5) and sialic acid-deficient (Lec2) CHO cells showed no difference in receptor preference between AAV-AS, AAV9.47 and AAV9 vectors (**Figure 3.8**).

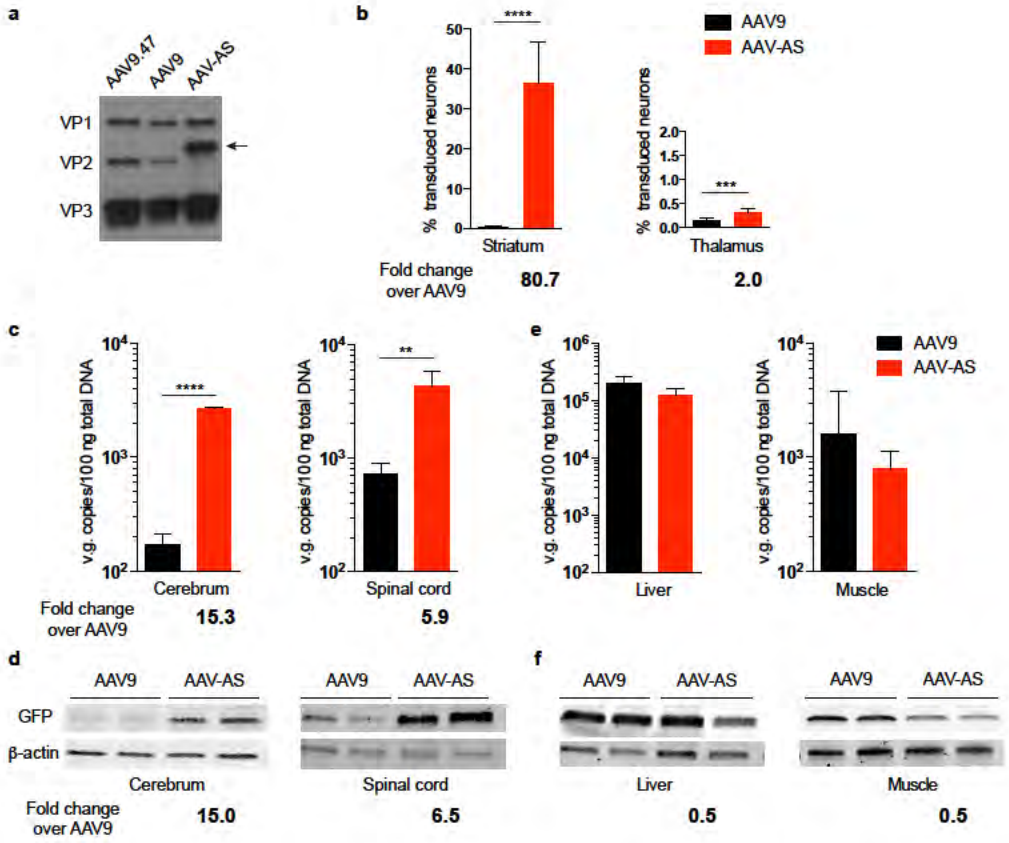

Figure 3.5: Quantitative assessment of AAV-AS CNS transduction efficacy. **a.** Western blot analysis of capsid protein composition of AAV vectors (1 x 10^{10} vg/lane) showed the presence of VP1, VP2 and VP3 capsid proteins. The poly-alanine VP2 fusion protein of AAV-AS capsid (indicated by black arrow) has a higher molecular weight than VP2 protein. **b.** Quantification of percentage of GFP-positive neurons in striatum and thalamus of mice injected with AAV-AS-GFP or AAV9-GFP vectors. Data shown is mean ± SD (n=4 biological replicates per group). **c.** AAV vector genome content in cerebrum and spinal cords (n=4 animals per group). Age matched non-injected mice were included as controls (not shown). **d.** Western blot analysis of GFP expression in cerebrum and spinal cord of 2 animals per group. Signal intensity of GFP was normalized to corresponding β-actin signal intensity for quantitative comparison. **e.** AAV vector genome content in liver and skeletal muscle (quadriceps) (n=4 animals per group). Data shown is mean ± SD. **f.** Western blot analysis of GFP protein expression in liver and skeletal muscle (quadriceps). *p<0.05, **p < 0.01, ***p < 0.001, ****p < 0.0001 by Student's unpaired two-tailed t-test.

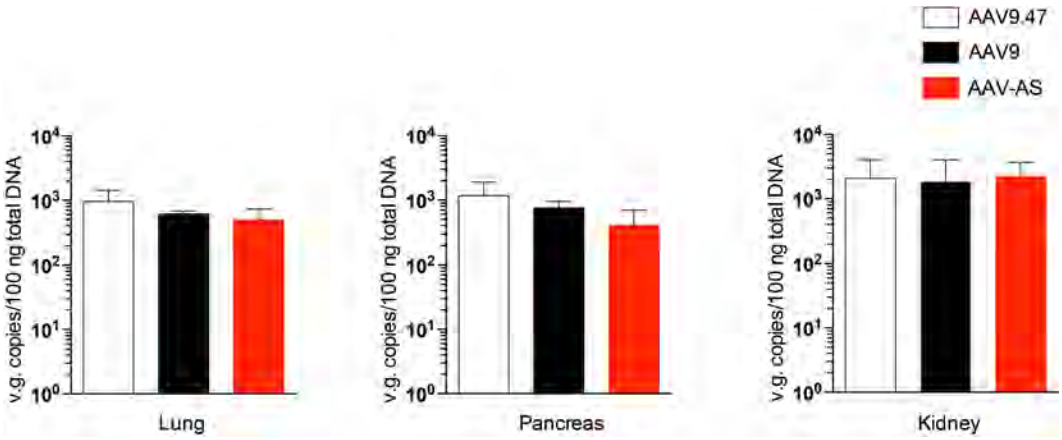

Figure 3.6: Biodistribution profile of AAV9.47, AAV9 and AAV-AS vectors in lung, pancreas and kidney. AAV vector genome content in mice injected intravenously with $5x10^{11}$ vg (n=4 animals per group). Data shown as mean ± SD.

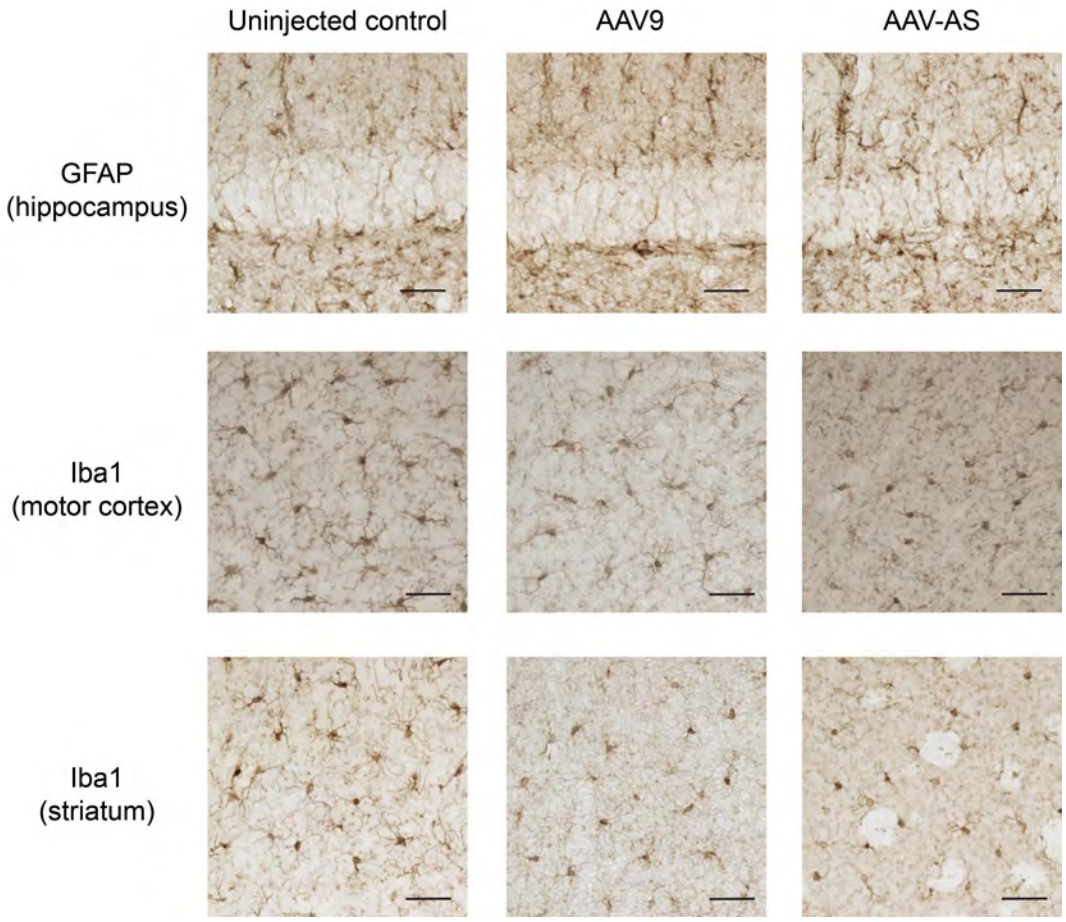

Figure 3.7: Assessment of gliosis markers in brain upon AAV infusion. Bar = 50 μm.

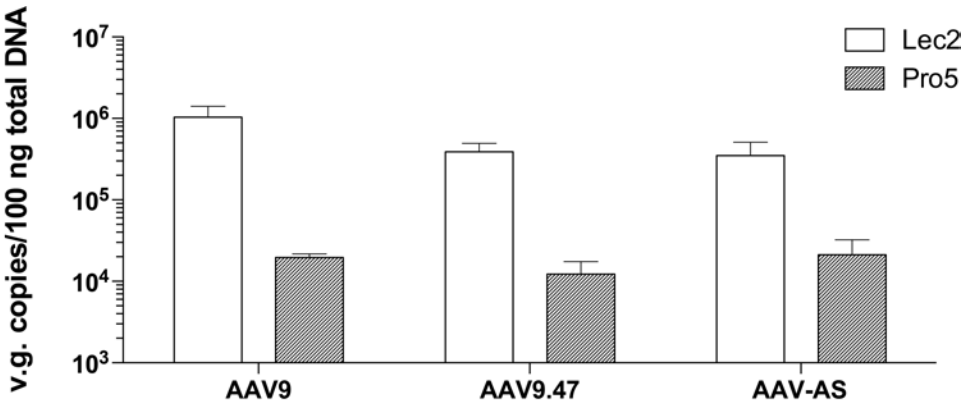

Figure 3.8: Cell binding studies of native and peptide-modified AAV vector. Data shown as mean ± SD. Experiment was performed with N=3 biological replicates.

Interestingly, while insertion of the 19-mer poly-alanine into AAVrh8 also led to an increase in CNS transduction efficiency (**Figure 3.9a**), it did not appear to enhance neuronal transduction, but instead noticeably increased glial and endothelial transduction (**Figure 3.9b**). Similar to AAV-AS, AAVrh8-AS exhibited significantly increased transduction of cerebrum, cerebellum and spinal cord (**Figure 3.9c**), while liver transduction remained unchanged (**Figure 3.9d**).

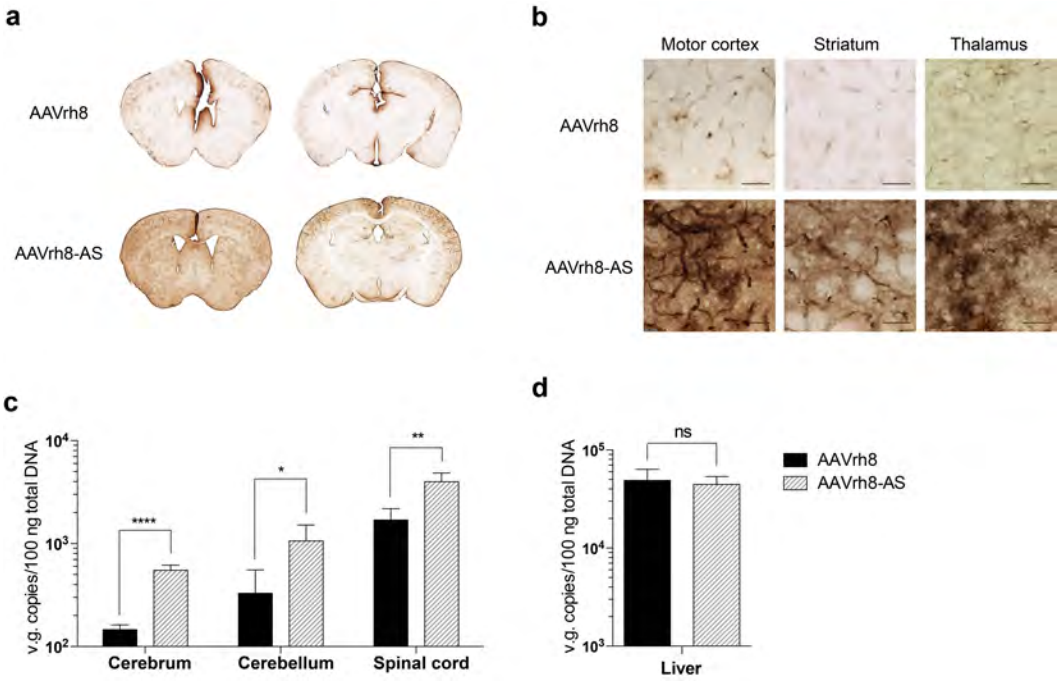

Figure 3.9: Biodistribution of AAVrh8-AS vector. (**a, b**) Distribution of GFP-positive cells in immunostained histological brain sections. Sections represented in (**a**) correspond to coronal planes +0.5mm and -1.80mm from the bregma plane. Bar = 50 µm. (**c, d**) Quantification of AAV vector genome content in (**c**) different CNS regions or (**d**) liver. Data shown as mean ± SD. Experiment was performed with N=3 per group. *p < 0.05, **p < 0.01, ****p < 0.0001 by Student's unpaired two-tailed t-test.

AAV-AS transduces neurons throughout the cat brain after systemic administration

Next we assessed whether the neuronal transduction properties of AAV-AS are reproducible in cats as there are numerous models of neurodegenerative diseases in this species. Consistent with results in mice, AAV-AS transduced diverse neuronal populations across the cat brain and spinal cord, including neurons in cerebral cortex, striatum and reticular formation, Purkinje neurons in cerebellum and motor neurons in the oculomotor nucleus located in ventral midbrain, spinal nucleus of the trigeminal nerve in brainstem and throughout the spinal cord (**Figure 3.10a, b**). Curiously, no endothelial and only sparse glial transduction was apparent in the cat brain in this study.

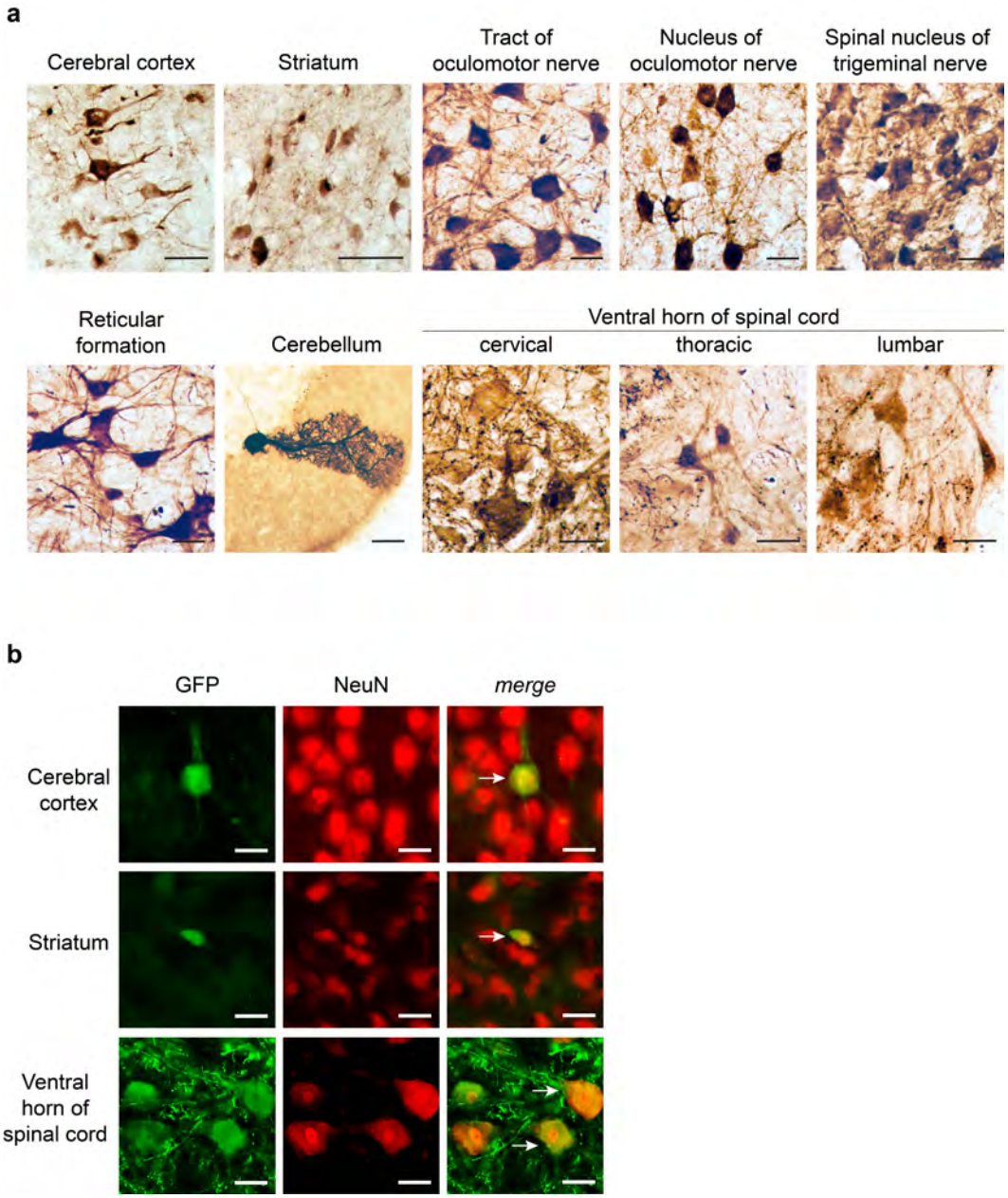

Figure 3.10: Neuronal transduction in cat after systemic delivery of AAV-AS vectors. a. Transduction of neurons in the cat brain after systemic delivery of AAV-AS vector ($1.29x10^{13}$ vg). Representative images (left) show GFP-positive cells with neuronal morphology in various structures in the brain and spinal cord. Bar = 50 µm. **b.** Double immunofluorescence staining for GFP and NeuN (right) confirm the neuronal identity of GFP-positive cells in brain and spinal cord. White arrows indicate examples of GFP-positive neurons. Bar = 50 µm.

Widespread knockdown of Htt in CNS after systemic delivery of AAV-AS vector

Finally, we evaluated the therapeutic potential of AAV-AS vector for Huntington's disease, a fatal autosomal dominant neurodegenerative disease caused by expansion of a CAG repeat in the huntingtin gene[333]. Currently there is no treatment for this devastating disease, but experimental RNAi[110, 111] and oligonucleotide[334] therapies have shown promising results. AAV-AS and AAV9 vectors encoding GFP and an U6-driven artificial microRNA specific for mouse *Htt* (miR^{Htt}) were infused systemically in C57BL/6 mice. The knockdown efficiency of this AAV-miR^{Htt} construct was 93% in a transient transfection assay in cell culture (**Figure 3.11).** Huntingtin mRNA and protein levels in CNS and liver were assessed at 4 weeks post injection (**Figure 3.12**). AAV-AS vector resulted in 33-50% reduction in *Htt* mRNA in striatum, motor cortex and spinal cord, and was better than AAV9 in all brain regions, but comparable in the spinal cord (**Figure 3.12a**). Conversely, AAV-AS was less potent than AAV9 in lowering *Htt* mRNA in liver (**Figure 3.12a**). Western blot analysis of Htt protein levels corroborated the differences between AAV9 and AAV-AS in the striatum, motor cortex and thalamus as well as in liver (**Figure 3.12b**). As anticipated, the reduction in Htt protein levels was inversely proportional to GFP protein levels, which indicates that higher CNS transduction efficiency leads to greater reduction in huntingtin mRNA and protein.

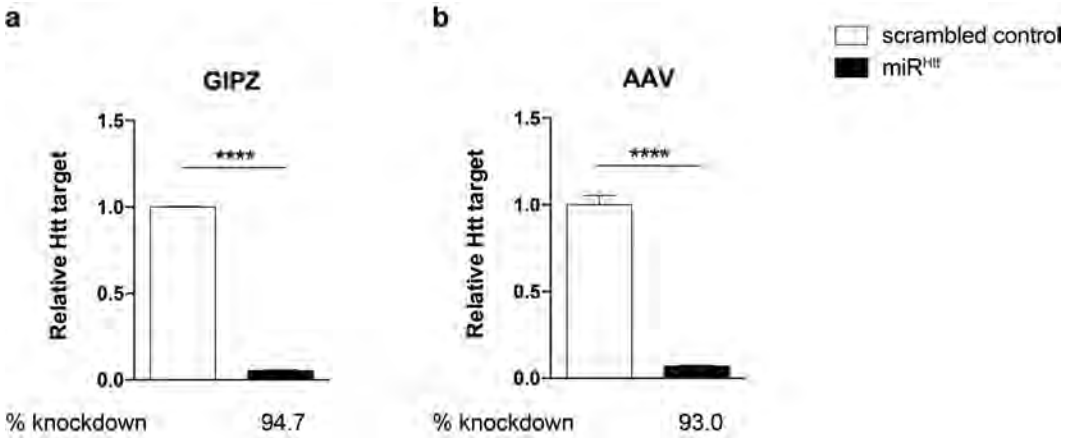

Figure 3.11: *In vitro* assessment of knockdown efficiency of miR^{Htt} construct. Changes in levels of luciferase reporter for *Htt* in HeLa cells transfected with **(a)** GIPZ expression plasmid, and **(b)** AAV transgene plasmid (used for *in vivo Htt* knockdown studies), containing either *Htt* targeting- artificial miRNA sequence (miR^{Htt}) or scrambled miRNA sequence. Values were normalized to luciferase levels in scrambled miRNA controls. % knockdown was calculated in comparison to scrambled controls. ****p < 0.0001 by Student's unpaired two-tailed t-test. Data shown is mean ± SD.

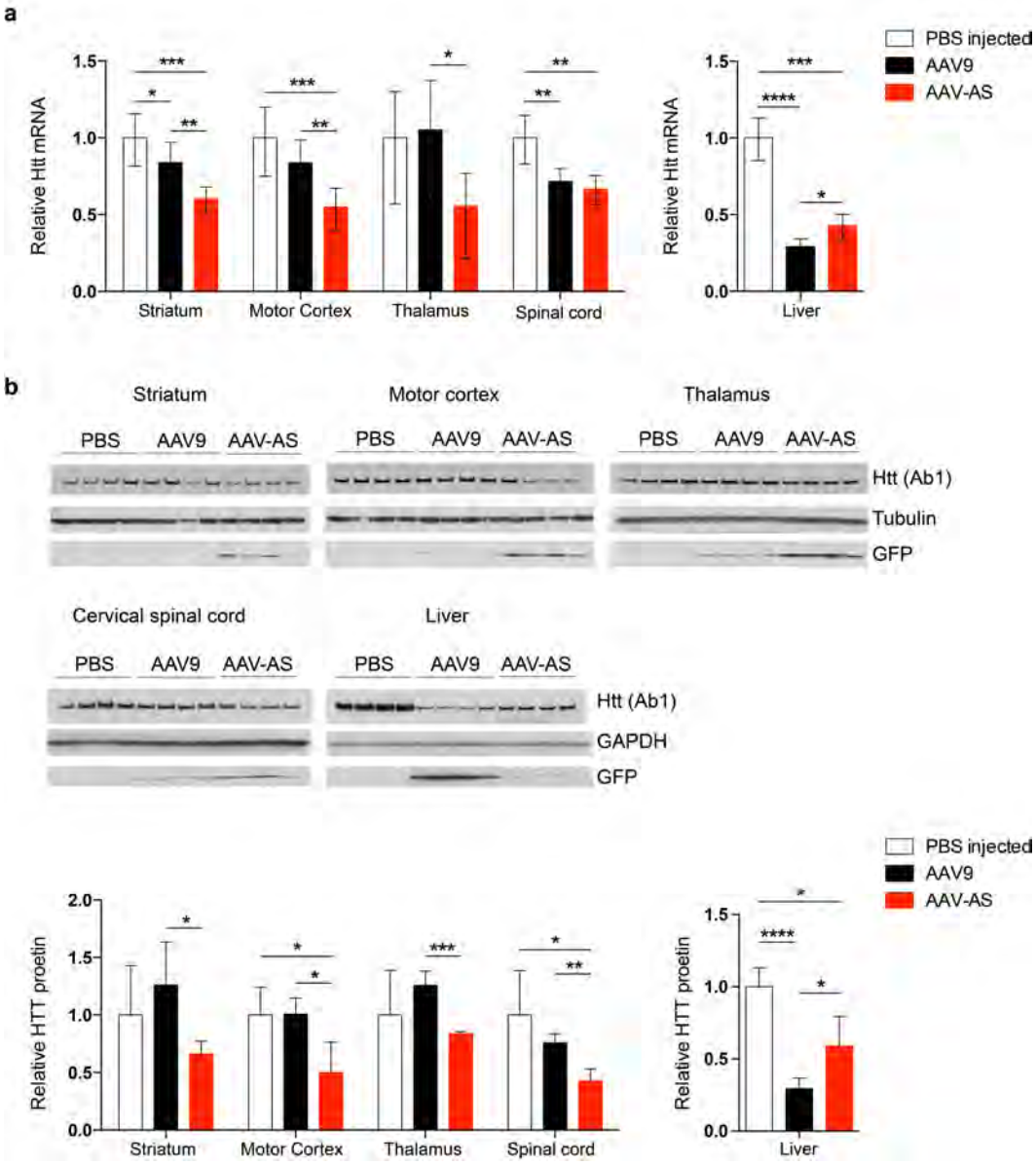

Figure 3.12: Htt knockdown in mice upon intravenous administration of AAV-AS-miR^{Htt} vector.

Figure 3.12: Htt knockdown in mice upon intravenous administration of AAV-AS-miR^{Htt} vector. a. Changes in *Htt* mRNA levels in brain structures, cervical spinal cord and liver in wild type mice injected systemically with AAV-AS or AAV9 vectors (n=4 per group) ($9.4x10^{11}$ vg/mouse) encoding a U6 promoter-driven artificial microRNA (miR^{Htt}) targeting mouse huntingtin mRNA. Values for each region were normalized to *Htt* mRNA levels in age-matched PBS-injected mice. *p < 0.05, **p < 0.01, ***p < 0.001, ****p < 0.0001 by Student's unpaired two-tailed t-test. Data shown is mean ± error. **b.** Western blot analysis of Htt and GFP protein levels in brain structures, cervical spinal cord and liver of the same AAV-injected mice and PBS-injected controls. Values for each region were normalized to HTT protein levels in age-matched PBS-injected mice. *p < 0.05, **p < 0.01, ***p < 0.001, ****p < 0.0001 by Student's unpaired two-tailed t-test. Data shown is mean ± SD.

CHAPTER IV

In vivo selection yields novel AAV-B1 capsid for CNS and muscle gene therapy

Abstract

Adeno-associated viral (AAV) vectors have shown promise as a platform for gene therapy of neurological disorders. Achieving global gene delivery to the central nervous system (CNS) is key for development of effective therapies for many of these diseases. Here we report the isolation of a novel CNS tropic AAV capsid, AAV-B1, after a single round of *in vivo* selection from an AAV capsid library. Systemic injection of AAV-B1 vector in adult mice and cat resulted in widespread gene transfer throughout the CNS with transduction of multiple neuronal sub-populations. In addition, AAV-B1 transduces muscle, beta cells, pulmonary alveoli and retinal vasculature at high efficiency. This vector is more efficient than AAV9 for gene delivery to mouse brain, spinal cord, muscle, pancreas and lung. Together with reduced sensitivity to neutralization by antibodies in pooled human sera, the broad transduction profile of AAV-B1 represents an important improvement over AAV9 for CNS gene therapy.

Results

Single round of selection in mouse yields novel synthetic capsids

We sought to isolate chimeric AAV variants capable of CNS transduction upon systemic delivery in adult mice after one round of library selection (**Figure 4.1a**). We constructed an AAV capsid library by DNA shuffling of AAV1, 2, 4, 5, 6, 8, 9, rh8, rh10, rh39 and AAVrh43 capsid genes. The parental capsids were chosen for their ability to transduce CNS upon intravenous delivery in neonatal mice[69]. The plasmid library had a maximum diversity of $2x10^7$ capsids, based on transformation efficiency. Sanger sequencing of individual capsids from the viral library confirmed the chimeric nature of capsid genes in the library (**Figure 4.2**). The AAV library was infused into adult C57BL/6 mice via the tail vein at $1x10^{11}$ or $5x10^{11}$ genome copies, and tissue resident capsid genes were PCR amplified from brain and liver after 3 days. Of capsids isolated from brain, AAV-B1 was the only one amplified from the mouse infused at the lower dose, while AAV-B2, B3 and B4 were isolated from the high dose. In contrast, numerous capsids were found in liver of mice infused at either dose, the major depot organ of systemically infused AAV. All new AAV capsid genes were chimeric, but the VP3 capsid genes of brain clones (AAV-B1 through B4) were mostly comprised of DNA derived from either AAV8 or AAVrh43 (**Figure 4.1b**), while liver-isolated capsid genes were more diverse (**Figure 4.1c**). Analysis of capsid protein sequences revealed greater homology between capsids isolated from brain (97.3% pairwise homology) (**Figure 4.1d**) compared to capsids isolated from liver (88.6% pairwise homology) (**Figure 4.1e**).

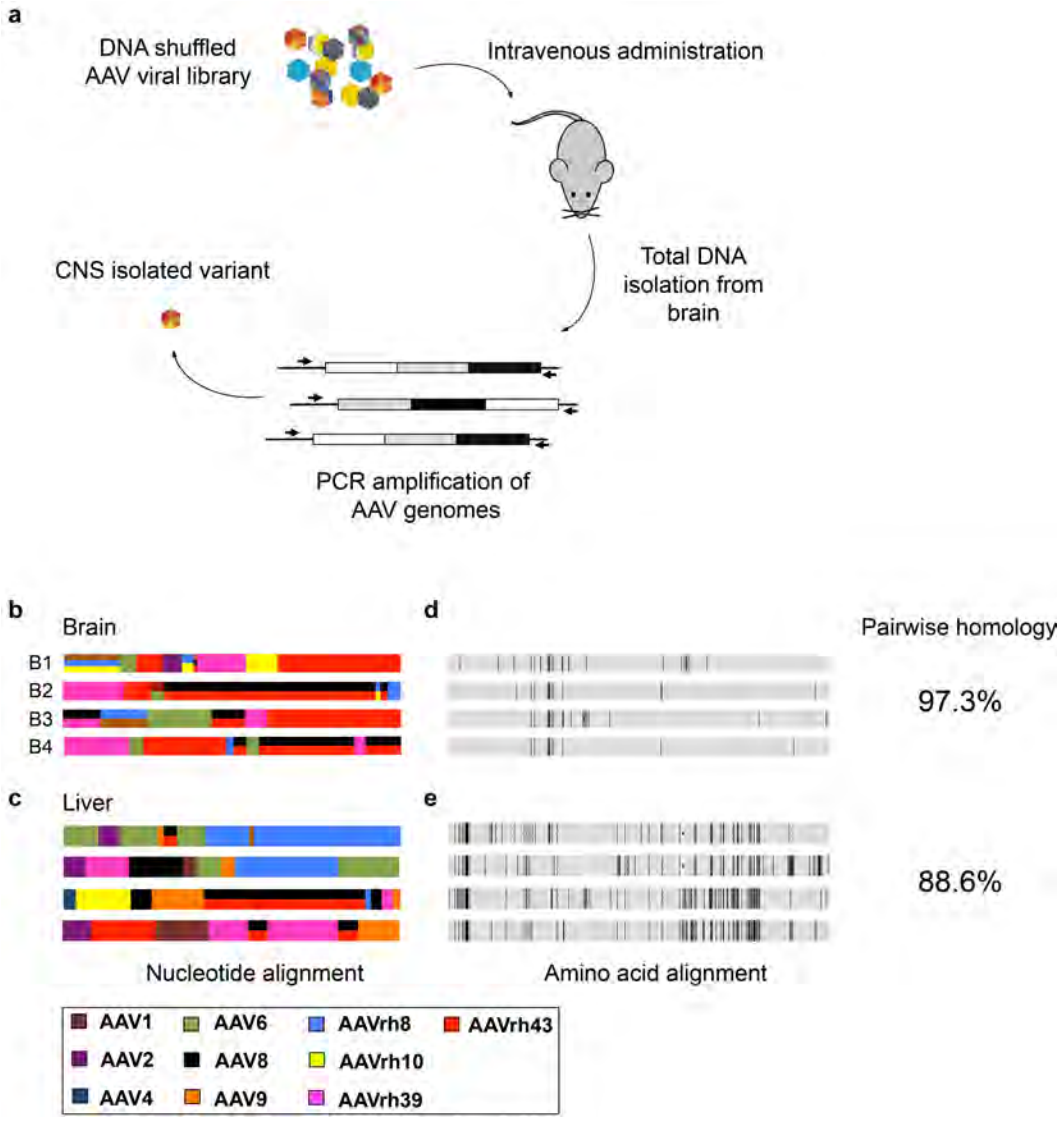

Figure 4.1: Single round *in vivo* biopanning. (**a**) Selection strategy. (**b, c**). Parental capsid gene contribution to new chimeric capsid genes isolated from (**b**) brain (AAV-B1, -B2, -B3, and -B4) and (**c**) liver. (**d, e**) Amino acid homology among capsids isolated from (**d**) brain and (**e**) liver. Grey areas indicate homology; black lines indicate non-homologous amino acids. % homology is calculated for amino acid composition.

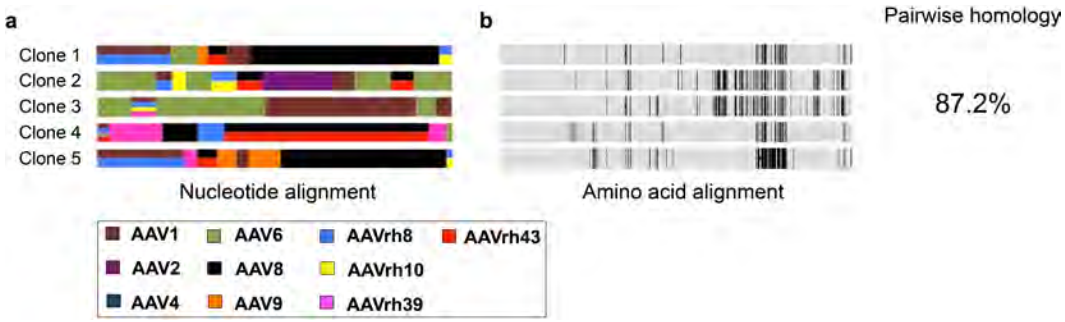

Figure 4.2: Chimeric nature of packaged viral library. a. Parental capsid contribution to five capsid genes PCR amplified from packaged viral library. **b.** Homology between capsids at the amino acid level. Grey areas indicate homology; black lines indicate non-homologous amino acids. % homology is calculated for amino acid composition.

Brain-selected AAV-B1 transduces mouse neuronal populations, and is superior to AAV9 for CNS gene transfer

The CNS transduction profile of AAV-B1 was assessed after systemic delivery in adult mice using a green fluorescent protein (GFP) expression cassette (**Figure 4.3a**). AAV-B1 vector transduced neuronal, glial and endothelial populations throughout the CNS (**Figure 4.3b, Figure 4.4, Figure 4.5**). Neuronal transduction was apparent in multiple regions of the cerebral cortex, including the primary (**Figure 4.3b**) and secondary (**Figure 4.4**) motor and somatosensory cortices, cingulate cortex and piriform (olfactory) cortex (**Figure 4.3b**). A sparse number of DARPP32-positive medium spiny neurons in the striatum were found transduced (**Figure 4.5a**). In the hippocampal formation, we found transduced granule cells in dentate gyrus (**Figure 4.3b, Figure 4.5b**) and pyramidal neurons in CA1-CA3 areas (**Figure 4.4**). Similar patterns of gene transfer to hippocampal neurons have been reported for AAV9[73]. Neurons in the thalamus (**Figure 4.3b, Figure 4.5b**), hypothalamus, amygdala (**Figure 4.3b**) and tyrosine hydroxylase (TH)-positive dopaminergic neurons in the substantia nigra (**Figure 4.5b**) were similarly transduced with AAV-B1. In the cerebellum, AAV-B1 vector transduced Purkinje cells (identified by calbindin D-28K co-staining) (**Figure 4.3b, Figure 4.5c**) as well as neurons in the granular layer. Finally, AAV-B1 vector transduced motor neurons throughout the spinal cord (**Figure 4.3b, Figure 4.4, Figure 4.5d**).

In addition to the neuronal tropism, AAV-B1 also transduced endothelial cells in the brain and spinal cord identified by the distinct morphology of blood vessels in CNS and confirmed by co-staining for CD31 (**Figure 4.5e**). AAV-B1 also transduced glial cells such as mature oligodendrocytes (identified by co-staining

for APC) (**Figure 4.5f**) and astrocytes (identified by morphology) (**Figure 4.5g**). Strong transduction of the choroid plexus was also apparent (**Figure 4.4**).

Quantitative analysis of AAV vector genomes in different regions of the CNS revealed 5.8- to 14.5-fold higher content for AAV-B1 compared to AAV9 (**Figure 4.3c**).

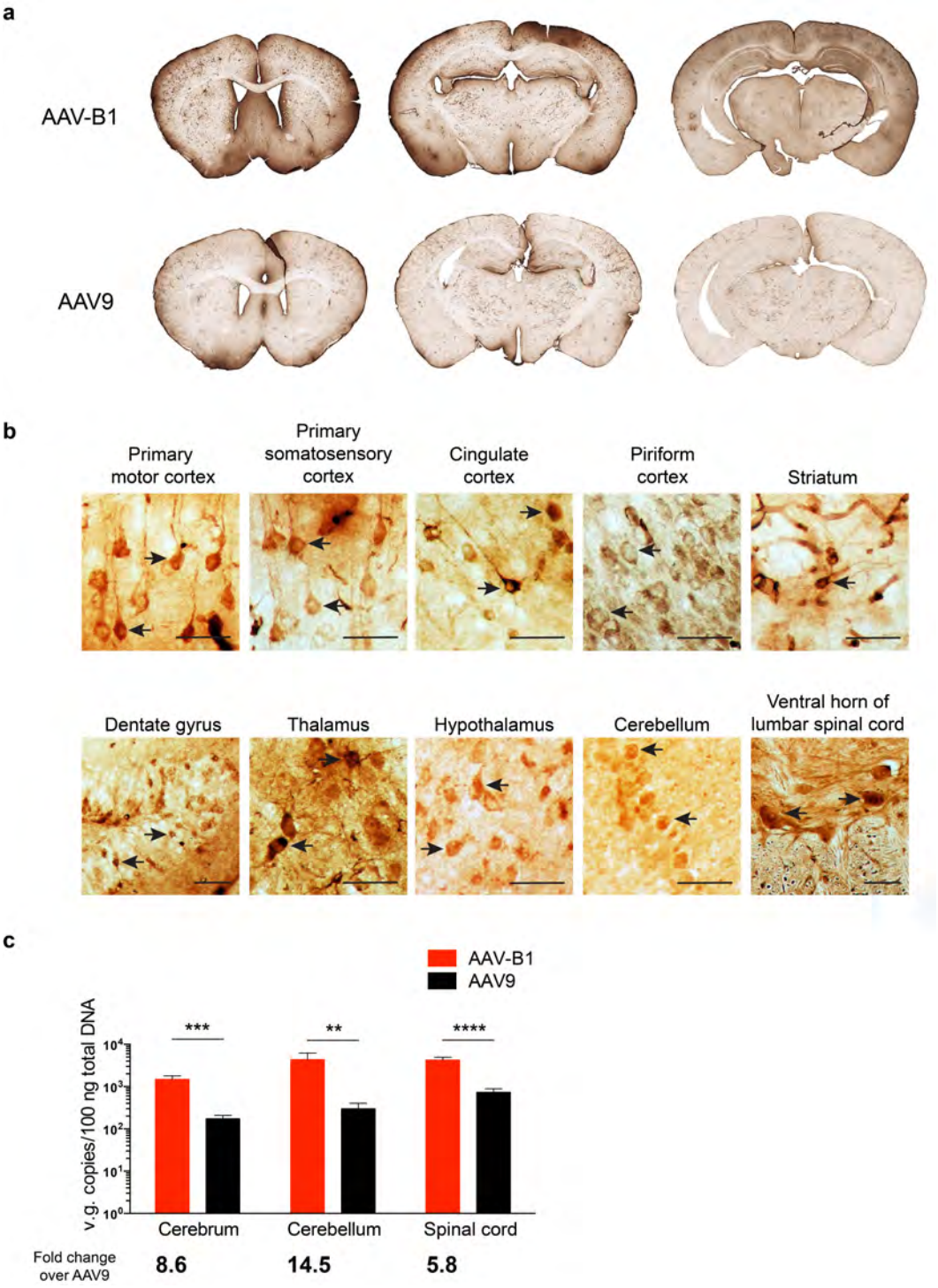

Figure 4.3: CNS transduction profile of AAV-B1 vector after intravascular infusion in adult mice.

Figure 4.3: CNS transduction profile of AAV-B1 vector after intravascular infusion in adult mice. (**a**) Overview of GFP distribution in brains of AAV-B1 and AAV9 injected mice ($2x10^{12}$ vg/mouse)**.** Representative images of coronal brain sections located at +0.5mm, -1.80mm and -3.00mm (left to right) in relation to bregma are shown. (**b**) Transduction of neuronal populations in different CNS regions of AAV-B1 injected mice. Black arrows indicate examples of GFP-positive neurons identified by morphology. Bar = 50 µm. (**c**) Comparison of AAV vector genome content in cerebrum, cerebellum and spinal cord of mice injected with $5x10^{11}$ vg AAV-B1 or AAV9 (N=4 animals per group). Age matched non-injected mice were included as controls (not shown). **p < 0.01, ***p < 0.001, ****p < 0.0001 by Student's two-tailed unpaired t-test.

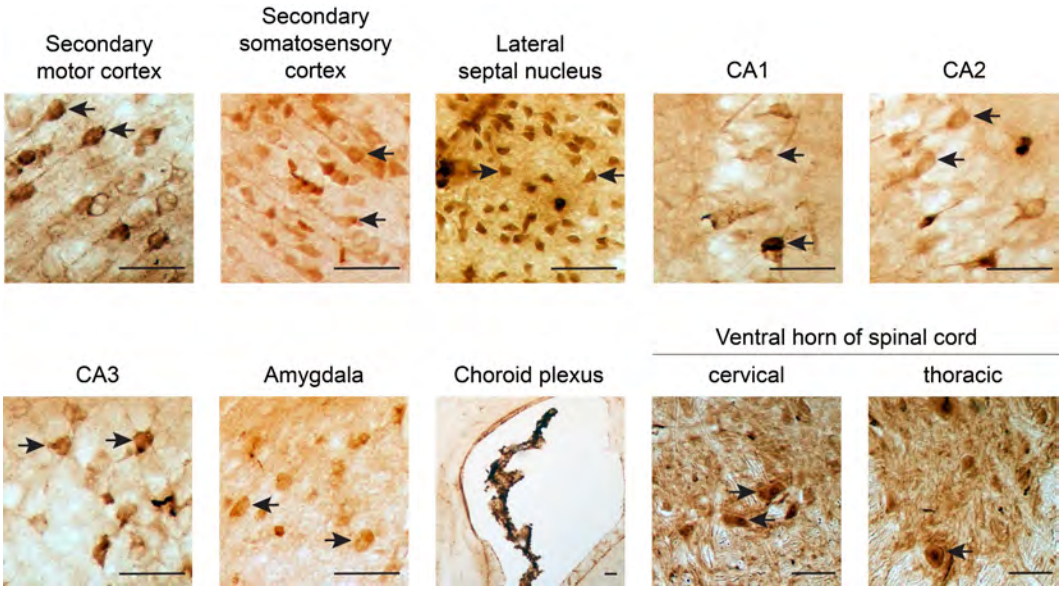

Figure 4.4: Transduction profile of AAV-B1 vector across multiple CNS regions after systemic delivery. Black arrows indicate examples of GFP-positive neurons. Bar = 50 μm.

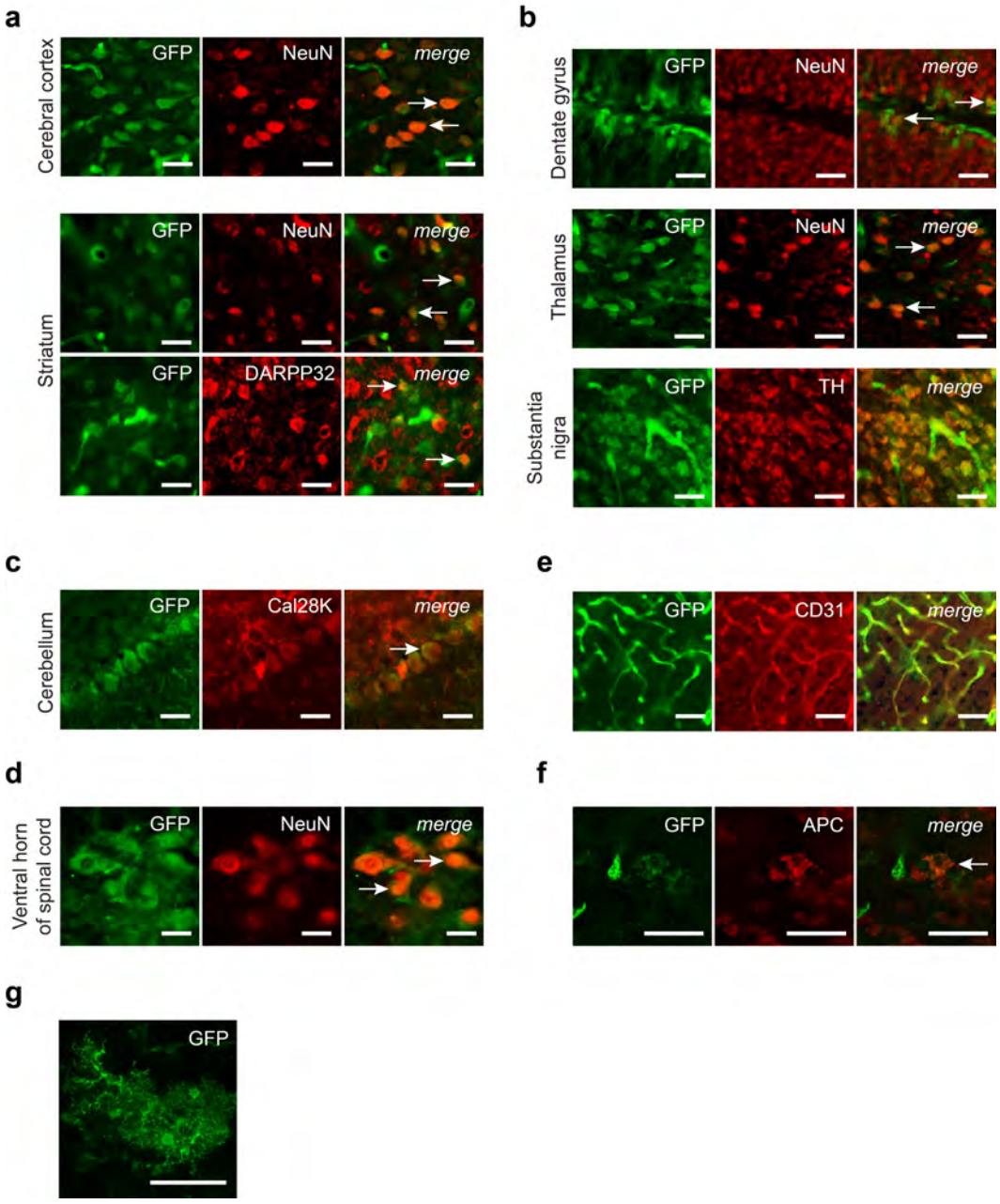

Figure 4.5: Phenotype of GFP positive cells in CNS after systemic delivery of AAV-B1. Transduced cells were identified by double immunofluorescence staining with antibodies to GFP, pan-neuronal marker NeuN (**a**, **b** and **d**), striatal medium spiny neuron marker DARPP32 (**a**), dopaminergic neuron marker tyrosine hydroxylase (TH) (**b**), Purkinje neuron marker calbindin-D-28k (Cal28K) (**c**), endothelial marker CD31 (**e**), and mature oligodendrocyte marker APC (**f**). The large size, morphology and location of GFP-positive neurons in the ventral spinal cord suggest a motor neuron identity. GFP-positive astrocytes (**g**) were identified based on their morphology. White arrows indicate examples of co-localization. Bar = 10 μm.

CNS tropism of mouse-selected AAV-B1 extends to a large animal species

Several novel therapies have been tested in feline models of neurological disorders prior to clinical trials[314, 335-337]. To investigate whether the CNS tropism of mouse-selected AAV-B1 is reproducible in a large animal species relevant to translational research, we infused AAV-B1 vector systemically into a normal juvenile cat through the carotid artery. We observed widespread neuronal gene transfer throughout the cat brain (**Figure 4.6**)**.** Mirroring the neuronal transduction pattern in mouse, AAV-B1 transduced neurons in the cat cerebral cortex, striatum, hippocampus, thalamus and Purkinje neurons in the cerebellum (**Figure 4.6**). In addition, we observed transduced motor neurons throughout the midbrain. Unlike in mouse, we found no indication that AAV-B1 transduced endothelial cells in the cat CNS.

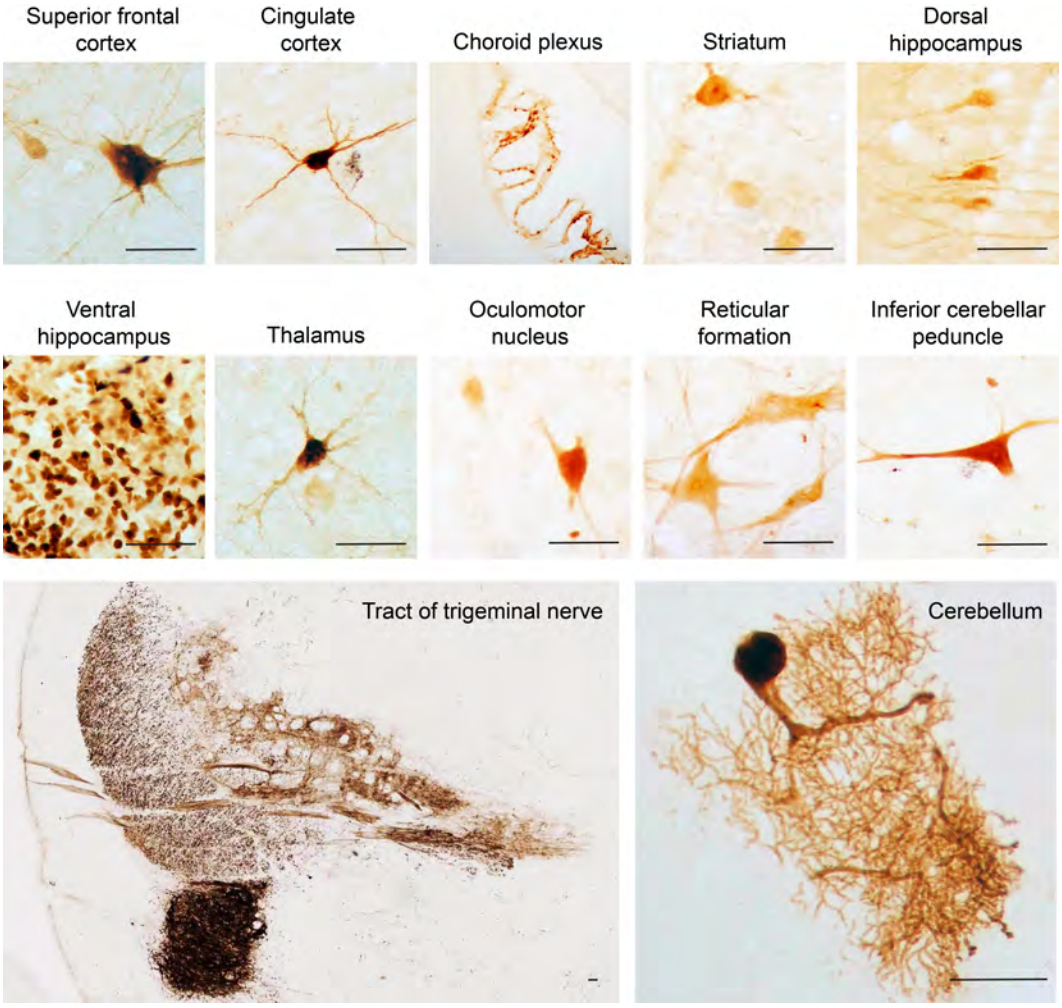

Figure 4.6: Neuronal transduction in cat brain after systemic delivery of AAV-B1 vectors. GFP distribution in the cat brain after systemic delivery of $3.4x10^{12}$ vg AAV-B1 vector. Representative images show GFP-positive cells with neuronal morphology in various structures in the brain. Image of tract of trigeminal nerve shows GFP staining of nerve fibers. Bar = 50 µm.

AAV-B1 as a global gene therapy vector

Next we assessed the peripheral transduction profile of AAV-B1. Liver transduction by AAV-B1 was lower than AAV9 as assessed by histological examination of GFP expression (**Figure 4.7a**). The vector genome content of AAV-B1 liver was 3-fold lower than AAV9 (**Figure 4.7b**). AAV-B1 proved to be highly efficient in transducing skeletal muscle and heart (**Figure 4.7c**) where vector genome content was 10.4- to 26.6-fold and 14.4-fold higher than AAV9, respectively (**Figure 4.7d**). AAV-B1 also transduced insulin-positive beta cells (**Figure 4.7e**) and lung alveoli (**Figure 4.7f**) at high efficiency. The vector genome content in pancreas and lung was 21.3- fold and 14.1-fold higher for AAV-B1 than AAV9, respectively (**Figure 4.7g, h**). Finally retinal endothelium was also transduced at high efficiency (**Figure 4.7i**), a property that is unique to AAV-B1[338].

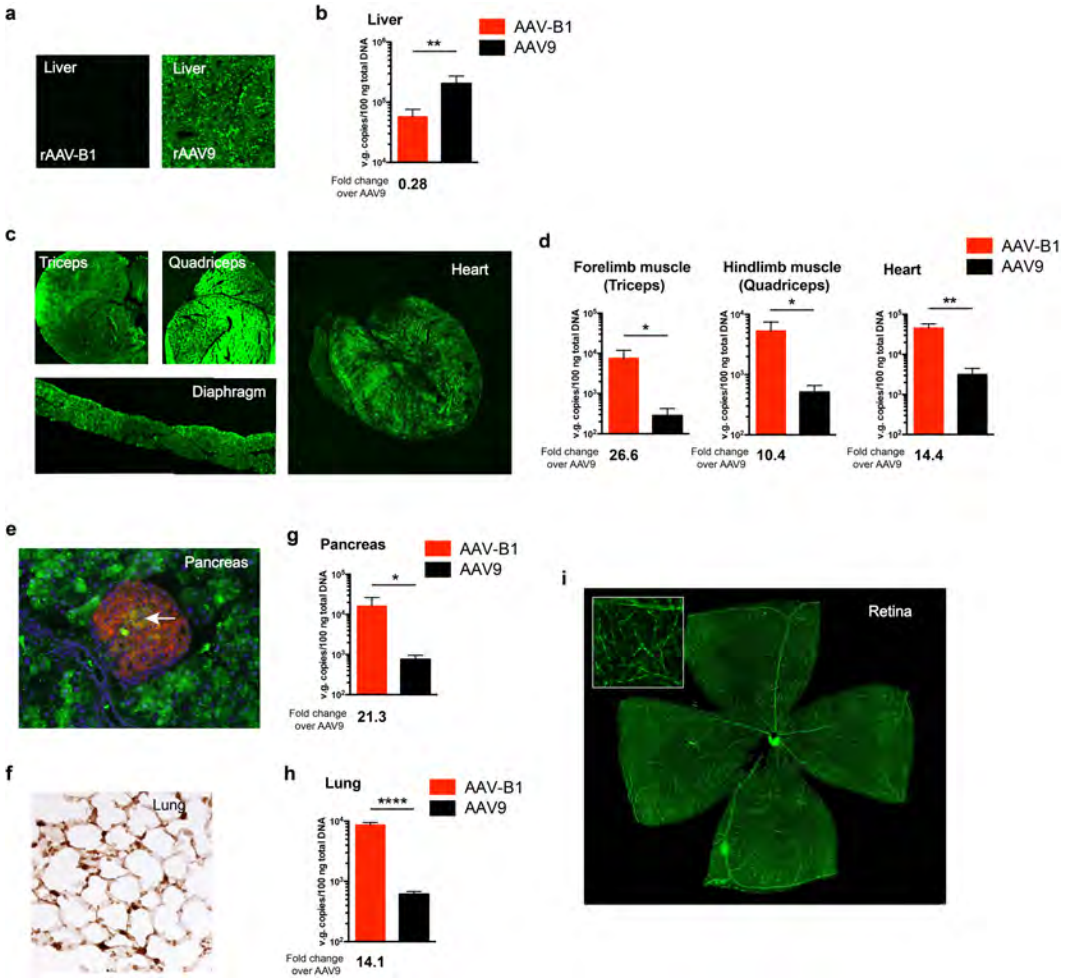

Figure 4.7: AAV-B1 biodistribution to other mouse tissues after intravascular delivery. GFP expression in (**a**) liver of AAV-B1 and AAV9 injected mice ($2x10^{12}$ vg/mouse), (**c**) skeletal muscle (triceps and quadriceps), diaphragm and heart, (**e**) pancreas, (**f**) lung, and (**i**) retina of AAV-B1 injected mice ($5x10^{11}$ vg/mouse). White arrow in **e.** indicates GFP (green)-positive insulin (red)-producing beta cells. Inset in **i.** shows individual GFP-positive blood vessels. Comparison of AAV vector genome content in (**b**) liver, (**d**) muscle groups, (**g**) pancreas and (**h**) lung of mice injected with $5x10^{11}$ vg AAV-B1 or AAV9 is shown (N=4 animals per group). *p<0.05, **p < 0.01, ****p < 0.0001 by Student's two-tailed unpaired t-test.

Biophysical characteristics of AAV-B1

AAV-B1 differs from AAV8, its closest parental capsid, by 19 amino acids (A24D, Q84K, A98V, L129F, P148Q, R152E, T157S, S223N, L235M, A268S, Q412E, T414S, T416Q, T452S, N458R, T461Q, G463L, G467A and F502S) (**Figure 4.8**). Structural modeling of AAV-B1 capsid based on the AAV8 template showed that most amino acids in VP3 that differ between the two capsids cluster in two regions, the βG strand (Q412E, T414S, T416Q) and the VR-IV loop (T452S, T461Q, G463L, and G467A) that were apparently derived from the AAVrh10 *cap* gene. The A268S substitution in the VR-I loop is a small side chain residue in representative AAV serotypes and is considered a conservative change. All surface exposed residues in VR-IV were of AAVrh10 origin except for N458R, which is not identified with any representative AAV genotypes (**Figure 4.9a**, **b)**. Despite the high degree of homology between AAV-B1 and AAV8, we confirmed that AAV-B1 and AAV8 have distinct biodistribution profiles after systemic infusion in adult mice (**Figure 4.10**).

Pre-existing humoral immunity is a major challenge for AAV-based clinical gene therapy[306]. We used a pooled human immunoglobulin-G (IVIG) neutralization assay to assess the immunological properties of AAV-B1 and found it to be more resistant to neutralization than AAV9 at all concentrations tested (**Figure 4.9c**).

To determine whether AAV-B1 uses the same cell-surface receptor as AAV9 given the shared CNS and muscle tropism, we performed cell binding assays using parental (Pro5) and sialic acid-deficient (Lec2) CHO cells. Surface exposed sialic acid residues allow for binding of capsids such as AAV1[200], AAV4[48], AAV5[48]

and AAV6[200] to Pro5 cells, while surface glycans on Lec2 cells are non-sialylated and thus have exposed galactose residues used by AAV9 as a receptor [50, 205]. AAV-B1 did not exhibit preferential binding to either cell line, indicating that neither terminal sialic acid nor terminal galactose preferentially act as primary glycan receptors for AAV-B1 capsid (**Figure 4.9d**).

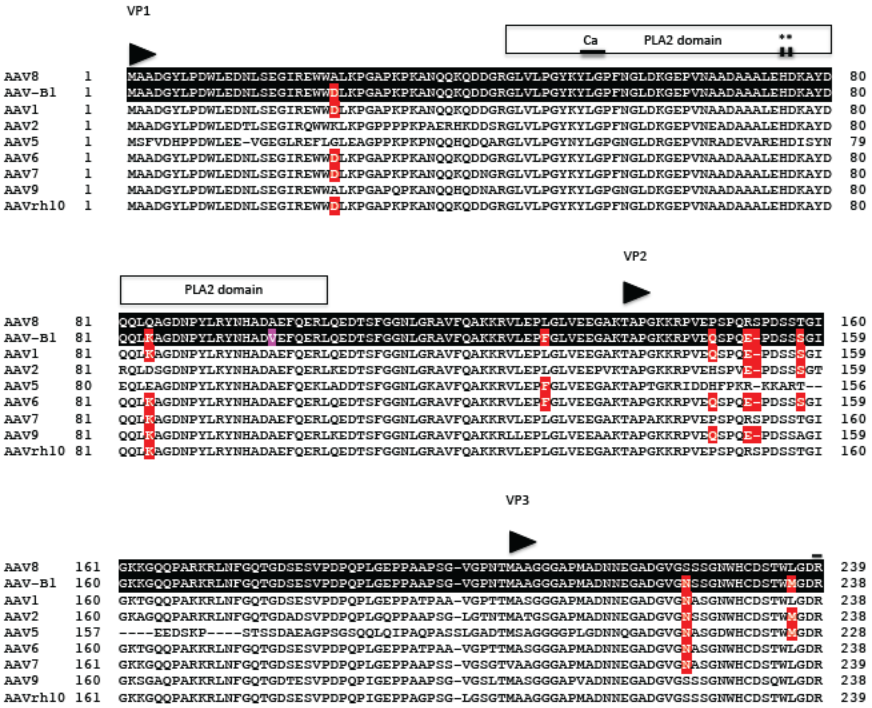
VP1
Ca
PLA2 domain
VP2
PLA2 domain
VP3

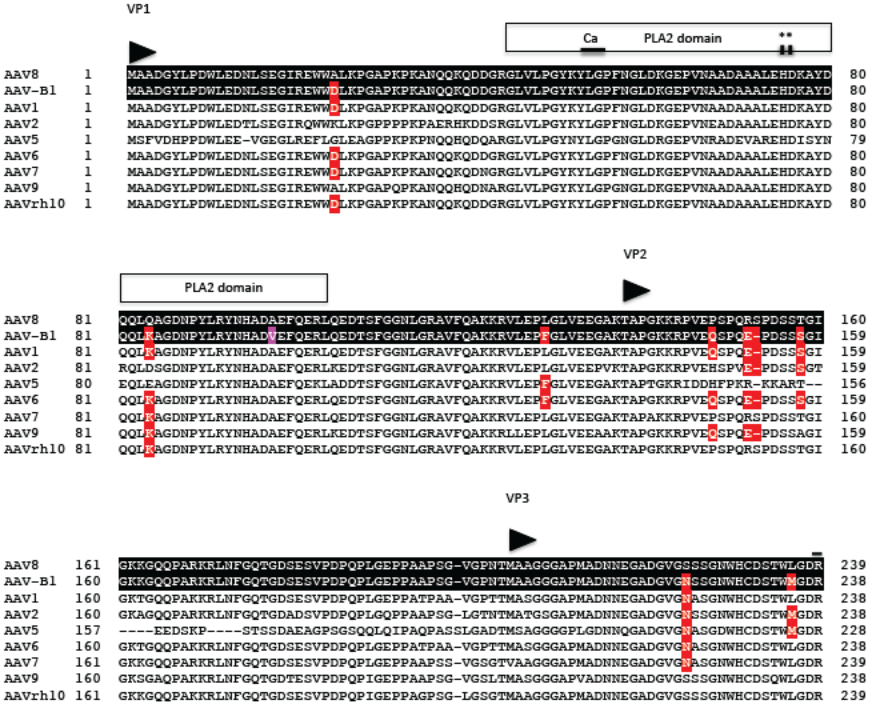
VP1
Ca
PLA2 domain
VP2
PLA2 domain
VP3

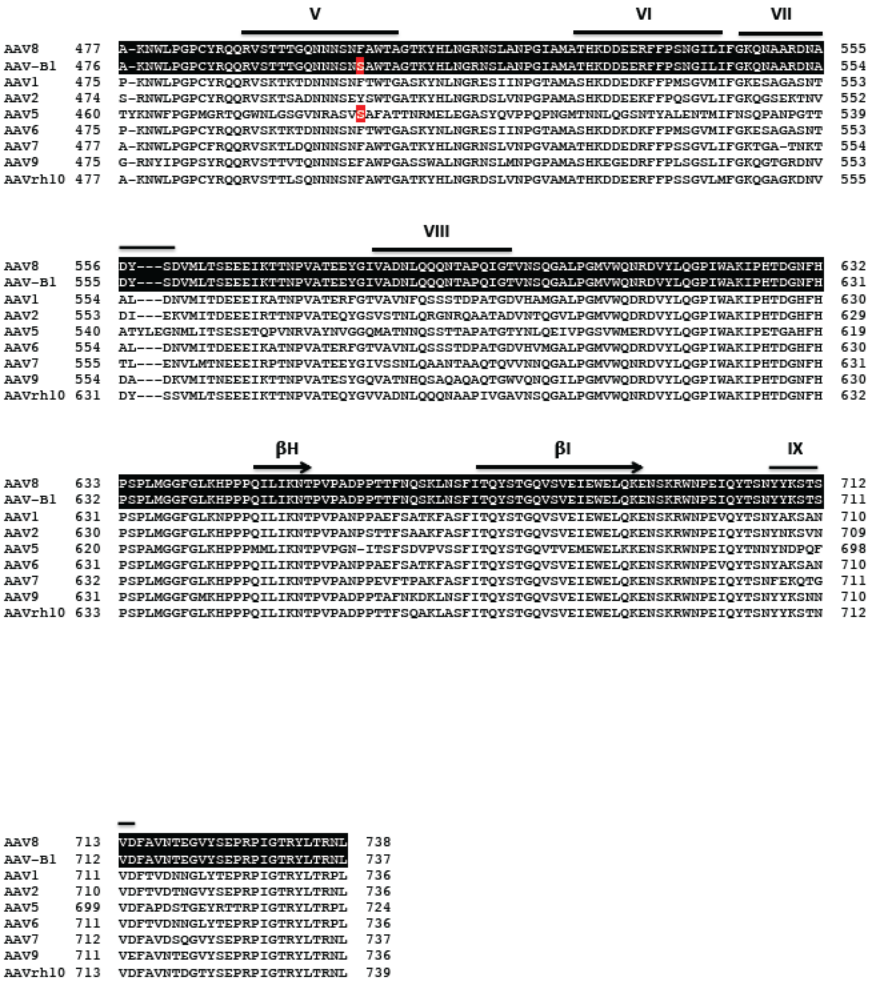

Figure 4.8: Comparison of AAV-B1 capsid protein sequence to AAV8 and other natural AAV isolates. The top two lines highlight the similarities and differences between amino acid sequences of AAV8 and AAV-B1, with singleton residue variants relative to AAV8 highlighted in red. The residues highlighted in pink indicate variant residues with no corresponding orthologs in the nine AAV species presented in the alignment. Translation start sites for VP1, VP2, and VP3 are indicated with filled triangles. The conserved parvovirus phospholipase A2 domain (approximately residues 44 to 104) in the VP1 unique region with the conserved AAV calcium-binding motif (Y-X-G-P-G/F) and catalytic residues (H-D-X-X-Y) are indicated with filled rectangles. The secondary structural elements are labeled with the corresponding text and the following symbols: β sheets B, C, D, E, F, G, and I are indicated with a horizontal overlined arrow. The positions of the variable loops (VR), I through IX, are indicated. The position of the conserved α helix is indicated with three parallel horizontal lines.

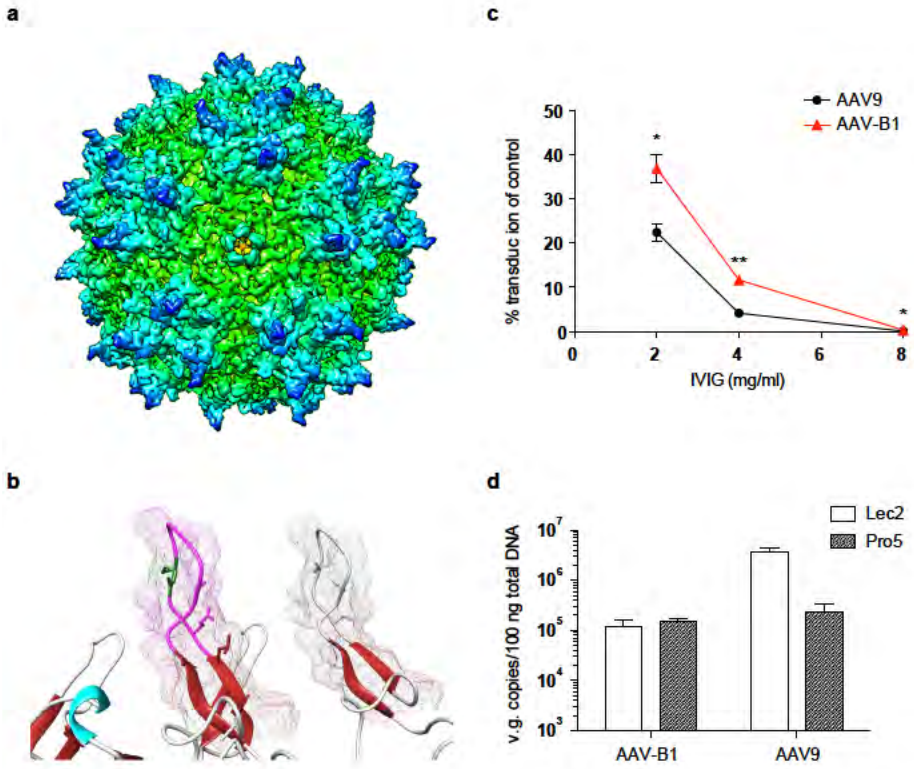

Figure 4.9: Structure, binding and neutralizing antibody analysis of AAV-B1. (**a**) Predicted molecular model of AAV-B1 capsid. (**b**) Surface exposed variable region-IV (VR-IV) of AAV-B1 (left) and AAV8 (right). (**c**) Pooled human IVIg neutralization assay and (**d**) CHO cell binding assay of AAV-B1 and AAV9 vectors. Data shown as mean ± SEM in (**c**), and as mean ± SD in (**d**). Experiment was performed with N=3 biological replicates. *p<0.05 by one-way ANOVA.

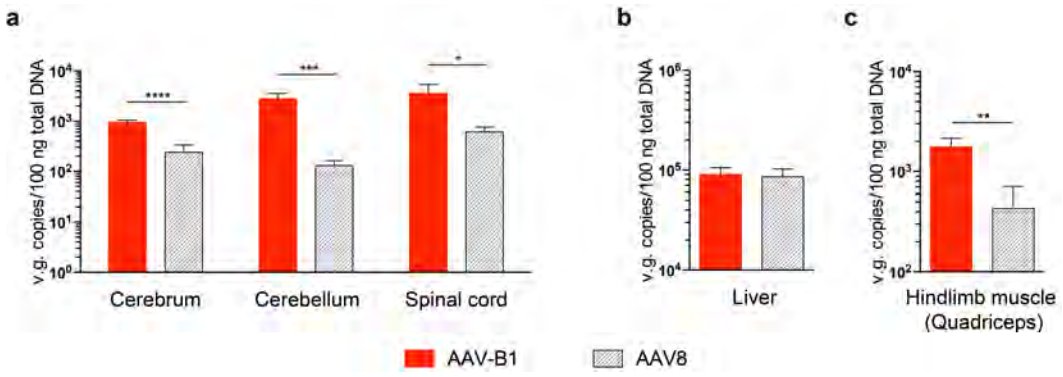

Figure 4.10: Biodistribution profile of AAV-B1 and AAV8 vectors infused systemically at 5x10^{11} vg. AAV vector genome content (N=4 animals per group) in **a.** CNS, **b.** liver and **c.** skeletal muscle (quadriceps) is shown. *p<0.05, **p < 0.01, ***p < 0.001, ****p < 0.0001 by Student's unpaired two-tailed t-test.

CHAPTER V

Discussion

Viral vector-mediated gene therapy holds great promise for treatment of neurological disorders. The current benchside efforts continue to be targeted towards generating better vectors, both at the virion level (e.g., developing capsids capable of crossing the BBB and targeting specific cell types) and at the transgene level (e.g., promoter and transgene design to improve efficacy in desired cell populations). Better non-invasive vector delivery routes for global and widespread CNS gene delivery are also being investigated for multi-focal neurological disorders. The result of this has been a slew of clinical trials for CNS disorders, which have been shown to be safe and non-toxic in Phase I, but few have been as efficacious in demonstrating therapeutic outcomes as perhaps may have been expected based on preclinical studies. These early trials have shed light on a myriad of challenges that must be surmounted for unequivocal clinical success. One of the major problems is the lack of good predictive animal models and inherent differences between species, which could be a primary cause of the failure of favorable preclinical outcomes to translate to the clinic. The potential of immune responses, both against the vector and expressed transgene, is often overlooked for neurological gene therapy, as the CNS is considered immune-privileged. This assumption has had to be revised in recent years as studies have demonstrated not only the generation of anti-capsid neutralizing antibodies, but also immune-mediated clearance of transduced antigen-presenting cells in the CNS[339, 340], which raises concerns for the next generation of CNS gene therapy clinical trials. More insight into the etiology of neurological disorders and particularly the development of biomarkers for early detection of disease will be of great help moving forward, as delivering therapies prior to onset of neurodegeneration will be key to improving efficacy of clinical intervention. Finally, recent advances in gene editing technologies, particularly CRISPR-Cas9, could

lead to a move away from the current gene replacement therapies towards more permanent genome editing. The regulatory approval of Glybera, an AAV1 clinical vector for lipoprotein lipase deficiency, in the European Union, the US FDA regulatory approval for the oncolytic HSV-based T-VEC for therapy of advanced melanoma, and the recent encouraging results of Phase III clinical trials of AAV2-based SPK-RPE65 vector for inherited retinal dystrophies (IRDs) has raised hopes that similar success may follow for gene therapy of neurological disorders in the future.

As outlined in **Chapter I**, the utility of AAV vectors for gene transfer is determined by the capsid, which is involved in several key cell entry steps. In-depth understanding of the capsid structure-function relationship, either through elucidation of AAV structure or through functional studies, has resulted in development of improved variants that possess a number of features such as enhanced transduction of a particular cell population *in vitro* or *in vivo*, altered tropism, or increased evasion of neutralizing antibodies, among others. Several challenges exist, however, before a greatly expanded toolbox of such vectors can be created for clinical use. Chief among them is the translatability of properties of capsids selected in cell culture or even in mice or NHPs, to humans. Even reproducibility of transduction profiles from *in vitro* to *in vivo* application is difficult, due to additional complicating factors such as blood-organ barriers that prevent the virus from interacting with target cells *in vivo*. The lack of exhaustive knowledge of all capsid interactions with the host cell, or even the host cell glycan receptors for every serotype, further compounds the challenge. The mechanism by which re-engineered capsids (particularly those isolated by library approaches) derive their superior gene transfer properties is almost entirely

unknown, which means that most capsid re-engineering efforts are semi-mechanistic at best. A consequence of the non- or semi-mechanistic approach to capsid engineering is that the designed capsid may exhibit properties different from the desired one. For example, AAVM41, originally selected from skeletal muscle, targets cardiac muscle preferentially[247]. Finally, variability in observed biological properties of a capsid between reports is concerning. Numerous examples abound, such as whether the human hepatocyte-selected AAVLK03 is superior to AAV8 or the very similar AAV3B at targeting hepatocytes of human origin[249, 341], or whether surface tyrosine-mutated AAV8 and AAV9 vectors enhance gene transfer[286], to mention a couple. Many factors could be responsible, such as injected dose and volume[342, 343], or even method of vector production[344], all of which can influence the tropism of a particular capsid. Even the use of ubiquitous promoters, which conventionally can drive expression in numerous cell types, can skew the apparent transduction profile of a capsid. For example, intraparenchymal injections with ubiquitous CBA-[315, 345], CMV-[346, 347] or RSV-[31] encoded AAV vectors indicate an almost exclusive neurotropic profile for most AAV serotypes with negligible gene transfer to other cell populations in the CNS; however, the same serotypes can mediate robust transduction of other cell types such as astrocytes[348] and oligodendrocytes[348, 349] when expression is driven by cell-specific promoters. One field that is likely to benefit in particular from further insight into capsid biology, is gene therapy for neurological disorders, where capsid re-engineering can lead to improved vectors allowing widespread genetic access across the brain and spinal cord.

The enhanced CNS transduction properties of AAV-AS represent an important improvement from AAV9 toward the ultimate goal of achieving gene transfer to

the majority of cells in the CNS, particularly neurons. The neuronal transduction efficiency of recently discovered capsids capable of crossing the adult BBB (such as AAVrh8 and AAVrh10) is not quantitatively higher than AAV9[70]. In contrast, the new AAV-AS vector described here is more efficient than AAV9 at transducing neurons in striatum and cerebral cortex. In addition, transduced motor neurons are evident in the spinal cord of AAV-AS injected mice, in contrast to AAV9 used in these experiments and in prior work[68]. Nonetheless the CNS transduction profile of AAV9 in this study appears less robust than in previous publications[73, 323], possibly due to the lower dose and the relatively weak intron-less promoter used in this study. While we are unable to completely exclude the possibility that the potency of our AAV9 vector is lower than those from other laboratories, we believe this is unlikely a major factor in the results reported here because the AAV vectors were prepared by the same method and titers determined in the same qPCR reaction to ensure that animals received comparable doses of the two vectors. Moreover, the CNS neuronal transduction profile of AAV-AS was also reproduced in a normal cat, although some differences such as the absence of transduced endothelium were apparent, which could be the result of variability in promoter efficiency across species. An important aspect to consider is that the widespread neuronal transduction profile of AAV-AS was achieved with a dose ($5x10^{11}$ vg/mouse) approximately 8-10 fold lower than in previous studies characterizing the CNS tropism of AAV9[68] and other natural AAV capsids[70] in adult mice. The extent of striatal neuronal transduction far exceeds any previous publication with systemic delivery of any AAV capsid, regardless of dose. Nonetheless, it is important to note the neuronal transduction properties of this new AAV-AS capsid are not uniform across the

brain as evidenced by the considerable difference in percentage of GFP-positive neurons between striatum and thalamus.

The variability in neuronal transduction with AAV-AS in different brain structures is likely to be determined by the CNS distribution of cell surface receptor(s) used by this new AAV vector to cross the BBB and transduce neurons. Glycans with terminal galactose have been identified as the primary factor for AAV9 attachment to the cell surface[50, 205] and the galactose-binding domain on the AAV9 capsid surface has been identified[204]. Integrin binding appears to have a role in AAV9 transduction[213]. Nonetheless, the mechanism that AAV9 and other AAV capsids use to cross the BBB, or cerebrospinal fluid (CSF)-blood barrier as previously suggested[69] is presently unknown. To our knowledge, there is no evidence suggesting that poly-alanine peptides target the CNS after vascular infusion, or are present in proteins such as transferrin or insulin that are known to cross the brain through transcytosis. The topological location of the N-terminus of AAV VP2 is uncertain since there is no crystallographic information on the location of VP1 or VP2 proteins for any of the AAV capsids with characterized structures[180, 187]. A recent study however indicates that the N-terminus of chimeric VP2 proteins is exposed on the capsid surface of at least 70% of capsids[239], suggesting this may also be the case for the poly-alanine peptide in AAV-AS. The results from our study on CHO cells show that cell surface binding of AAV-AS is identical to AAV9 and AAV9.47, suggesting the interaction with glycans with exposed terminal galactose residues is not affected by the poly-alanine peptide. The impact of the poly-alanine residues, however, on the interaction of AAV9.47 capsid with co-receptors on the luminal surface of brain microvascular endothelial cells or other cells along the BBB and CSF-blood barrier is presently

unknown. Further studies will be necessary to uncover the mechanism that underlies this increased efficiency.

The potential of AAV-AS for development of potent therapies for neurological diseases is apparent by its efficacy in reducing huntingtin (Htt) mRNA by 40-50% in striatum and motor cortex - two structures relevant to HD pathophysiology - after a single systemic infusion. Earlier studies investigating direct striatal injection of AAV vectors encoding Htt-specific shRNA or microRNAs in adult mice have consistently reported no higher than 40-60% silencing of *Htt* mRNA at the injection site[110, 111, 350]. A recent study investigating the therapeutic efficacy of a systemically delivered AAV9-miR vector in HD mouse models was unable to demonstrate *Htt* mRNA knockdown in the brain of transgenic BACHD mice, and 33% mRNA knockdown in the striatum but no significant difference in the frontal cortex of N171-82Q mice upon administration of a higher dose[112], which agrees well with the extent of knockdown documented in this study with AAV9 vector.

There is an apparent discrepancy between the differential in GFP transduction efficiency of striatal neurons between AAV-AS and AAV9 vectors (36% vs <1 %) and the comparatively modest increase in *Htt* knockdown in the same structure with AAV-miR^{Htt} vectors. It is key to note that knockdown is a sum effect of all transduced cells in a particular structure, and not just the neuronal population. This is exemplified by the comparatively smaller 6-15 fold increase in AAV-AS transduction compared to AAV9 when measured by vector genome quantification, where the contribution of every transduced CNS cell is taken into account. This could indicate that AAV9 transduces other cell types to some extent, but the resulting GFP expression level from the CBA promoter used in this study is

below the detection limit of our immunohistochemical staining. By the same measure, it is possible the degree of enhancement of neuronal transduction between the two vectors may not be as large as suggested by the histological quantification results. Importantly, as mentioned above, AAV-mediated *Htt* silencing in the striatum after direct injection has been reported at a maximum of 40-60%, even at the site of local injection where the percentage of transduced cells is very high. The reasons for this maximum effect are unknown at the moment, but could be due to only a fraction of *Htt* mRNA in CNS cells being accessible to the RNAi pathway. Therefore the 33-50% reduction documented by systemic infusion of AAV-AS is likely to be near or at the maximum *Htt* silencing possible with AAV vectors engaging the RNAi pathway in the brain, irrespective of any further gene transfer efficacy. The use of differing promoters and vector doses further confounds drawing any direct quantitative correlation between the two experiments.

Treatment of diffuse and multifocal neurological pathologies by direct intraparenchymal injection is unlikely to lead to even distribution of the therapeutic molecule in the CNS, even with the use of advanced infusion techniques such as convection enhanced delivery[56], or by injection into axonally connected structures [51, 320-322]. In contrast, a single systemic infusion of AAV-B1 can mediate gene transfer to neuronal populations in multiple structures throughout the CNS, making it an attractive candidate for development of AAV-based gene therapies for neurological disorders. AAV-B1 is demonstrably superior to AAV9 for CNS transduction (approximately one log higher). Another important characteristic of AAV-B1 is the consistency of pan-neuronal transduction in both mouse and cat brain, as numerous naturally occurring

models of neurodegenerative diseases in the latter intermediate size species are often used in the translation of proof-of-concept experiments in mice to clinical trials in humans.

In addition to being extremely potent for CNS gene transfer as expected from the screening strategy of this study, AAV-B1 is also highly effective for gene transfer to a number of peripheral tissues including skeletal muscle, heart and lung. The broad transduction profile of AAV-B1 suggests several gene therapy applications, including those for systemic correction of monogenic neurometabolic disorders, muscular dystrophies and diabetes, as well as disorders involving the alveolar epithelium such as surfactant deficiencies. One such potential therapy application is for Pompe disease, a lysosomal storage disease that manifests as muscular atrophy, cardiorespiratory failure and glycogen storage in motor neurons[351]. AAV9 has limited therapeutic effect in adult Pompe disease mice [352], possibly due to inefficient mannose-6-phosphate receptor-mediated enzyme uptake in skeletal muscle [353] and insufficient AAV9 gene transfer efficiency. In addition, the unique retinal vasculature transduction profile of AAV-B1 may be useful for gene therapy of ocular vascular disorders like diabetic retinopathy and wet age-related macular degeneration. The higher resistance of AAV-B1 to pre-existing neutralizing antibodies in pooled human sera suggests that systemic gene therapies based on this new capsid may be applicable to a broader population of patients.

The isolation of AAV-B1 is the first instance where an AAV capsid capable of crossing a non-compromised blood brain barrier (BBB) has been selected from a chimeric capsid library. While the AAV-B1 capsid was selected at the lower

library dose, it does not exclude the possibility of stochastic selection. This could theoretically be resolved by repeating the selection to isolate the same or homologous capsid variants. An argument against AAV-B1 being selected stochastically, however, is the greater VP3 protein homology between brain-selected capsids compared to liver-resident variants, which suggests a structure-function relationship. One or more of the amino acid differences in surface-exposed domains of AAV-B1 and AAV8 likely account for the difference in tropism between these highly homologous capsids, although the present lack of structural data for AAV VP1 and VP2 N-terminal regions[180, 187] makes it difficult to speculate about the contribution of the numerous amino acid differences found in those regions to overall tropism. At the cell entry level, AAV-B1 appears to use neither sialic acid nor galactose preferentially as its cell surface receptor, similar to AAV8 whose primary receptor remains unknown. Further biophysical studies for this capsid may shed light on the unique biological properties of AAV-B1.

The mechanisms by which either of the re-engineered vectors AAV-AS and AAV-B1, or for that matter, even known natural AAV isolates such as AAV9, enter the brain after being injected into the vasculature is unknown. Speculation on how these modified AAV vectors gain access to the brain parenchyma will be useful for development of next generation CNS-targeted gene therapies.

The blood–brain barrier (BBB) provides an obstacle to free diffusion of vascular components into the brain parenchyma. In capillaries of peripheral organs, endothelial cells are separated by intercellular clefts and fenestra, which allow for non-selective diffusion across the capillary wall. In contrast, the BBB comprises of a network of specialized non-fenestrated endothelial cells (that have

intercellular junctions to restrict movement through inter-endothelial gaps). The capillary wall is further fortressed by a laminin-rich basement membrane, vascular pericytes, and astrocytic endfeet. Brain capillaries are therefore deficient in vesicular transport due to blocked free diffusion across the vessel. Instead, entry into the CSF can be achieved primarily in one of three ways: by passive diffusion of lipid-soluble molecules; by active receptor-mediated transport of water-soluble molecules (such as glucose and amino acids); and by ion channels.

The upper limit of pore size of BBB is <1 nm, which precludes passive transport of viruses across the capillary wall. Several viruses have therefore developed strategies to move into the nervous system through both circulatory and axonal routes. Viruses like human immunodeficiency virus (HIV) employ a ‘Trojan horse’ approach by infecting monocytes that pass through the BBB during normal turnover of perivascular macrophages or as result of the production of pro-inflammatory molecules, such as CC-chemokine ligand 2 (CCL2) that compromise the BBB. The human T-lymphotropic virus type 1 (HTLV1) binds to endothelial receptors such as glucose transporter type 1 (GLUT1), allowing for infection of endothelial cells and subsequent BBB leakage by release of pro-inflammatory mediators. Several other viruses such as Nipah virus, Japanese encephalitis virus (JEV), rabies virus, West Nile virus, and mouse adenovirus type 1 (MAV-1) also similarly disrupt the tight junction complex by induction of inflammatory cytokines or chemokines.

Whether any of these mechanisms are operative in this case is not clear. There is no evidence of neuroinflammation upon systemic administration of either re-

engineered vector or AAV9. It is possible therefore, that other novel mechanisms may be involved in AAV transport across the BBB.

Based on earlier reports using capsids with chimeric VP2, it is conceivable that the inserted polyalanine is expressed on the surface of the AAV-AS capsid. Such a surface exposed hydrophobic residue may change the physical properties of the capsid that may contribute to the transcytosis properties of AAV-AS. These may be tested *in vivo* by replacing the 19-mer polyalanine with polymers of other hydrophobic amino acids such as leucine, isoleucine and valine. The size and site of the polyalanine insertion may also play a role, as insertion of a 5-mer polyalanine into loop IV of the AAV2 capsid at site 587 is reported to not impact CNS targeting[237]. It has been reported that AAV capsids generated by the peptide insertion method used here, contain capsids that lack chimeric VP2 and increase off-targeting[239]. Though analysis of AAV-AS capsid proteins reveals that the peptide-fused VP2 is present, it is unclear what fraction of total capsids has all 3 VP proteins. Purification of VP2-containing capsids (by expressing a hexahistidine tag along with polyalanine and subsequent Ni^{2+} column purification, for example) could reduce AAV-AS gene transfer to peripheral tissues.

It is possible that AAV in general, or the two re-engineered capsids described here, may be transported across the BBB by ‘piggy-backing’ on receptor-mediated transcytosis systems, either by binding to known receptors such as transferrin receptor (TfR), insulin or insulin-like growth factor receptor and low density lipoprotein receptor-related proteins (LRPs), or an yet unknown one. The identity of this receptor can be ascertained by ligand-based receptor capture methods such as TRICEPS[354], a specifically designed reagent comprising of 3

orthogonal moieties: one that is coupled to amino groups on the AAV capsid surface, a second for the ligand-based capture of glycosylated receptors on brain microvascular endothelial cells (BMVECs) that constitute the BBB, and a biotin tag for purifying receptor peptides for analysis by quantitative mass spectrometry (MS). While not ideal, preliminary studies on the kinetics of AAV transcytosis can be performed using *in vitro* artificial BBB models.

Conversely, it is possible that these vectors do not change interaction of AAV at the BBB, but instead bind differently to serum proteins in the blood. For example, polysorbate 80-coated nanoparticles bind to apolipoproteins in the blood and therefore could undergo receptor-mediated endocytosis into the brain capillary endothelial cells via the LDL receptor family[355] and transcytosis into the brain parenchyma, which suggest exploring whether a similar phenomenon occurs for the polyalanine-coated nanoparticle-sized AAV-AS. This can be resolved by screening interacting partners in the serum by co-precipitation experiments. Human galectin-3 binding protein was identified as one such serum protein that bound to AAV6 and modulated vector distribution following intravenous delivery[356]. No such binding partner, however, has been identified for AAV8 (closest natural isolate of AAV-B1) or AAV9 (closest natural isolate of AAV-AS).

The question of how to select for an effective AAV capsid for human gene transfer remains a central and a particularly complex one. Rodents serve as ubiquitously important models for biomedical testing. However, rodents may have limited predictive capability for brain studies, as their brain circuitry, cognition and behavior differ significantly from humans. Non-human primates (NHPs) may be more appropriate for preclinical studies, as they share specialized brain

structures implicated in motor, perception and cognition capability (such as an expanded frontal cortex[357]) with humans that have no homolog in any other mammal.

However, gene transfer in animal models (which are used to test AAV vectors in a preclinical setting) may not translate to human populations. For example, systemic administration of AAV2 and AAV8 vectors in hemophilia B patients resulted in comparable levels of plasma factor IX expression[153, 306, 358]. In contrast, preclinical data from mouse and non-human primates clearly predict AAV8 to be the superior liver gene therapy vector[359-361]. One approach is to use humanized mouse models. These models are repopulated with particular human cell populations[362], and can be predictive of human transduction in efficacy studies. Humanized liver models have been used both as preclinical disease models for gene therapy[363], and also as a platform to select a chimeric capsid capable of enhanced human hepatocyte transduction[249], although whether this selected capsid is truly superior to natural isolates like AAV8 is debatable[341, 364]. Humanized brain mouse models are rare, primarily due to the embargo on research on human/non-human chimeras based on ethical considerations. Nevertheless, some models exist, such as human glial progenitor cell-engrafted mice that exhibit enhanced synaptic plasticity and learning[365]. Such models might be incredibly valuable to simulate the human brain for preclinical testing. However, many concerns exist for using humanized mouse models as predictive tools for clinical gene therapy, such as human donor-to-donor variability and disparity in extent of engraftment from mouse-to-mouse. Recent efforts in recapitulating human diversity in mouse models (such as Diversity Outbred mice[366] at The Jackson Laboratory) may be useful. Perhaps the biggest

drawback of humanized mouse models for AAV capsid and gene therapy studies is lack of a human immune system. Human preexisting neutralizing antibodies and capsid-specific T cell response, likely lacking in mouse models, inhibit AAV-mediated transduction in patients. This last factor can be reduced by steroid administration prior to AAV infusion. Reconstituting humanized mice models with Hu-CD34+ engraftment recapitulating the multilineage human immune system[367] will likely be more predictive of clinical gene therapy outcomes.

In conclusion, AAV-AS and AAV-B1 are the first AAV capsids with superior CNS gene transfer properties since the discovery of AAV9 and provide a potent new platform for development of novel gene therapies for neurological diseases.

Bibliography

1. Naldini, L. Gene therapy returns to centre stage. *Nature* **526(7573)**, 351-360. doi: 310.1038/nature15818 (2015).
2. Pierce, E.A. & Bennett, J. The status of RPE65 gene therapy trials: safety and efficacy. *Cold Spring Harb Perspect Med* **5(9)**, pii: a017285. doi: 017210.011101/cshperspect.a017285 (2015).
3. Biffi, A. et al. Lentiviral hematopoietic stem cell gene therapy benefits metachromatic leukodystrophy. *Science* **341(6148)**, 1233158. doi: 1233110.1231126/science.1233158 (2013).
4. Cartier, N. et al. Hematopoietic stem cell gene therapy with a lentiviral vector in X-linked adrenoleukodystrophy. *Science* **326(5954)**, 818-823. doi: 810.1126/science.1171242 (2009).
5. Piccioni, D.E. & Kesari, S. Clinical trials of viral therapy for malignant gliomas. *Expert Rev Anticancer Ther* **13(11)**, 1297-1305. doi: 1210.1586/14737140.14732013.14851160 (2013).
6. Tebas, P. et al. Gene editing of CCR5 in autologous CD4 T cells of persons infected with HIV. *The New England journal of medicine* **370(10)**, 901-910. doi: 910.1056/NEJMoa1300662 (2014).
7. Swiech, L. et al. In vivo interrogation of gene function in the mammalian brain using CRISPR-Cas9. *Nat Biotechnol* **33**, 102-106 (2015).
8. Bengtsson, N.E., Seto, J.T., Hall, J.K., Chamberlain, J.S. & Odom, G.L. Progress and prospects of gene therapy clinical trials for the muscular dystrophies. *Hum Mol Genet* **Oct 8**, pii: ddv420. [Epub ahead of print] (2015).
9. Bartus, R.T., Weinberg, M.S. & Samulski, R.J. Parkinson's disease gene therapy: success by design meets failure by efficacy. *Mol Ther* **22(3)**, 487-497. doi: 410.1038/mt.2013.1281 (2014).
10. Kay, M.A. et al. In vivo gene therapy of hemophilia B: sustained partial correction in factor IX-deficient dogs. *Science* **262(5130)**, 117-119 (1993).
11. Cavazzana-Calvo, M. et al. Gene therapy of human severe combined immunodeficiency (SCID)-X1 disease. *Science* **288(5466)**, 669-672 (2000).
12. Turner, D.L., Snyder, E.Y. & Cepko, C.L. Lineage-independent determination of cell type in the embryonic mouse retina. *Neuron* **4(6)**, 833-845 (1990).
13. Fields-Berry, S.C., Halliday, A.L. & Cepko, C.L. A recombinant retrovirus encoding alkaline phosphatase confirms clonal boundary assignment in lineage analysis of murine retina. *Proc Natl Acad Sci U S A* **89(2)**, 693-697 (1992).
14. Hacein-Bey-Abina, S. et al. LMO2-associated clonal T cell proliferation in two patients after gene therapy for SCID-X1. *Science* **302(5644)**, 415-419 (2003).
15. Hacein-Bey-Abina, S. et al. Efficacy of gene therapy for X-linked severe combined immunodeficiency. *The New England journal of medicine* **363(4)**, 355-364. doi: 310.1056/NEJMoa1000164 (2010).
16. Cattoglio, C. et al. Hot spots of retroviral integration in human CD34+ hematopoietic cells. *Blood* **110(6)**, 1770-1778 (2007).

17. Montini, E. et al. Hematopoietic stem cell gene transfer in a tumor-prone mouse model uncovers low genotoxicity of lentiviralvector integration. *Nat Biotechnol* **24(6)**, 687-696 (2006).
18. Blömer, U. et al. Highly efficient and sustained gene transfer in adult neurons with a lentivirus vector. *J Virol* **71(9)**, 6641-6649 (1997).
19. Brooks, A.I. et al. Functional correction of established central nervous system deficits in an animal model of lysosomal storage disease with feline immunodeficiency virus-based vectors. *Proc Natl Acad Sci U S A* **99(9)**, 6216-6221 (2002).
20. Barcia, C. et al. One-year expression from high-capacity adenoviral vectors in the brains of animals with pre-existing anti-adenoviral immunity: clinical implications. *Mol Ther* **15(12)**, 2154-2163 (2007).
21. Akli, S. et al. Transfer of a foreign gene into the brain using adenovirus vectors. *Nature genetics* **3(3)**, 224-228 (1993).
22. Davidson, B.L., Allen, E.D., Kozarsky, K.F., Wilson, J.M. & Roessler, B.J. A model system for in vivo gene transfer into the central nervous system using an adenoviral vector. *Nature genetics* **3(3)**, 219-223 (1993).
23. Dubensky, T.W. (Re-)Engineering tumor cell-selective replicating adenoviruses: a step in the right direction toward systemic therapy for metastatic disease. *Cancer Cell* **1(4)**, 307-309 (2002).
24. Wilson, J.M. Lessons learned from the gene therapy trial for ornithine transcarbamylase deficiency. *Mol Genet Metab* **96(4)**, 151-157 (2009).
25. Sheridan, C. Gene therapy finds its niche. *Nat Biotechnol* **29(2)**, 121-128. doi: 110.1038/nbt.1769 (2011).
26. Chiocca, E.A. et al. Transfer and expression of the lacZ gene in rat brain neurons mediated by herpes simplex virus insertion mutants. *New Biologist* **2**, 739-746 (1990).
27. Diefenbach, R.J., Miranda-Saksena, M., Douglas, M.W. & Cunningham, A.L. Transport and egress of herpes simplex virus in neurons. *Rev Med Virol* **18(1)**, 35-51 (2008).
28. Spaete, R.R. & Frenkel, N. The herpes simplex virus amplicon: a new eucaryotic defective-virus cloning-amplifying vector. *Cell* **30(1)**, 295-304 (1982).
29. Sena-Esteves, M., Saeki, Y., Fraefel, C. & Breakefield, X.O. HSV-1 amplicon vectors--simplicity and versatility. *Mol Ther* **2(1)**, 9-15 (2000).
30. Costantini, L.C., Bakowska, J.C., Breakefield, X.O. & Isacson, O. Gene therapy in the CNS. *Gene Ther* **7(2)**, 93-109 (2000).
31. Davidson, B.L. et al. Recombinant adeno-associated virus type 2, 4, and 5 vectors: transduction of variant cell types and regions in the mammalian central nervous system. *Proc Natl Acad Sci U S A* **97**, 3428-3432 (2000).
32. McCarty, D.M., Young, S.M. & Samulski, R.J. Integration of adeno-associated virus (AAV) and recombinant AAV vectors. *Annu Rev Genet* **38**, 819-845 (2004).
33. Bessis, N., GarciaCozar, F.J. & Boissier, M.C. Immune responses to gene therapy vectors: influence on vector function and effector mechanisms. *Gene Ther* **Suppl 1**, S10-17 (2004).
34. Xiao, W. et al. Gene therapy vectors based on adeno-associated virus type 1. *J Virol* **73**, 3994-4003 (1999).
35. Urabe, M., Ding, C. & Kotin, R.M. Insect cells as a factory to produce adeno-associated virus type 2 vectors. *Hum Gene Ther* **13(16)**, 1935-1943 (2002).

36. Leone, P. et al. Long-term follow-up after gene therapy for canavan disease. *Science translational medicine* **4**, 165ra163 (2012).
37. Maguire, C.A. et al. Microvesicle-associated AAV vector as a novel gene delivery system. *Mol Ther* **20(5)**, 960-971 (2012).
38. György, B., Fitzpatrick, Z., Crommentuijn, M.H., Mu, D. & Maguire, C.A. Naturally enveloped AAV vectors for shielding neutralizing antibodies and robust gene delivery in vivo. *Biomaterials* **35(26)**, 7598-7609. doi: 7510.1016/j.biomaterials.2014.7505.7032 (2014).
39. Bledsoe, A.W., Jackson, C.A., McPherson, S. & Morrow, C.D. Cytokine production in motor neurons by poliovirus replicon vector gene delivery. *Nat Biotechnol* **18(9)**, 964-969 (2000).
40. Jackson, C.A., Cobbs, C., Peduzzi, J.D., Novak, M. & Morrow, C.D. Repetitive intrathecal injections of poliovirus replicons result in gene expression in neurons of the central nervous system without pathogenesis. *Hum Gene Ther* **12(15)**, 1827-1841 (2001).
41. Ehrengruber, M.U. et al. Recombinant Semliki Forest virus and Sindbis virus efficiently infect neurons in hippocampal slice cultures. *Proc Natl Acad Sci U S A* **96(12)**, 7041-7046 (1999).
42. Ehrengruber, M.U. et al. Gene transfer into neurons from hippocampal slices: comparison of recombinant Semliki Forest Virus, adenovirus, adeno-associated virus, lentivirus, and measles virus. *Molecular and cellular neurosciences* **17(5)**, 855-871 (2001).
43. Altman-Hamamdzic, S. et al. Expression of beta-galactosidase in mouse brain: utilization of a novel nonreplicative Sindbis virus vector as a neuronal gene delivery system. *Gene Ther* **4(8)**, 815-822 (1997).
44. Cordelier, P., Van Bockstaele, E., Calarota, S.A. & Strayer, D.S. Inhibiting AIDS in the central nervous system: gene delivery to protect neurons from HIV. *Mol Ther* **7(6)**, 801-810 (2003).
45. Louboutin, J.P., Chekmasova, A.A., Marusich, E., Chowdhury, J.R. & Strayer, D.S. Efficient CNS gene delivery by intravenous injection. *Nat Methods* **7(11)**, 905-907. doi: 910.1038/nmeth.1518 (2010).
46. Cearley, C.N. & Wolfe, J.H. Transduction characteristics of adeno-associated virus vectors expressing cap serotypes 7, 8, 9, and Rh10 in the mouse brain. *Mol Ther* **13**, 528-537 (2006).
47. Liu, G., Martins, I.H., Chiorini, J.A. & Davidson, B.L. Adeno-associated virus type 4 (AAV4) targets ependyma and astrocytes in the subventricular zone and RMS. *Gene Ther* **12**, 1503-1508 (2005).
48. Kaludov, N., Brown, K.E., Walters, R.W., Zabner, J. & Chiorini, J.A. Adeno-associated virus serotype 4 (AAV4) and AAV5 both require sialic acid binding for hemagglutination and efficient transduction but differ in sialic acid linkage specificity. *J Virol* **75**, 6884-6893 (2001).
49. Shen, S., Bryant, K.D., Brown, S.M., Randell, S.H. & Asokan, A. Terminal N-linked galactose is the primary receptor for adeno-associated virus 9. *The Journal of biological chemistry* **286(15)**, 13532-13540. doi: 13510.11074/jbc.M13110.210922 (2011).
50. Bell, C.L. et al. The AAV9 receptor and its modification to improve in vivo lung gene transfer in mice. *The Journal of clinical investigation* **121**, 2427-2435 (2011).
51. Cearley, C.N. & Wolfe, J.H. A single injection of an adeno-associated virus vector into nuclei with divergent connections results in widespread

vector distribution in the brain and global correction of a neurogenetic disease. *J Neurosci* **27**, 9928-9940 (2007).
52. Castle, M.J., Perlson, E., Holzbaur, E.L. & Wolfe, J.H. Long-distance axonal transport of AAV9 is driven by dynein and kinesin-2 and is trafficked in a highly motile Rab7-positive compartment. *Mol Ther* **22(3)**, 554-566. doi: 510.1038/mt.2013.1237 (2014).
53. Wang, N. et al. Neuronal targets for reducing mutant huntingtin expression to ameliorate disease in a mouse model of Huntington's disease. *Nat Med* **20**, 536-541 (2014).
54. Kells, A.P. et al. Efficient gene therapy-based method for the delivery of therapeutics to primate cortex. *Proc Natl Acad Sci U S A* **106(7)**, 2407-2411. doi: 2410.1073/pnas.0810682106 (2009).
55. Broekman, M.L. et al. Mechanisms of distribution of mouse beta-galactosidase in the adult GM1-gangliosidosis brain. *Gene Ther* **16**, 303-308 (2009).
56. Bankiewicz, K.S. et al. Convection-enhanced delivery of AAV vector in parkinsonian monkeys; in vivo detection of gene expression and restoration of dopaminergic function using pro-drug approach. *Exp Neurol* **164**, 2-14 (2000).
57. Wang, S., Olumolade, O.O., Sun, T., Samiotaki, G. & Konofagou, E.E. Noninvasive, neuron-specific gene therapy can be facilitated by focused ultrasound and recombinant adeno-associated virus. *Gene Ther* **22(1)**, 104-110. doi: 110.1038/gt.2014.1091 (2015).
58. Vite, C.H., Passini, M.A., Haskins, M.E. & Wolfe, J.H. Adeno-associated virus vector-mediated transduction in the cat brain. *Gene Ther* **10(22)**, 1874-1881 (2003).
59. Kim, J.Y., Grunke, S.D., Levites, Y., Golde, T.E. & Jankowsky, J.L. Intracerebroventricular viral injection of the neonatal mouse brain for persistent and widespread neuronal transduction. *J Vis Exp* **91**, 51863. doi: 51810.53791/51863 (2014).
60. McLean, J.R. et al. Widespread neuron-specific transgene expression in brain and spinal cord following synapsin promoter-driven AAV9 neonatal intracerebroventricular injection. *Neuroscience letters* **576**, 73-78. doi: 10.1016/j.neulet.2014.1005.1044 (2014).
61. Snyder, B.R. et al. Comparison of adeno-associated viral vector serotypes for spinal cord and motor neuron gene delivery. *Hum Gene Ther* **22**, 1129-1135 (2011).
62. Federici, T. et al. Robust spinal motor neuron transduction following intrathecal delivery of AAV9 in pigs. *Gene Ther* **19(8)**, 852-859. doi: 810.1038/gt.2011.1130 (2012).
63. Samaranch, L. et al. Adeno-associated virus serotype 9 transduction in the central nervous system of nonhuman primates. *Hum Gene Ther* **23(4)**, 382-389. doi: 310.1089/hum.2011.1200 (2012).
64. Gray, S.J., Nagabhushan Kalburgi, S., McCown, T.J. & Jude Samulski, R. Global CNS gene delivery and evasion of anti-AAV-neutralizing antibodies by intrathecal AAV administration in non-human primates. *Gene Ther* **20**, 450-459 (2013).
65. Samaranch, L. et al. Adeno-associated virus serotype 9 transduction in the central nervous system of nonhuman primates. *Hum Gene Ther* **23**, 382-389 (2012).

66. Schuster, D.J. et al. Biodistribution of adeno-associated virus serotype 9 (AAV9) vector after intrathecal and intravenous delivery in mouse. *Front Neuroanat* **8**, 42. doi: 10.3389/fnana.2014.00042 (2014).
67. Wong, A.D. et al. The blood-brain barrier: an engineering perspective. *Front Neuroeng* **6**, 7. doi: 10.3389/fneng.2013.00007 (2013).
68. Foust, K.D. et al. Intravascular AAV9 preferentially targets neonatal neurons and adult astrocytes. *Nat Biotechnol* **27**, 59-65 (2009).
69. Zhang, H. et al. Several rAAV vectors efficiently cross the blood-brain barrier and transduce neurons and astrocytes in the neonatal mouse central nervous system. *Mol Ther* **19**, 1440-1448 (2011).
70. Yang, B. et al. Global CNS transduction of adult mice by intravenously delivered rAAVrh.8 and rAAVrh.10 and nonhuman primates by rAAVrh.10. *Mol Ther* **22**, 1299-1309 (2014).
71. Fu, H. et al. Self-complementary adeno-associated virus serotype 2 vector: global distribution and broad dispersion of AAV-mediated transgene expression in mouse brain. *Mol Ther* **8(6)**, 911-917 (2003).
72. McCarty, D.M., DiRosario, J., Gulaid, K., Muenzer, J. & Fu, H. Mannitol-facilitated CNS entry of rAAV2 vector significantly delayed the neurological disease progression in MPS IIIB mice. *Gene Ther* **16(11)**, 1340-1352. doi: 1310.1038/gt.2009.1385 (2009).
73. Gray, S.J. et al. Preclinical differences of intravascular AAV9 delivery to neurons and glia: a comparative study of adult mice and nonhuman primates. *Mol Ther* **19**, 1058-1069 (2011).
74. Gray, S.J. et al. Optimizing promoters for recombinant adeno-associated virus-mediated gene expression in the peripheral and central nervous system using self-complementary vectors. *Hum Gene Ther* **22**, 1143-1153 (2011).
75. Grimm, D. et al. Fatality in mice due to oversaturation of cellular microRNA/short hairpin RNA pathways. *Nature* **441**, 537-541 (2006).
76. Bevan, A.K. et al. Systemic gene delivery in large species for targeting spinal cord, brain, and peripheral tissues for pediatric disorders. *Mol Ther* **19**, 1971-1980 (2011).
77. Hordeaux, J. et al. Efficient central nervous system AAVrh10-mediated intrathecal gene transfer in adult and neonate rats. *Gene Ther* **22(4)**, 316-324. doi: 310.1038/gt.2014.1121 (2015).
78. Chakrabarty, P. et al. Capsid serotype and timing of injection determines AAV transduction in the neonatal mice brain. *PloS one* **8(6)**, e67680. doi: 67610.61371/journal.pone.0067680 (2013).
79. Foust, K.D. et al. Rescue of the spinal muscular atrophy phenotype in a mouse model by early postnatal delivery of SMN. *Nat Biotechnol* **28**, 271-274 (2010).
80. Kaul, R., Gao, G.P., Balamurugan, K. & Matalon, R. Cloning of the human aspartoacylase cDNA and a common missense mutation in Canavan disease. *Nature genetics* **5(2)**, 118-123 (1993).
81. Leone, P. et al. Aspartoacylase gene transfer to the mammalian central nervous system with therapeutic implications for Canavan disease. *Ann Neurol* **48(1)**, 27-38 (2000).
82. Janson, C. et al. Clinical protocol. Gene therapy of Canavan disease: AAV-2 vector for neurosurgical delivery of aspartoacylase gene (ASPA) to the human brain. *Hum Gene Ther* **13(11)**, 1391-1412 (2002).

83. McPhee, S.W. et al. Immune responses to AAV in a phase I study for Canavan disease. *J Gene Med* **8(5)**, 577-588 (2006).
84. Ahmed, S.S. et al. A single intravenous rAAV injection as late as P20 achieves efficacious and sustained CNS Gene therapy in Canavan mice. *Mol Ther* **21**, 2136-2147 (2013).
85. Wang, R.Y., Bodamer, O.A., Watson, M.S., Wilcox, W.R. & ACMG, W., Group, on Diagnostic Confirmation of Lysosomal Storage Diseases Lysosomal storage diseases: diagnostic confirmation and management of presymptomatic individuals. *Genetics in medicine : official journal of the American College of Medical Genetics* **13(5)**, 457-484. doi: 410.1097/GIM.1090b1013e318211a318217e318211 (2011).
86. Sands, M.S. & Davidson, B.L. Gene therapy for lysosomal storage diseases. *Mol Ther* **13(5)**, 839-849 (2006).
87. Hinderer, C. et al. Intrathecal AAV9-mediated gene delivery corrects lysosomal storage throughout the CNS in a large animal model of mucopolysaccharidosis type I. *Molecular Therapy* **22**, S233-234 (2014).
88. Ruzo, A. et al. Correction of pathological accumulation of glycosaminoglycans in central nervous system and peripheral tissues of MPSIIIA mice through systemic AAV9 gene transfer. *Hum Gene Ther* **23**, 1237-1246 (2012).
89. Fu, H. et al. Significantly increased lifespan and improved behavioral performances by rAAV gene delivery in adult mucopolysaccharidosis IIIB mice. *Gene Ther* **14**, 1065-1077 (2007).
90. Fu, H., Dirosario, J., Killedar, S., Zaraspe, K. & McCarty, D.M. Correction of neurological disease of mucopolysaccharidosis IIIB in adult mice by rAAV9 trans-blood-brain barrier gene delivery. *Mol Ther* **19**, 1025-1033 (2011).
91. Miyake, N., Miyake, K., Asakawa, N., Yamamoto, M. & Shimada, T. Long-term correction of biochemical and neurological abnormalities in MLD mice model by neonatal systemic injection of an AAV serotype 9 vector. *Gene Ther* **21**, 427-433 (2014).
92. Sevin, C. et al. Intracerebral adeno-associated virus-mediated gene transfer in rapidly progressive forms of metachromatic leukodystrophy. *Hum Mol Genet* **15(1)**, 53-64 (2006).
93. Spampanato, C. et al. Efficacy of a combined intracerebral and systemic gene delivery approach for the treatment of a severe lysosomal storage disorder. *Mol Ther* **19(5)**, 860-869. doi: 810.1038/mt.2010.1299 (2011).
94. Passini, M.A. et al. AAV vector-mediated correction of brain pathology in a mouse model of Niemann-Pick A disease. *Mol Ther* **11(5)**, 754-762 (2005).
95. Falk, D.J. et al. Intrapleural administration of AAV9 improves neural and cardiorespiratory function in Pompe disease. *Mol Ther* **21(9)**, 1661-1667. doi: 1610.1038/mt.2013 (2013).
96. Weismann, C.M. et al. Systemic AAV9 gene transfer in adult GM1 gangliosidosis mice reduces lysosomal storage in CNS and extends lifespan. *Hum Mol Genet* **24**, 4353-4364 (2015).
97. Cachon-Gonzalez, M.B. et al. Effective gene therapy in an authentic model of Tay-Sachs-related diseases. *Proc Natl Acad Sci U S A* **103**, 10373-10378 (2006).

98. Sargeant, T.J. et al. Adeno-associated virus-mediated expression of β-hexosaminidase prevents neuronal loss in the Sandhoff mouse brain. *Hum Mol Genet* **20(22)**, 4371-4380. doi: 4310.1093/hmg/ddr4364 (2011).
99. Worgall, S. et al. Treatment of late infantile neuronal ceroid lipofuscinosis by CNS administration of a serotype 2 adeno-associated virus expressing CLN2 cDNA. *Hum Gene Ther* **19**, 463-474 (2008).
100. Tardieu, M. et al. Intracerebral Administration of Adeno-Associated Viral Vector Serotype rh.10 Carrying Human SGSH and SUMF1 cDNAs in Children with Mucopolysaccharidosis Type IIIA Disease: Results of a Phase I/II Trial. *Hum Gene Ther* (2014).
101. Gong, Y. et al. Adenoassociated virus seroytpe 9-mediated gene therapy for X-linked adrenoleukodystrophy. *Mol Ther* **23(5)**, 824-834. doi: 810.1038/mt.2015.1036 (2015).
102. Bevan, A.K. et al. Early heart failure in the SMNDelta7 model of spinal muscular atrophy and correction by postnatal scAAV9-SMN delivery. *Hum Mol Genet* **19**, 3895-3905 (2010).
103. Passini, M.A. et al. Translational Fidelity of Intrathecal Delivery of Self-Complementary AAV9-Survival Motor Neuron 1 for Spinal Muscular Atrophy. *Hum Gene Ther* (2014).
104. Meyer, K. et al. Improving Single Injection CSF Delivery of AAV9-mediated Gene Therapy for SMA: A Dose-response Study in Mice and Nonhuman Primates. *Mol Ther* **23**, 477-487 (2015).
105. Duque, S.I. et al. A large animal model of spinal muscular atrophy and correction of phenotype. *Ann Neurol* **77(3)**, 399-414. doi: 310.1002/ana.24332 (2015).
106. Garg, S.K. et al. Systemic delivery of MeCP2 rescues behavioral and cellular deficits in female mouse models of Rett syndrome. *J Neurosci* **33**, 13612-13620 (2013).
107. Foust, K.D. et al. Therapeutic AAV9-mediated suppression of mutant SOD1 slows disease progression and extends survival in models of inherited ALS. *Mol Ther* **21**, 2148-2159 (2013).
108. Yamashita, T. et al. Rescue of amyotrophic lateral sclerosis phenotype in a mouse model by intravenous AAV9-ADAR2 delivery to motor neurons. *EMBO Mol Med* **5(11)**, 1710-1719. doi: 1710.1002/emmm.201302935 (2013).
109. Patel, P. et al. Adeno-associated virus-mediated delivery of a recombinant single-chain antibody against misfolded superoxide dismutase for treatment of amyotrophic lateral sclerosis. *Mol Ther* **22(3)**, 498-510. doi: 410.1038/mt.2013.1239 (2014).
110. Harper, S.Q. et al. RNA interference improves motor and neuropathological abnormalities in a Huntington's disease mouse model. *Proc Natl Acad Sci U S A* **102**, 5820-5825 (2005).
111. McBride, J.L. et al. Artificial miRNAs mitigate shRNA-mediated toxicity in the brain: implications for the therapeutic development of RNAi. *Proc Natl Acad Sci U S A* **105**, 5868-5873 (2008).
112. Dufour, B.D., Smith, C.A., Clark, R.L., Walker, T.R. & McBride, J.L. Intrajugular vein delivery of AAV9-RNAi prevents neuropathological changes and weight loss in Huntington's disease mice. *Mol Ther* **22**, 797-810 (2014).

113. Rodríguez-Lebrón, E. et al. Silencing mutant ATXN3 expression resolves molecular phenotypes in SCA3 transgenic mice. *Mol Ther* **21(10)**, 1909-1918. doi: 1910.1038/mt.2013.1152 (2013).
114. Samii, A., Nutt, J.G. & Ransom, B.R. Parkinson's disease. *Lancet* **363(9423)**, 1783-1793 (2004).
115. Kaplitt, M.G. et al. Safety and tolerability of gene therapy with an adeno-associated virus (AAV) borne GAD gene for Parkinson's disease: an open label, phase I trial. *Lancet* **369**, 2097-2105 (2007).
116. LeWitt, P.A. et al. AAV2-GAD gene therapy for advanced Parkinson's disease: a double-blind, sham-surgery controlled, randomised trial. *Lancet Neurol* **10(4)**, 309-319. doi: 310.1016/S1474-4422(1011)70039-70034 (2011).
117. Christine, C.W. et al. Safety and tolerability of putaminal AADC gene therapy for Parkinson disease. *Neurology* **73**, 1662-1669 (2009).
118. Muramatsu, S. et al. A phase I study of aromatic L-amino acid decarboxylase gene therapy for Parkinson's disease. *Mol Ther* **18**, 1731-1735 (2010).
119. Mittermeyer, G. et al. Long-term evaluation of a phase 1 study of AADC gene therapy for Parkinson's disease. *Hum Gene Ther* **23(4)**, 377-381. doi: 310.1089/hum.2011.1220 (2012).
120. Palfi, S. et al. Long-term safety and tolerability of ProSavin, a lentiviral vector-based gene therapy for Parkinson's disease: a dose escalation, open-label, phase 1/2 trial. *Lancet* **383(9923)**, 1138-1146. doi: 1110.1016/S0140-6736(1113)61939-X (2014).
121. Kordower, J.H. et al. Delivery of neurturin by AAV2 (CERE-120)-mediated gene transfer provides structural and functional neuroprotection and neurorestoration in MPTP-treated monkeys. *Ann Neurol* **60(6)**, 706-715 (2006).
122. Gasmi, M. et al. AAV2-mediated delivery of human neurturin to the rat nigrostriatal system: long-term efficacy and tolerability of CERE-120 for Parkinson's disease. *Neurobiol Dis* **27(1)**, 67-76 (2007).
123. Gasmi, M. et al. Striatal delivery of neurturin by CERE-120, an AAV2 vector for the treatment of dopaminergic neuron degeneration in Parkinson's disease. *Mol Ther* **15(1)**, 62-68 (2007).
124. Marks, W.J.J. et al. Safety and tolerability of intraputaminal delivery of CERE-120 (adeno-associated virus serotype 2-neurturin) to patients with idiopathic Parkinson's disease: an open-label, phase I trial. *Lancet Neurol* **7(5)**, 400-408. doi: 410.1016/S1474-4422(1008)70065-70066 (2008).
125. Marks, W.J.J. et al. Gene delivery of AAV2-neurturin for Parkinson's disease: a double-blind, randomised, controlled trial. *Lancet Neurol* **9**, 1164-1172 (2010).
126. Herzog, C.D. et al. Enhanced neurotrophic distribution, cell signaling and neuroprotection following substantia nigral versus striatal delivery of AAV2-NRTN (CERE-120). *Neurobiol Dis* **58**, 38-48. doi: 10.1016/j.nbd.2013.1004.1011 (2013).
127. Zharikov, A.D. et al. shRNA targeting α-synuclein prevents neurodegeneration in a Parkinson's disease model. *The Journal of clinical investigation* **125(7)**, 2721-2735. doi: 2710.1172/JCI64502 (2015).
128. Hwu, W.L. et al. Gene therapy for aromatic L-amino acid decarboxylase deficiency. *Science translational medicine* **4**, 134ra161 (2012).

129. Burns, A. & Iliffe, S. Alzheimer's disease. *BMJ* **338**, b158. doi: 110.1136/bmj.b1158 (2009).
130. Ballard, C. et al. Alzheimer's disease. *Lancet* **377(9770)**, 1019-1031. doi: 1010.1016/S0140-6736(1010)61349-61349 (2011).
131. Breunig, J.J., Guillot-Sestier, M.V. & Town, T. Brain injury, neuroinflammation and Alzheimer's disease. *Front Againg Neurosci* **5**, 26. doi: 10.3389/fnagi.2013.00026 (2013).
132. Bedse, G., Di Domenico, F., Serviddio, G. & Cassano, T. Aberrant insulin signaling in Alzheimer's disease: current knowledge. *Front Neurosci* **9**, 204. doi: 210.3389/fnins.2015.00204 (2015).
133. Cechetto, D.F., Hachinski, V. & Whitehead, S.N. Vascular risk factors and Alzheimer's disease. *Expert Rev Neurother* **8(5)**, 743-750. doi: 710.1586/14737175.14737178.14737175.14737743 (2008).
134. Grothe, M., Heinsen, H. & Teipel, S.J. Atrophy of the cholinergic Basal forebrain over the adult age range and in early stages of Alzheimer's disease. *Biological psychiatry* **71(9)**, 805-813. doi: 810.1016/j.biopsych.2011.1006.1019 (2012).
135. O'Connor, D.M. & Boulis, N.M. Gene therapy for neurodegenerative diseases. *Trends Mol Med* **21(8)**, 504-512. doi: 510.1016/j.molmed.2015.1006.1001 (2015).
136. Li, Y., Wang, J., Zhang, S. & Liu, Z. Neprilysin gene transfer: A promising therapeutic approach for Alzheimer's disease. *Journal of neuroscience research* **93(9)**, 1325-1329. doi: 1310.1002/jnr.23564 (2015).
137. Lebson, L. et al. Trafficking CD11b-positive blood cells deliver therapeutic genes to the brain of amyloid-depositing transgenic mice. *J Neurosci* **30**, 9651-9658 (2010).
138. Levites, Y. et al. A human monoclonal IgG that binds aβ assemblies and diverse amyloids exhibits anti-amyloid activities in vitro and in vivo. *J Neurosci* **35(16)**, 6265-6276. doi: 6210.1523/JNEUROSCI.5109-6214.2015 (2015).
139. Nawrot, B. Targeting BACE with small inhibitory nucleic acids - a future for Alzheimer's disease therapy? *Acta Biochim Pol* **51(2)**, 431-444 (2004).
140. Huang, Y. et al. Loss of GPR3 reduces the amyloid plaque burden and improves memory in Alzheimer's disease mouse models. *Science translational medicine* **7(309)**, 309ra164. doi: 310.1126/scitranslmed.aab3492 (2015).
141. Kiyota, T. et al. AAV2/1 CD74 gene transfer reduces β-amyloidosis and improves learning and memory in a mouse model of Alzheimer's disease. *Mol Ther* **Jul 31**, doi: 10.1038/mt.2015.1142. [Epub ahead of print] (2015).
142. Hudry, E. et al. Gene transfer of human Apoe isoforms results in differential modulation of amyloid deposition and neurotoxicity in mouse brain. *Science translational medicine* **5(212)**, 212ra161. doi: 210.1126/scitranslmed.3007000 (2013).
143. Liao, F. et al. Anti-ApoE antibody given after plaque onset decreases Aβ accumulation and improves brain function in a mouse model of Aβ amyloidosis. *J Neurosci* **34(21)**, 7281-7292. doi: 7210.1523/JNEUROSCI.0646-7214.2014 (2014).
144. Murphy, S.R. et al. Acat1 knockdown gene therapy decreases amyloid-β in a mouse model of Alzheimer's disease. *Mol Ther* **21(8)**, 1497-1506. doi: 1410.1038/mt.2013.1118 (2013).

145. Burlot, M.A. et al. Cholesterol 24-hydroxylase defect is implicated in memory impairments associated with Alzheimer-like Tau pathology. *Hum Mol Genet* **24(21)**, 5965-5976. doi: 5910.1093/hmg/ddv5268 (2015).
146. Hudry, E. et al. Adeno-associated virus gene therapy with cholesterol 24-hydroxylase reduces the amyloid pathology before or after the onset of amyloid plaques in mouse models of Alzheimer's disease. *Mol Ther* **18(1)**, 44-53. doi: 10.1038/mt.2009.1175 (2010).
147. Gant, J.C. et al. Reversal of aging-related neuronal Ca2+ dysregulation and cognitive impairment by delivery of a transgene encoding FK506-binding protein 12.6/1b to the hippocampus. *J Neurosci* **35(30)**, 10878-10887. doi: 10810.11523/JNEUROSCI.11248-10815.12015 (2015).
148. Kemppainen, S. et al. Cerebral dopamine neurotrophic factor improves long-term memory in APP/PS1 transgenic mice modeling Alzheimer's disease as well as in wild-type mice. *Behavioural brain research* **291**, 1-11. doi: 10.1016/j.bbr.2015.1005.1002 (2015).
149. Pascual-Lucas, M. et al. Insulin-like growth factor 2 reverses memory and synaptic deficits in APP transgenic mice. *EMBO Mol Med* **6(10)**, 1246-1262. doi: 1210.15252/emmm.201404228 (2014).
150. Nagahara, A.H. et al. Early BDNF treatment ameliorates cell loss in the entorhinal cortex of APP transgenic mice. *J Neurosci* **33(39)**, 15596-15602. doi: 15510.11523/JNEUROSCI.15195-15512.12013 (2013).
151. Tuszynski, M.H. et al. Nerve Growth Factor Gene Therapy: Activation of Neuronal Responses in Alzheimer Disease. *JAMA Neurol* **72(10)**, 1139-1147. doi: 1110.1001/jamaneurol.2015.1807 (2015).
152. Gaudet, D. et al. Efficacy and long-term safety of alipogene tiparvovec (AAV1-LPLS447X) gene therapy for lipoprotein lipase deficiency: an open-label trial. *Gene Ther* **20**, 361-369 (2013).
153. Nathwani, A.C. et al. Long-term safety and efficacy of factor IX gene therapy in hemophilia B. *The New England journal of medicine* **371(21)**, 1994-2004. doi: 1910.1056/NEJMoa1407309 (2014).
154. Miller, D.G. et al. Large-scale analysis of adeno-associated virus vector integration sites in normal human cells. *J Virol* **79(17)**, 11434-11442 (2005).
155. Nakai, H. et al. Large-scale molecular characterization of adeno-associated virus vector integration in mouse liver. *J Virol* **79(6)**, 3606-3614 (2005).
156. Nakai, H. et al. AAV serotype 2 vectors preferentially integrate into active genes in mice. *Nature genetics* **34(3)**, 297-302 (2003).
157. Russell, D.W. & Hirata, R.K. Human gene targeting by viral vectors. *Nature genetics* **18(4)**, 325-330 (1998).
158. Kohli, M., Rago, C., Lengauer, C., Kinzler, K.W. & Vogelstein, B. Facile methods for generating human somatic cell gene knockouts using recombinant adeno-associated viruses. *Nucleic Acids Res* **32(1)**, e3 (2004).
159. Topaloglu, O., Hurley, P.J., Yildirim, O., Civin, C.I. & Bunz, F. Improved methods for the generation of human gene knockout and knockin cell lines. *Nucleic Acids Res* **33(18)**, e158 (2005).
160. Miller, D.G. et al. Gene targeting in vivo by adeno-associated virus vectors. *Nat Biotechnol* **24(8)**, 1022-1026 (2006).

161. Paulk, N.K. et al. Adeno-associated virus gene repair corrects a mouse model of hereditary tyrosinemia in vivo. *Hepatology* **51(4)**, 1200-1208. doi: 1210.1002/hep.23481 (2010).
162. Barzel, A. et al. Promoterless gene targeting without nucleases ameliorates haemophilia B in mice. *Nature* **517(7534)**, 360-364. doi: 310.1038/nature13864 (2015).
163. Cox, D.B., Platt, R.J. & Zhang, F. Therapeutic genome editing: prospects and challenges. *Nat Med* **21(2)**, 121-131. doi: 110.1038/nm.3793 (2015).
164. Li, H. et al. In vivo genome editing restores haemostasis in a mouse model of haemophilia. *Nature* **475(7355)**, 217-221. doi: 210.1038/nature10177 (2011).
165. Anguela, X.M. et al. Robust ZFN-mediated genome editing in adult hemophilic mice. *Blood* **122(19)**, 3283-3287. doi: 3210.1182/blood-2013-3204-497354 (2013).
166. Garriga-Canut, M. et al. Synthetic zinc finger repressors reduce mutant huntingtin expression in the brain of R6/2 mice. *Proc Natl Acad Sci U S A* **109(45)**, E3136-3145. doi: 3110.1073/pnas.1206506109 (2012).
167. Hsu, P.D., Lander, E.S. & Zhang, F. Development and applications of CRISPR-Cas9 for genome engineering. *Cell* **157**, 1262-1278 (2014).
168. Ran, F.A. et al. In vivo genome editing using Staphylococcus aureus Cas9. *Nature* **520(7546)**, 186-191. doi: 110.1038/nature14299 (2015).
169. Zetsche, B. et al. Cpf1 Is a Single RNA-Guided Endonuclease of a Class 2 CRISPR-Cas System. *Cell* **163**, 759-771 (2015).
170. Berns, K.I. in Fields Virology, Vol. 3. (eds. B.N. Fields, D.M. Knipe & M. Howley) 2173-2197 (Lippincott-Raven, Philadelphia, PA; 1996).
171. Srivastava, A., Lusby, E.W. & Berns, K.I. Nucleotide sequence and organization of the adeno-associated virus 2 genome. *J Virol* **45**, 555-564 (1993).
172. Atchison, R.W., Casto, B.C. & Hammon, W.M. Adenovirus-Associated Defective Virus Particles. *Science* **149**, 754-756 (1965).
173. Hoggan, M.D., Blacklow, N.R. & Rowe, W.P. Studies of small DNA viruses found in various adenovirus preparations: physical, biological, and immunological characteristics. *Proc Natl Acad Sci U S A* **55**, 1467-1474 (1966).
174. Gao, G. et al. Clades of Adeno-associated viruses are widely disseminated in human tissues. *J Virol* **78**, 6381-6388 (2004).
175. Gao, G.P. et al. Novel adeno-associated viruses from rhesus monkeys as vectors for human gene therapy. *Proc Natl Acad Sci U S A* **99**, 11854-11859 (2002).
176. Mori, S., Wang, L., Takeuchi, T. & Kanda, T. Two novel adeno-associated viruses from cynomolgus monkey: pseudotyping characterization of capsid protein. *Virology* **330**, 375-383 (2004).
177. Schmidt, M. et al. Molecular characterization of the heparin-dependent transduction domain on the capsid of a novel adeno-associated virus isolate, AAV(VR-942). *J Virol* **82**, 8911-8916 (2008).
178. Schmidt, M. et al. Adeno-associated virus type 12 (AAV12): a novel AAV serotype with sialic acid- and heparan sulfate proteoglycan-independent transduction activity. *J Virol* **82**, 1399-1406 (2008).
179. Miller, E.B. et al. Production, purification and preliminary X-ray crystallographic studies of adeno-associated virus serotype 1. *Acta Crystallogr Sect F Struct Biol Cryst Commun* **62**, 1271-1274 (2006).

180. Xie, Q. et al. The atomic structure of adeno-associated virus (AAV-2), a vector for human gene therapy. *Proc Natl Acad Sci U S A* **99**, 10405-10410 (2002).
181. Lerch, T.F., Xie, Q. & Chapman, M.S. The structure of adeno-associated virus serotype 3B (AAV-3B): insights into receptor binding and immune evasion. *Virology* **403**, 26-36 (2010).
182. Govindasamy, L. et al. Structurally mapping the diverse phenotype of adeno-associated virus serotype 4. *J Virol* **80**, 11556-11570 (2006).
183. Walters, R.W. et al. Structure of adeno-associated virus serotype 5. *J Virol* **78**, 3361-3371 (2004).
184. Xie, Q., Ongley, H.M., Hare, J. & Chapman, M.S. Crystallization and preliminary X-ray structural studies of adeno-associated virus serotype 6. *Acta Crystallogr Sect F Struct Biol Cryst Commun* **64**, 1074-1078 (2008).
185. Quesada, O. et al. Production, purification and preliminary X-ray crystallographic studies of adeno-associated virus serotype 7. *Acta Crystallogr Sect F Struct Biol Cryst Commun* **63**, 1073-1076 (2007).
186. Nam, H.J. et al. Structure of adeno-associated virus serotype 8, a gene therapy vector. *J Virol* **81**, 12260-12271 (2007).
187. DiMattia, M.A. et al. Structural insight into the unique properties of adeno-associated virus serotype 9. *J Virol* **86**, 6947-6958 (2012).
188. Halder, S. et al. Structure of neurotropic adeno-associated virus AAVrh.8. *Journal of structural biology* **192**, 21-36 (2015).
189. Mikals, K. et al. The structure of AAVrh32.33, a novel gene delivery vector. *Journal of structural biology* **186**, 308-317 (2014).
190. Lerch, T.F. et al. Structure of AAV-DJ, a retargeted gene therapy vector: cryo-electron microscopy at 4.5 A resolution. *Structure* **20**, 1310-1320 (2012).
191. Agbandje-McKenna, M. & Kleinschmidt, J. AAV capsid structure and cell interactions. *Methods Mol Biol* **807**, 47-92 (2011).
192. Kronenberg, S., Bottcher, B., von der Lieth, C.W., Bleker, S. & Kleinschmidt, J.A. A conformational change in the adeno-associated virus type 2 capsid leads to the exposure of hidden VP1 N termini. *J Virol* **79**, 5296-5303 (2005).
193. Ruffing, M., Zentgraf, H. & Kleinschmidt, J.A. Assembly of viruslike particles by recombinant structural proteins of adeno-associated virus type 2 in insect cells. *J Virol* **66**, 6922-6930 (1992).
194. Steinbach, S., Wistuba, A., Bock, T. & Kleinschmidt, J.A. Assembly of adeno-associated virus type 2 capsids in vitro. *J Gen Virol* **78 (Pt 6)**, 1453-1462 (1997).
195. Hoque, M. et al. Nuclear transport of the major capsid protein is essential for adeno-associated virus capsid formation. *J Virol* **73**, 7912-7915 (1999).
196. Warrington, K.H., Jr. et al. Adeno-associated virus type 2 VP2 capsid protein is nonessential and can tolerate large peptide insertions at its N terminus. *J Virol* **78**, 6595-6609 (2004).
197. Rabinowitz, J.E., Xiao, W. & Samulski, R.J. Insertional mutagenesis of AAV2 capsid and the production of recombinant virus. *Virology* **265**, 274-285 (1999).
198. Sonntag, F., Schmidt, K. & Kleinschmidt, J.A. A viral assembly factor promotes AAV2 capsid formation in the nucleolus. *Proc Natl Acad Sci U S A* **107**, 10220-10225 (2010).

199. Seisenberger, G. et al. Real-time single-molecule imaging of the infection pathway of an adeno-associated virus. *Science* **294**, 1929-1932 (2001).
200. Wu, Z., Miller, E., Agbandje-McKenna, M. & Samulski, R.J. Alpha2,3 and alpha2,6 N-linked sialic acids facilitate efficient binding and transduction by adeno-associated virus types 1 and 6. *J Virol* **80**, 9093-9103 (2006).
201. Summerford, C. & Samulski, R.J. Membrane-associated heparan sulfate proteoglycan is a receptor for adeno-associated virus type 2 virions. *J Virol* **72**, 1438-1445 (1998).
202. Lerch, T.F. & Chapman, M.S. Identification of the heparin binding site on adeno-associated virus serotype 3B (AAV-3B). *Virology* **423**, 6-13 (2012).
203. Walters, R.W. et al. Binding of adeno-associated virus type 5 to 2,3-linked sialic acid is required for gene transfer. *The Journal of biological chemistry* **276**, 20610-20616 (2001).
204. Bell, C.L., Gurda, B.L., Van Vliet, K., Agbandje-McKenna, M. & Wilson, J.M. Identification of the galactose binding domain of the adeno-associated virus serotype 9 capsid. *J Virol* **86**, 7326-7333 (2012).
205. Shen, S., Bryant, K.D., Brown, S.M., Randell, S.H. & Asokan, A. Terminal N-linked galactose is the primary receptor for adeno-associated virus 9. *The Journal of biological chemistry* **286**, 13532-13540 (2011).
206. Wu, Z. et al. Single amino acid changes can influence titer, heparin binding, and tissue tropism in different adeno-associated virus serotypes. *J Virol* **80**, 11393-11397 (2006).
207. Ng, R. et al. Structural characterization of the dual glycan binding adeno-associated virus serotype 6. *J Virol* **84**, 12945-12957 (2010).
208. Asokan, A., Hamra, J.B., Govindasamy, L., Agbandje-McKenna, M. & Samulski, R.J. Adeno-associated virus type 2 contains an integrin alpha5beta1 binding domain essential for viral cell entry. *J Virol* **80**, 8961-8969 (2006).
209. Qing, K. et al. Human fibroblast growth factor receptor 1 is a co-receptor for infection by adeno-associated virus 2. *Nat Med* **5**, 71-77 (1999).
210. Ling, C. et al. Human hepatocyte growth factor receptor is a cellular coreceptor for adeno-associated virus serotype 3. *Hum Gene Ther* **21**, 1741-1747 (2010).
211. Di Pasquale, G. et al. Identification of PDGFR as a receptor for AAV-5 transduction. *Nat Med* **9**, 1306-1312 (2003).
212. Akache, B. et al. The 37/67-kilodalton laminin receptor is a receptor for adeno-associated virus serotypes 8, 2, 3, and 9. *J Virol* **80**, 9831-9836 (2006).
213. Shen, S. et al. Functional analysis of the putative integrin recognition motif on adeno-associated virus 9. *The Journal of biological chemistry* **290**, 1496-1504 (2015).
214. Sanlioglu, S. et al. Endocytosis and nuclear trafficking of adeno-associated virus type 2 are controlled by rac1 and phosphatidylinositol-3 kinase activation. *J Virol* **74**, 9184-9196 (2000).
215. Lux, K. et al. Green fluorescent protein-tagged adeno-associated virus particles allow the study of cytosolic and nuclear trafficking. *J Virol* **79**, 11776-11787 (2005).
216. Sonntag, F., Bleker, S., Leuchs, B., Fischer, R. & Kleinschmidt, J.A. Adeno-associated virus type 2 capsids with externalized VP1/VP2 trafficking domains are generated prior to passage through the cytoplasm

and are maintained until uncoating occurs in the nucleus. *J Virol* **80**, 11040-11054 (2006).
217. Nonnenmacher, M. & Weber, T. Adeno-associated virus 2 infection requires endocytosis through the CLIC/GEEC pathway. *Cell Host Microbe* **10**, 563-576 (2011).
218. Bantel-Schaal, U., Braspenning-Wesch, I. & Kartenbeck, J. Adeno-associated virus type 5 exploits two different entry pathways in human embryo fibroblasts. *J Gen Virol* **90**, 317-322 (2009).
219. Ding, W., Zhang, L.N., Yeaman, C. & Engelhardt, J.F. rAAV2 traffics through both the late and the recycling endosomes in a dose-dependent fashion. *Mol Ther* **13**, 671-682 (2006).
220. Zhong, L. et al. Tyrosine-phosphorylation of AAV2 vectors and its consequences on viral intracellular trafficking and transgene expression. *Virology* **381**, 194-202 (2008).
221. Zhong, L. et al. Next generation of adeno-associated virus 2 vectors: point mutations in tyrosines lead to high-efficiency transduction at lower doses. *Proc Natl Acad Sci U S A* **105**, 7827-7832 (2008).
222. Zhong, L. et al. A dual role of EGFR protein tyrosine kinase signaling in ubiquitination of AAV2 capsids and viral second-strand DNA synthesis. *Mol Ther* **15**, 1323-1330 (2007).
223. Kelkar, S. et al. A common mechanism for cytoplasmic dynein-dependent microtubule binding shared among adeno-associated virus and adenovirus serotypes. *J Virol* **80**, 7781-7785 (2006).
224. Xiao, P.J. & Samulski, R.J. Cytoplasmic trafficking, endosomal escape, and perinuclear accumulation of adeno-associated virus type 2 particles are facilitated by microtubule network. *J Virol* **86(19)**, 10462-10461-10473. doi: 10410.11128/JVI.00935-10412 (2012).
225. Wu, P. et al. Mutational analysis of the adeno-associated virus type 2 (AAV2) capsid gene and construction of AAV2 vectors with altered tropism. *J Virol* **74**, 8635-8647 (2000).
226. Xiao, W., Warrington, K.H., Jr., Hearing, P., Hughes, J. & Muzyczka, N. Adenovirus-facilitated nuclear translocation of adeno-associated virus type 2. *J Virol* **76**, 11505-11517 (2002).
227. Hansen, J., Qing, K. & Srivastava, A. Infection of purified nuclei by adeno-associated virus 2. *Mol Ther* **4**, 289-296 (2001).
228. Cohen, S., Behzad, A.R., Carroll, J.B. & Pante, N. Parvoviral nuclear import: bypassing the host nuclear-transport machinery. *J Gen Virol* **87**, 3209-3213 (2006).
229. Bartlett, J.S., Wilcher, R. & Samulski, R.J. Infectious entry pathway of adeno-associated virus and adeno-associated virus vectors. *J Virol* **74**, 2777-2785 (2000).
230. Murphy, S.L., Bhagwat, A., Edmonson, S., Zhou, S. & High, K.A. High-throughput screening and biophysical interrogation of hepatotropic AAV. *Mol Ther* **16**, 1960-1967 (2008).
231. Kotin, R.M. et al. Site-specific integration by adeno-associated virus. *Proc Natl Acad Sci U S A* **87**, 1963-1973 (1990).
232. Kotin, R.M., Linden, R.M. & Berns, K.I. Characterization of a preferred site on human chromosome 19q for integration of adeno-associated virus DNA by non-homologous recombination. *The EMBO journal* **11**, 5071-5078 (1992).

233. Linden, R.M., Ward, P., Giraud, C., Winocour, E. & Berns, K.I. Site-specific integration by adeno-associated virus. *Proc Natl Acad Sci U S A* **93**, 11288-11294 (1996).
234. Linden, R.M., Winocour, E. & Berns, K.I. The recombination signals for adeno-associated virus site-specific integration. *Proc Natl Acad Sci U S A* **93**, 7966-7972 (1996).
235. Weitzman, M.D., Kyostio, S.R., Kotin, R.M. & Owens, R.A. Adeno-associated virus (AAV) Rep proteins mediate complex formation between AAV DNA and its integration site in human DNA. *Proc Natl Acad Sci U S A* **91**, 5808-5812 (1994).
236. Cideciyan, A.V. et al. Vision 1 year after gene therapy for Leber's congenital amaurosis. *The New England journal of medicine* **361**, 725-727 (2009).
237. Chen, Y.H., Chang, M. & Davidson, B.L. Molecular signatures of disease brain endothelia provide new sites for CNS-directed enzyme therapy. *Nat Med* **15**, 1215-1218 (2009).
238. Munch, R.C. et al. Displaying high-affinity ligands on adeno-associated viral vectors enables tumor cell-specific and safe gene transfer. *Mol Ther* **21**, 109-118 (2013).
239. Munch, R.C. et al. Off-target-free gene delivery by affinity-purified receptor-targeted viral vectors. *Nature communications* **6**, 6246 (2015).
240. Vandenberghe, L.H. et al. Naturally occurring singleton residues in AAV capsid impact vector performance and illustrate structural constraints. *Gene Ther* **16**, 1416-1428 (2009).
241. Lin, J. et al. A new genetic vaccine platform based on an adeno-associated virus isolated from a rhesus macaque. *J Virol* **83**, 12738-12750 (2009).
242. Calcedo, R., Vandenberghe, L.H., Gao, G., Lin, J. & Wilson, J.M. Worldwide epidemiology of neutralizing antibodies to adeno-associated viruses. *The Journal of infectious diseases* **199**, 381-390 (2009).
243. Asokan, A. et al. Reengineering a receptor footprint of adeno-associated virus enables selective and systemic gene transfer to muscle. *Nat Biotechnol* **28**, 79-82 (2010).
244. Bowles, D.E. et al. Phase 1 gene therapy for Duchenne muscular dystrophy using a translational optimized AAV vector. *Mol Ther* **20**, 443-455 (2012).
245. Pulicherla, N. et al. Engineering liver-detargeted AAV9 vectors for cardiac and musculoskeletal gene transfer. *Mol Ther* **19**, 1070-1078 (2011).
246. Grimm, D. et al. In vitro and in vivo gene therapy vector evolution via multispecies interbreeding and retargeting of adeno-associated viruses. *J Virol* **82**, 5887-5911 (2008).
247. Yang, L. et al. A myocardium tropic adeno-associated virus (AAV) evolved by DNA shuffling and in vivo selection. *Proc Natl Acad Sci U S A* (2009).
248. Dalkara, D. et al. In vivo-directed evolution of a new adeno-associated virus for therapeutic outer retinal gene delivery from the vitreous. *Science translational medicine* **5**, 189ra176 (2013).
249. Lisowski, L. et al. Selection and evaluation of clinically relevant AAV variants in a xenograft liver model. *Nature* **506**, 382-386 (2014).
250. Zinn, E. et al. In Silico Reconstruction of the Viral Evolutionary Lineage Yields a Potent Gene Therapy Vector. *Cell reports* **12**, 1056-1068 (2015).

251. Loiler, S.A. et al. Targeting recombinant adeno-associated virus vectors to enhance gene transfer to pancreatic islets and liver. *Gene Ther* **10**, 1551-1558 (2003).
252. Shi, W., Arnold, G.S. & Bartlett, J.S. Insertional mutagenesis of the adeno-associated virus type 2 (AAV2) capsid gene and generation of AAV2 vectors targeted to alternative cell-surface receptors. *Hum Gene Ther* **12**, 1697-1711 (2001).
253. Girod, A. et al. Genetic capsid modifications allow efficient re-targeting of adeno-associated virus type 2. *Nature Med* **5**, 1438 (1999).
254. Shi, W. & Bartlett, J.S. RGD inclusion in VP3 provides adeno-associated virus type 2 (AAV2)-based vectors with a heparan sulfate-independent cell entry mechanism. *Mol Ther* **7**, 515-525 (2003).
255. Nicklin, S.A. et al. Efficient and selective AAV2-mediated gene transfer directed to human vascular endothelial cells. *Mol Ther* **4**, 174-181 (2001).
256. Grifman, M. et al. Incorporation of tumor-targeting peptides into recombinant adeno-associated virus capsids. *Mol Ther* **3**, 964-975 (2001).
257. Perabo, L. et al. In vitro selection of viral vectors with modified tropism: the adeno-associated virus display. *Mol Ther* **8**, 151-157 (2003).
258. Muller, O.J. et al. Random peptide libraries displayed on adeno-associated virus to select for targeted gene therapy vectors. *Nat Biotechnol* **21**, 1040-1046 (2003).
259. Work, L.M. et al. Development of efficient viral vectors selective for vascular smooth muscle cells. *Mol Ther* **9**, 198-208 (2004).
260. Work, L.M. et al. Vascular bed-targeted in vivo gene delivery using tropism-modified adeno-associated viruses. *Mol Ther* **13**, 683-693 (2006).
261. Waterkamp, D.A., Muller, O.J., Ying, Y., Trepel, M. & Kleinschmidt, J.A. Isolation of targeted AAV2 vectors from novel virus display libraries. *J Gene Med* **8**, 1307-1319 (2006).
262. White, S.J. et al. Targeted gene delivery to vascular tissue in vivo by tropism-modified adeno-associated virus vectors. *Circulation* **109**, 513-519 (2004).
263. Chen, Y.H., Clafin, K., Geoghegan, J.C. & Davidson, B.L. Sialic acid deposition impairs the utility of AAV9, but not peptide-modified AAVs for brain gene therapy in a mouse model of lysosomal storage disease. *Mol Ther* **7**, 1393-1399 (2012).
264. Opie, S.R., Warrington, K.H., Jr., Agbandje-McKenna, M., Zolotukhin, S. & Muzyczka, N. Identification of amino acid residues in the capsid proteins of adeno-associated virus type 2 that contribute to heparan sulfate proteoglycan binding. *J Virol* **77**, 6995-7006 (2003).
265. Judd, J. et al. Random Insertion of mCherry Into VP3 Domain of Adeno-associated Virus Yields Fluorescent Capsids With no Loss of Infectivity. *Mol Ther Nucleic Acids* **1**, e54 (2012).
266. Michelfelder, S. et al. Successful expansion but not complete restriction of tropism of adeno-associated virus by in vivo biopanning of random virus display peptide libraries. *PloS one* **4**, e5122 (2009).
267. Michelfelder, S. et al. Peptide ligands incorporated into the threefold spike capsid domain to re-direct gene transduction of AAV8 and AAV9 in vivo. *PloS one* **6**, e23101 (2011).
268. Yu, C.Y. et al. A muscle-targeting peptide displayed on AAV2 improves muscle tropism on systemic delivery. *Gene Ther* **16**, 953-962 (2009).

269. Lee, N.C. et al. An acidic oligopeptide displayed on AAV2 improves axial muscle tropism after systemic delivery. *Genetic vaccines and therapy* **10**, 3 (2012).
270. Ying, Y. et al. Heart-targeted adeno-associated viral vectors selected by in vivo biopanning of a random viral display peptide library. *Gene Ther* **17**, 980-990 (2010).
271. Hauck, B., Chen, L. & Xiao, W. Generation and characterization of chimeric recombinant AAV vectors. *Mol Ther* **7**, 419-425 (2003).
272. Rabinowitz, J.E. et al. Cross-dressing the virion: the transcapsidation of adeno-associated virus serotypes functionally defines subgroups. *J Virol* **78**, 4421-4432 (2004).
273. Shen, S. et al. Engraftment of a galactose receptor footprint onto adeno-associated viral capsids improves transduction efficiency. *The Journal of biological chemistry* **288**, 28814-28823 (2013).
274. Hauck, B. et al. Efficient AAV1-AAV2 hybrid vector for gene therapy of hemophilia. *Hum Gene Ther* **17**, 46-54 (2006).
275. Grieger, J.C., Snowdy, S. & Samulski, R.J. Separate basic region motifs within the adeno-associated virus capsid proteins are essential for infectivity and assembly. *J Virol* **80**, 5199-5210 (2006).
276. Limberis, M.P., Vandenberghe, L.H., Zhang, L., Pickles, R.J. & Wilson, J.M. Transduction efficiencies of novel AAV vectors in mouse airway epithelium in vivo and human ciliated airway epithelium in vitro. *Mol Ther* **17**, 294-301 (2009).
277. Lochrie, M.A. et al. Mutations on the external surfaces of adeno-associated virus type 2 capsids that affect transduction and neutralization. *J Virol* **80**, 821-834 (2006).
278. Li, C. et al. Single amino acid modification of adeno-associated virus capsid changes transduction and humoral immune profiles. *J Virol* **86**, 7752-7759 (2012).
279. Petrs-Silva, H. et al. High-efficiency transduction of the mouse retina by tyrosine-mutant AAV serotype vectors. *Mol Ther* **17**, 463-471 (2009).
280. Qiao, C. et al. Adeno-associated virus serotype 6 capsid tyrosine-to-phenylalanine mutations improve gene transfer to skeletal muscle. *Hum Gene Ther* **21**, 1343-1348 (2010).
281. Markusic, D.M. et al. High-efficiency transduction and correction of murine hemophilia B using AAV2 vectors devoid of multiple surface-exposed tyrosines. *Mol Ther* **18**, 2048-2056 (2010).
282. Petrs-Silva, H. et al. Novel properties of tyrosine-mutant AAV2 vectors in the mouse retina. *Mol Ther* **19**, 293-301 (2011).
283. Dalkara, D. et al. Enhanced gene delivery to the neonatal retina through systemic administration of tyrosine-mutated AAV9. *Gene Ther* **19**, 176-181 (2012).
284. Hakim, C.H. et al. Systemic gene transfer reveals distinctive muscle transduction profile of tyrosine mutant AAV-1, -6, and -9 in neonatal dogs. *Molecular therapy. Methods & clinical development* **1**, 14002 (2014).
285. Yue, Y. et al. Safe and bodywide muscle transduction in young adult Duchenne muscular dystrophy dogs with adeno-associated virus. *Hum Mol Genet* **24**, 5880-5890 (2015).
286. Qiao, C. et al. Single tyrosine mutation in AAV8 and AAV9 capsids is insufficient to enhance gene delivery to skeletal muscle and heart. *Human gene therapy methods* **23**, 29-37 (2012).

287. Le, H.T., Yu, Q.C., Wilson, J.M. & Croyle, M.A. Utility of PEGylated recombinant adeno-associated viruses for gene transfer. *J Control Release* **108**, 161-177 (2005).
288. Carlisle, R.C. et al. Coating of adeno-associated virus with reactive polymers can ablate virus tropism, enable retargeting and provide resistance to neutralising antisera. *J Gene Med* **10**, 400-411 (2008).
289. Horowitz, E.D., Weinberg, M.S. & Asokan, A. Glycated AAV vectors: chemical redirection of viral tissue tropism. *Bioconjugate chemistry* **22**, 529-532 (2011).
290. Bartlett, J.S., Kleinschmidt, J., Boucher, R.C. & Samulski, R.J. Targeted adeno-associated virus vector transduction of nonpermissive cells mediated by a bispecific F(ab'gamma)2 antibody. *Nat Biotechnol* **17**, 181-186 (1999).
291. Ponnazhagan, S., Mahendra, G., Kumar, S., Thompson, J.A. & Castillas, M., Jr. Conjugate-based targeting of recombinant adeno-associated virus type 2 vectors by using avidin-linked ligands. *J Virol* **76**, 12900-12907 (2002).
292. Perabo, L. et al. Combinatorial engineering of a gene therapy vector: directed evolution of adeno-associated virus. *J Gene Med* **8**, 155-162 (2006).
293. Maheshri, N., Koerber, J.T., Kaspar, B.K. & Schaffer, D.V. Directed evolution of adeno-associated virus yields enhanced gene delivery vectors. *Nat Biotechnol* **24**, 198-204 (2006).
294. Koerber, J.T., Jang, J.H. & Schaffer, D.V. DNA shuffling of adeno-associated virus yields functionally diverse viral progeny. *Mol Ther* **16**, 1703-1709 (2008).
295. Li, W. et al. Engineering and selection of shuffled AAV genomes: a new strategy for producing targeted biological nanoparticles. *Mol Ther* **16**, 1252-1260 (2008).
296. Nonnenmacher, M., van Bakel, H., Hajjar, R.J. & Weber, T. High capsid-genome correlation facilitates creation of AAV libraries for directed evolution. *Mol Ther* **23**, 675-682 (2015).
297. Excoffon, K.J. et al. Directed evolution of adeno-associated virus to an infectious respiratory virus. *Proc Natl Acad Sci U S A* **106**, 3865-3870 (2009).
298. Li, W. et al. Generation of novel AAV variants by directed evolution for improved CFTR delivery to human ciliated airway epithelium. *Mol Ther* **17**, 2067-2077 (2009).
299. Koerber, J.T. et al. Molecular evolution of adeno-associated virus for enhanced glial gene delivery. *Mol Ther* **17**, 2088-2095 (2009).
300. Maguire, C.A. et al. Directed evolution of adeno-associated virus for glioma cell transduction. *Journal of neuro-oncology* **96**, 337-347 (2010).
301. Jang, J.H. et al. An evolved adeno-associated viral variant enhances gene delivery and gene targeting in neural stem cells. *Mol Ther* **19**, 667-675 (2011).
302. Asuri, P. et al. Directed evolution of adeno-associated virus for enhanced gene delivery and gene targeting in human pluripotent stem cells. *Mol Ther* **20**, 329-338 (2012).
303. Kotterman, M.A., Vazin, T. & Schaffer, D.V. Enhanced selective gene delivery to neural stem cells in vivo by an adeno-associated viral variant. *Development* **142**, 1885-1892 (2015).

304. Li, C. et al. Development of Patient-specific AAV Vectors After Neutralizing Antibody Selection for Enhanced Muscle Gene Transfer. *Mol Ther* (2015).
305. Boutin, S. et al. Prevalence of serum IgG and neutralizing factors against adeno-associated virus (AAV) types 1, 2, 5, 6, 8, and 9 in the healthy population: implications for gene therapy using AAV vectors. *Hum Gene Ther* **21**, 704-712 (2010).
306. Manno, C.S. et al. Successful transduction of liver in hemophilia by AAV-Factor IX and limitations imposed by the host immune response. *Nat Med* **12**, 342-347 (2006).
307. Stroes, E.S. et al. Intramuscular administration of AAV1-lipoprotein lipase S447X lowers triglycerides in lipoprotein lipase-deficient patients. *Arteriosclerosis, thrombosis, and vascular biology* **28**, 2303-2304 (2008).
308. Klimczak, R.R., Koerber, J.T., Dalkara, D., Flannery, J.G. & Schaffer, D.V. A novel adeno-associated viral variant for efficient and selective intravitreal transduction of rat Muller cells. *PloS one* **4**, e7467 (2009).
309. Gray, S.J. et al. Directed evolution of a novel adeno-associated virus (AAV) vector that crosses the seizure-compromised blood-brain barrier (BBB). *Mol Ther* **18**, 570-578 (2010).
310. Adachi, K., Enoki, T., Kawano, Y., Veraz, M. & Nakai, H. Drawing a high-resolution functional map of adeno-associated virus capsid by massively parallel sequencing. *Nature communications* **5**, 3075 (2014).
311. Marsic, D. et al. Vector design Tour de Force: integrating combinatorial and rational approaches to derive novel adeno-associated virus variants. *Mol Ther* **22**, 1900-1909 (2014).
312. Santiago-Ortiz, J. et al. AAV ancestral reconstruction library enables selection of broadly infectious viral variants. *Gene Ther* **22**, 934-946 (2015).
313. Vite, C.H. et al. Effective gene therapy for an inherited CNS disease in a large animal model. *Ann Neurol* **57**, 355-364 (2005).
314. McCurdy, V.J. et al. Sustained normalization of neurological disease after intracranial gene therapy in a feline model. *Science translational medicine* **6**, 231ra248 (2014).
315. Burger, C. et al. Recombinant AAV viral vectors pseudotyped with viral capsids from serotypes 1, 2, and 5 display differential efficiency and cell tropism after delivery to different regions of the central nervous system. *Mol Ther* **10**, 302-317 (2004).
316. Broekman, M.L., Comer, L.A., Hyman, B.T. & Sena-Esteves, M. Adeno-associated virus vectors serotyped with AAV8 capsid are more efficient than AAV-1 or -2 serotypes for widespread gene delivery to the neonatal mouse brain. *Neuroscience* **138**, 501-510 (2006).
317. Sondhi, D. et al. Enhanced Survival of the LINCL Mouse Following CLN2 Gene Transfer Using the rh.10 Rhesus Macaque-derived Adeno-associated Virus Vector. *Mol Ther* **15**, 481-491 (2007).
318. Fiandaca, M.S., Forsayeth, J.R., Dickinson, P.J. & Bankiewicz, K.S. Image-guided convection-enhanced delivery platform in the treatment of neurological diseases. *Neurotherapeutics : the journal of the American Society for Experimental NeuroTherapeutics* **5**, 123-127 (2008).
319. Eberling, J.L. et al. Results from a phase I safety trial of hAADC gene therapy for Parkinson disease. *Neurology* **70**, 1980-1983 (2008).

320. Kells, A.P. et al. Efficient gene therapy-based method for the delivery of therapeutics to primate cortex. *Proc Natl Acad Sci U S A* **106**, 2407-2411 (2009).
321. Salegio, E.A. et al. Axonal transport of adeno-associated viral vectors is serotype-dependent. *Gene Ther* **20**, 348-352 (2013).
322. San Sebastian, W. et al. Adeno-associated virus type 6 is retrogradely transported in the non-human primate brain. *Gene Ther* **20**, 1178-1183 (2013).
323. Yang, B. et al. Global CNS Transduction of Adult Mice by Intravenously Delivered rAAVrh.8 and rAAVrh.10 and Nonhuman Primates by rAAVrh.10. *Mol Ther* (2014).
324. Duque, S. et al. Intravenous Administration of Self-complementary AAV9 Enables Transgene Delivery to Adult Motor Neurons. *Mol Ther* (2009).
325. Gombash, S.E. et al. Intravenous AAV9 efficiently transduces myenteric neurons in neonate and juvenile mice. *Frontiers in molecular neuroscience* **7**, 81 (2014).
326. Benskey, M.J. et al. Targeted gene delivery to the enteric nervous system using AAV: a comparison across serotypes and capsid mutants. *Mol Ther* **23**, 488-500 (2015).
327. Zolotukhin, S. et al. Recombinant adeno-associated virus purification using novel methods improves infectious titer and yield. *Gene Ther* **6**, 973-985 (1999).
328. Grieger, J.C., Choi, V.W. & Samulski, R.J. Production and characterization of adeno-associated viral vectors. *Nature protocols* **1**, 1412-1428 (2006).
329. Livak, K.J. & Schmittgen, T.D. Analysis of relative gene expression data using real-time quantitative PCR and the 2(-Delta Delta C(T)) Method. *Methods* **25**, 402-408 (2001).
330. DiFiglia, M. et al. Huntingtin is a cytoplasmic protein associated with vesicles in human and rat brain neurons. *Neuron* **14**, 1075-1081 (1995).
331. Biasini, M. et al. SWISS-MODEL: modelling protein tertiary and quaternary structure using evolutionary information. *Nucleic Acids Res* **42**, W252-258 (2014).
332. Gyorgy, B., Fitzpatrick, Z., Crommentuijn, M.H., Mu, D. & Maguire, C.A. Naturally enveloped AAV vectors for shielding neutralizing antibodies and robust gene delivery in vivo. *Biomaterials* **35**, 7598-7609 (2014).
333. A novel gene containing a trinucleotide repeat that is expanded and unstable on Huntington's disease chromosomes. The Huntington's Disease Collaborative Research Group. *Cell* **72**, 971-983 (1993).
334. Kordasiewicz, H.B. et al. Sustained therapeutic reversal of Huntington's disease by transient repression of huntingtin synthesis. *Neuron* **74**, 1031-1044 (2012).
335. Bradbury, A.M. et al. Therapeutic response in feline sandhoff disease despite immunity to intracranial gene therapy. *Mol Ther* **21**, 1306-1315 (2013).
336. Yoon, S.Y., Bagel, J.H., O'Donnell, P.A., Vite, C.H. & Wolfe, J.H. Clinical Improvement of Alpha-mannosidosis Cat Following a Single Cisterna Magna Infusion of AAV1. *Mol Ther* (2015).
337. Vite, C.H. et al. Intracisternal cyclodextrin prevents cerebellar dysfunction and Purkinje cell death in feline Niemann-Pick type C1 disease. *Science translational medicine* **7**, 276ra226 (2015).

338. Bemelmans, A.P. et al. A single intravenous AAV9 injection mediates bilateral gene transfer to the adult mouse retina. *PloS one* **8**, e61618 (2013).
339. Ciesielska, A. et al. Cerebral infusion of AAV9 vector-encoding non-self proteins can elicit cell-mediated immune responses. *Mol Ther* **21**, 158-166 (2013).
340. Samaranch, L. et al. AAV9-mediated expression of a non-self protein in nonhuman primate central nervous system triggers widespread neuroinflammation driven by antigen-presenting cell transduction. *Mol Ther* **22**, 329-337 (2014).
341. Wang, L. et al. Comparative Study of Liver Gene Transfer With AAV Vectors Based on Natural and Engineered AAV Capsids. *Mol Ther* (2015).
342. Nathanson, J.L., Yanagawa, Y., Obata, K. & Callaway, E.M. Preferential labeling of inhibitory and excitatory cortical neurons by endogenous tropism of adeno-associated virus and lentivirus vectors. *Neuroscience* **161**, 441-450 (2009).
343. Vandenberghe, L.H. et al. Dosage thresholds for AAV2 and AAV8 photoreceptor gene therapy in monkey. *Science translational medicine* **3**, 88ra54 (2011).
344. Klein, R.L., Dayton, R.D., Tatom, J.B., Henderson, K.M. & Henning, P.P. AAV8, 9, Rh10, Rh43 vector gene transfer in the rat brain: effects of serotype, promoter and purification method. *Mol Ther* **16**, 89-96 (2008).
345. Dodiya, H.B. et al. Differential transduction following basal ganglia administration of distinct pseudotyped AAV capsid serotypes in nonhuman primates. *Mol Ther* **18**, 579-587 (2010).
346. Cearley, C.N. et al. Expanded Repertoire of AAV Vector Serotypes Mediate Unique Patterns of Transduction in Mouse Brain. *Mol Ther* (2008).
347. Taymans, J.M. et al. Comparative analysis of adeno-associated viral vector serotypes 1, 2, 5, 7, and 8 in mouse brain. *Hum Gene Ther* **18**, 195-206 (2007).
348. Lawlor, P.A., Bland, R.J., Mouravlev, A., Young, D. & During, M.J. Efficient gene delivery and selective transduction of glial cells in the mammalian brain by AAV serotypes isolated from nonhuman primates. *Mol Ther* **17**, 1692-1702 (2009).
349. Chen, H., McCarty, D.M., Bruce, A.T. & Suzuki, K. Oligodendrocyte-specific gene expression in mouse brain: use of a myelin-forming cell type-specific promoter in an adeno-associated virus. *Journal of neuroscience research* **55**, 504-513 (1999).
350. Boudreau, R.L. et al. Nonallele-specific silencing of mutant and wild-type huntingtin demonstrates therapeutic efficacy in Huntington's disease mice. *Mol Ther* **17**, 1053-1063 (2009).
351. DeRuisseau, L.R. et al. Neural deficits contribute to respiratory insufficiency in Pompe disease. *Proc Natl Acad Sci U S A* **106**, 9419-9424 (2009).
352. Falk, D.J. et al. Comparative impact of AAV and enzyme replacement therapy on respiratory and cardiac function in adult Pompe mice. *Molecular therapy. Methods & clinical development* **2**, 15007 (2015).
353. Cardone, M. et al. Abnormal mannose-6-phosphate receptor trafficking impairs recombinant alpha-glucosidase uptake in Pompe disease fibroblasts. *Pathogenetics* **1**, 6 (2008).

354. Frei, A.P., Moest, H., Novy, K. & Wollscheid, B. Ligand-based receptor identification on living cells and tissues using TRICEPS. *Nature protocols* **8**, 1321-1336 (2013).
355. Kreuter, J. et al. Apolipoprotein-mediated transport of nanoparticle-bound drugs across the blood-brain barrier. *J Drug Target* **10**, 317-325 (2002).
356. Denard, J. et al. Human galectin 3 binding protein interacts with recombinant adeno-associated virus type 6. *J Virol* **86**, 6620-6631 (2012).
357. Wise, S.P. Forward frontal fields: phylogeny and fundamental function. *Trends Neurosci* **31**, 599-608 (2008).
358. Nathwani, A.C. et al. Adenovirus-associated virus vector-mediated gene transfer in hemophilia B. *The New England journal of medicine* **365**, 2357-2365 (2011).
359. Nathwani, A.C. et al. Safe and efficient transduction of the liver after peripheral vein infusion of self-complementary AAV vector results in stable therapeutic expression of human FIX in nonhuman primates. *Blood* **109**, 1414-1421 (2007).
360. Nathwani, A.C. et al. Self-complementary adeno-associated virus vectors containing a novel liver-specific human factor IX expression cassette enable highly efficient transduction of murine and nonhuman primate liver. *Blood* **107**, 2653-2661 (2006).
361. Davidoff, A.M. et al. Comparison of the ability of adeno-associated viral vectors pseudotyped with serotype 2, 5, and 8 capsid proteins to mediate efficient transduction of the liver in murine and nonhuman primate models. *Mol Ther* **11**, 875-888 (2005).
362. Azuma, H. et al. Robust expansion of human hepatocytes in Fah-/-/Rag2-/-/Il2rg-/- mice. *Nat Biotechnol* **25**, 903-910 (2007).
363. Bissig-Choisat, B. et al. Development and rescue of human familial hypercholesterolaemia in a xenograft mouse model. *Nature communications* **6**, 7339 (2015).
364. Kay, M.A. Selecting the Best AAV Capsid for Human Studies. *Mol Ther* **23**, 1800-1801 (2015).
365. Han, X. et al. Forebrain engraftment by human glial progenitor cells enhances synaptic plasticity and learning in adult mice. *Cell Stem Cell* **12**, 342-353 (2013).
366. Chesler, E.J. et al. The Collaborative Cross at Oak Ridge National Laboratory: developing a powerful resource for systems genetics. *Mammalian genome : official journal of the International Mammalian Genome Society* **19**, 382-389 (2008).
367. Shultz, L.D. et al. Human lymphoid and myeloid cell development in NOD/LtSz-scid IL2R gamma null mice engrafted with mobilized human hemopoietic stem cells. *Journal of immunology* **174**, 6477-6489 (2005).